UCLA
UCLA Electronic Theses and Dissertations

Title
The Analytic Structure of Scattering Amplitudes in N = 4 Super-Yang-Mills Theory

Permalink
https://escholarship.org/uc/item/1x25r1hd

Author
Litsey, Sean

Publication Date
2016

Peer reviewed|Thesis/dissertation

The Analytic Structure of Scattering Amplitudes in $\mathcal{N} = 4$ Super-Yang-Mills Theory

A dissertation submitted in partial satisfaction

of the requirements for the degree

Doctor of Philosophy in Physics

by

Sean Christopher Litsey

2016

Abstract of the Dissertation

The Analytic Structure of Scattering Amplitudes in $\mathcal{N} = 4$ Super-Yang-Mills Theory

by

Sean Christopher Litsey

Doctor of Philosophy in Physics

University of California, Los Angeles, 2016

Professor Zvi Bern, Chair

We begin the dissertation in Chapter 1 with a discussion of tree-level amplitudes in Yang-Mills theories. The DDM and BCJ decompositions of the amplitudes are described and related to one another by the introduction of a transformation matrix. This is related to the Kleiss-Kuijf and BCJ amplitude identities, and we conjecture a connection to the existence of a BCJ representation via a condition on the generalized inverse of that matrix. Under two widely-believed assumptions, this relationship is proved. Switching gears somewhat, we introduce the RSVW formulation of the amplitude, and the extension of BCJ-like features to residues of the RSVW integrand is proposed. Using the previously proven connection of BCJ representations to the generalized inverse condition, this extension is validated, including a version of gravitational double copy.

The remainder of the dissertation involves an analysis of the analytic properties of loop amplitudes in $\mathcal{N} = 4$ super-Yang-Mills theory. Chapter 2 contains a review of the planar case, including an exposition of dual variables and momentum twistors, dual conformal symmetry, and their implications for the amplitude. After defining the integrand and on-shell diagrams, we explain the crucial properties that the amplitude has no poles at infinite momentum and that its leading singularities are dual-conformally-invariant cross ratios, and can therefore be normalized to unity. We define the concept of a $d$log form, and show that it is a feature of the planar integrand as well. This leads to the definition of a pure integrand basis. The

proceeding setup is connected to the amplituhedron formulation, and we put forward the hypothesis that the amplitude is determined by zero conditions.

Chapter 3 contains the primary computations of the dissertation. This chapter treats amplitudes in fully nonplanar $\mathcal{N} = 4$ super-Yang-Mills, analyzing the conjecture that they follow the pattern of having no poles at infinity, can be written in $d$log form, and can be decomposed into a pure integrand basis, with each basis element having unit leading singularity. Through explicit calculation, we show that this is true for the two-loop four-point, three-loop four-point, and two-loop five-point amplitudes, and discuss the features of each case. We then discuss the zero condition hypothesis, showing explicitly that it holds for the two-loop four-particle amplitude, and showing the set of conditions that fix the amplitude in the three-loop four-particle and two-loop five-particle cases without explicitly performing the fixing. This concludes the body of the dissertation.

Two appendices complete the dissertation. Appendix B includes an in-depth discussion of $d$log forms, including purely mathematical examples and a discussion of their appearance in one-loop amplitudes. Finally, Appendix C redoes portions of the analysis of Chapter 3 for the two- and three-loop four-particle amplitudes, but gives representations that are not in a pure integrand basis. Instead diagram symmetry is imposed on the basis elements, and diagrams that lack maximal cuts are pushed into maximal-cut diagrams. This gives representations closer in spirit to the previously-constructed representations of these amplitudes, such as the BCJ representations. It also highlights the role of color Jacobi identities and the freedom in the amplitude representation they can generate, and contains an explicit discussion of these features that is unpublished elsewhere.

The dissertation of Sean Christopher Litsey is approved.

Michael Gutperle

Terence Tao

Zvi Bern, Committee Chair

University of California, Los Angeles

2016

To my family, for putting up with me spending a few years of my life to learn about a subject I love.

TABLE OF CONTENTS

List of Figures

LIST OF TABLES

2010	B.S. (Mathematics & Physics), Yale University, New Haven, Connecticut.
2010-2016	Teaching Assistant, Department of Physics & Astronomy, UCLA, Los Angeles, California.
2012-2016	Graduate Student Researcher, Department of Physics & Astronomy, UCLA, Los Angeles, California.

PUBLICATIONS

Zvi Bern, Enrico Herrmann, Sean Litsey, James Stankowicz, and Jaroslav Trnka. "Evidence for a Nonplanar Amplituhedron." 2015. [arXiv:1512.08591 [hep-th]].

Zvi Bern, Enrico Herrmann, Sean Litsey, James Stankowicz, and Jaroslav Trnka. "Logarithmic Singularities and Maximally Supersymmetric Amplitudes." *JHEP* 1506 (2015) 202. [arXiv:1412.8584 [hept-th]].

Sean Litsey and James Stankowicz. "Kinematic Nmerators and a Double-Copy Formula for $\mathcal{N} = 4$ Super-Yang-Mills Residues." *Phys. Rev. D* **90** (2014) no.2, 025013. [arXiv:1309.7681 [hep-th]].

Sean Litsey and Marc Sher. "Higgs Masses in the Four Generation MSSM." *Phys. Rev. D* **80** (2009) 057701. [arXiv:0908.0502 [hep-ph]].

CHAPTER 1

Color-Kinematic Duality and Residues of Tree-Level Amplitudes

In this chapter, we focus on tree-level amplitudes. There has been much work examining the singularity structure of these amplitudes as functions of external momenta, for example the development of BCFW recursion in Refs. [4, 5]. We will take a different approach, focusing on the representation of the amplitude as an integral over a moduli space, and study the singularity structure of the integrand. This will be analogous to the view we take in later chapters when discussing loop-level amplitudes, although both the space of integration and properties of the singularities we study will be quite different. This chapter is based on Ref. [1], joint work done with James Stankowicz.

One of the more significant recent advances in the study of amplitudes is the discovery by Bern, Carrasco, and Johansson (BCJ) of a duality between color and kinematics [6]. In this duality, kinematic numerators of diagrams obey relations similar to the Jacobi identities obeyed by color factors. One consequence of these relations is that color-ordered tree-level partial amplitudes obey a set of nontrivial identities, known as BCJ amplitude identities. These amplitude identities are even more constraining than the Kleiss-Kuijf identities [7], and so reduce the number of partial amplitudes required to determine a full scattering amplitude. Color-kinematic duality has been conjectured to hold for any number of loops or legs in a wide variety of theories, including pure Yang-Mills theories and their supersymmetric extensions. While no proof exists at loop level, a variety of nontrivial constructions exist [8–15], and its original tree-level formulation has been fully proven.

One remarkable feature of color-kinematic duality is that one can use it to construct

gravity amplitudes directly from gauge-theory amplitudes. To do so, one replaces the color factors in a gauge-theory amplitude with corresponding kinematic numerators that obey the duality. This gives what is known as the double-copy form of gravity amplitudes [6, 9]. At tree level, this encodes the Kawai-Lewellen-Tye (KLT) relations [16] between gauge and gravity amplitudes [17]. The extension of the double-copy formula to loop level [9] requires first constructing loop-level Yang-Mills amplitudes in a form where the duality is manifest. Then, as at tree level, one obtains gravity amplitudes simply by replacing color factors with the corresponding kinematic-numerator.

A parallel direction of research originated from writing the tree-level scattering amplitude of $\mathcal{N} = 4$ super-Yang-Mills with the Roiban, Spradlin, Volovich, and Witten (RSVW) twistor string formula [18–22]. (This is also known as the "connected prescription".) The RSVW formula expresses the scattering amplitude as an integral over a moduli space of curves in $\mathbb{CP}^{3|4}$ supertwistor space, effectively reducing the entire scattering amplitude calculation to solving an algebraic system of equations.

This method for determining tree-level scattering amplitudes as integrals was extended to $\mathcal{N} = 8$ supergravity, first in specific cases [23–25], and later in general [26–29]. Like the RSVW formula, the integrals for $\mathcal{N} = 8$ supergravity can be interpreted as contour integrals, and hence as sums of residues. The formula appearing in Ref. [26] was originally a conjecture, in part because the formula required the KLT relations to hold for the residues in the same way that it holds for the amplitudes; this "KLT orthogonality conjecture" was proven in [30].

Contemporaneously with the work of [1], $\mathcal{N} = 4$ super-Yang-Mills amplitudes were constructed using the "scattering equations" [31], shown to have a color-kinematic structure, and were explicitly related to color-dual numerators [32], using what is now called the Cachazo-He-Yuan (CHY) formula. Because both the CHY formula and the kinematic numerator decomposition of amplitudes represent the same mathematical object, it is not surprising that the former can be written in terms of the latter. On the other hand, the discovery that global relations, such as the KLT relations, hold at the residue level is intriguing because it

suggests there is a Jacobi-like numerator structure for the residues as well.

Additional hints of a Jacobi-like numerator structure for residues appeared in a proof of the BCJ amplitude identities in $\mathcal{N} = 4$ super-Yang-Mills [33]. The proof uses the explicit structure of the RSVW integrand to prove the BCJ identities. Further, Ref. [33] discusses how the method of the proof indicates that the BCJ amplitude identities hold at the level of the residues themselves, analogously to the KLT orthogonality conjecture. Given that the original BCJ amplitude relations were originally derived by considering color-dual numerators, the reappearance of amplitude relations for residues strongly hints at an analogous set of numerators for the residues.

Following these hints, Ref. [1] defined objects called *residue numerators.* By construction, the residue numerators are analogous to the kinematic numerators of partial amplitudes, except that they hold for RSVW residues. Following Ref. [1], we use the KLT orthogonality conjecture to show that the residue numerators obey both a double-copy formula and an orthogonality condition. We also expound on the observation of Ref. [33] to verify that RSVW residues do indeed satisfy the BCJ relations. To do all this, we work in the linear algebra formalism of Refs. [34, 35]. To formally prove our results in this formalism, we prove a conjecture of Ref. [35], establishing that the BCJ amplitude identities are equivalent to an equation specifying a consistency condition for the existence of a solution to a certain system of equations.

The structure of this chapter is as follows. Section 1.1 outlines the necessary background material: the linear algebra formalism, the RSVW formula and its gravitational generalizations, and the concepts of color-kinematic duality and double copy. Section 1.1 also contains some novel material. Subsection 1.1.2 presents a proof that the BCJ amplitude identities are equivalent to a system of constraint equations in the linear algebra formalism. In subsection 1.1.4 we explicitly demonstrate that the BCJ amplitude identities (and hence the constraint equations) apply to RSVW residues, as was noted in [33]. Section 1.2 defines residue numerators, the central objects of this chapter, and proves their double-copy formula. Finally, Section 1.3 summarizes the results and discusses future directions.

1.1 Background Material and Lemmas

1.1.1 Linear Algebra

A convenient way of structuring discussions of kinematic numerators is the linear algebra approach pioneered in Ref. [34] and extended in Ref. [35] (whose notation we largely adopt). This formalism makes generalized gauge invariance manifest, and, as we shall demonstrate, also reinterprets the BCJ amplitude identities as algebraic consistency conditions.

To motivate this approach, recall that Yang-Mills scattering amplitudes in four dimensions can be written in a so-called Del Duca-Dixon-Maltoni (DDM) decomposition [36]. In this form, the full n-particle amplitude at tree level is written as

$$\mathcal{A}_n = g^{n-2} \sum_{\tau \in S_{n-2}} c_\tau A_n \left(1, \tau\left(2\right), \ldots, \tau\left(n-1\right), n\right), \tag{1.1}$$

where the coupling constant is g, the notation $\tau \in S_{n-2}$ indicates that the sum runs over permutations τ of the particle labels $2, \ldots, n-1$, the A_n are color-ordered partial amplitudes, and the c_τ are color factors[1] of cubic diagrams. Cubic diagrams are diagrams whose vertices are all degree three, and which conserve color and momentum at each vertex. Any diagrams containing higher-point contact terms are absorbed into cubic diagrams with the same color factor, with missing propagators P introduced by multiplying by $1 = \frac{P}{P}$. While there is no known Lagrangian from which this decomposition can be directly generated by Feynman rules (see however Ref. [37]), these cubic diagrams are a useful way of reorganizing the usual sum over Feynman diagrams.

Another decomposition of the tree level amplitude, which we will refer to as the BCJ decomposition, is

$$\mathcal{A}_n = g^{n-2} \sum_{i=1}^{(2n-5)!!} \frac{c_i n_i}{D_i}, \tag{1.2}$$

---

[1] These are a product of group-theory structure constants; see [36] for details.

$$c_\tau \quad = \quad \begin{array}{c} \overset{\displaystyle \tau(2) \quad \cdots \quad \tau(n-1)}{\underset{\displaystyle 1 \qquad\qquad\qquad\qquad n}{\rule{0pt}{0pt}\Big|\Big|\Big|\Big|\Big|}} \end{array}$$

Figure 1.1: The definition of the c_τ color factors appearing in the DDM decomposition, where the diagram represents its color factor. Notice that legs 1 and n are fixed, while τ permutes legs 2 through $n-1$.

where the sum is now over the unique set of $(2n-5)!!$ cubic diagrams, with color factors c_i, products of propagators D_i, and so-called "kinematic numerators" n_i. These last objects are functions only of the external momenta and helicities, and are not uniquely defined. This is because a generalized gauge transformation $n_i \mapsto n_i + \Delta_i$, for functions Δ_i that obey

$$\sum_{i=1}^{(2n-5)!!} \frac{c_i \Delta_i}{D_i} = 0, \tag{1.3}$$

will leave the BCJ decomposition Eq. (1.2) invariant. The notion of a generalized gauge transformation will turn out to be nicely expressed in the linear algebra formalism.

We can relate the DDM and BCJ decompositions in a useful way. It was shown in Ref. [36] that the $(n-2)!$ color factors c_τ form a basis of the space of color factors of cubic diagrams. This is possible because the Jacobi relations of the structure constants induce linear relations among the color factors. In other words, any of the $(2n-5)!!$ color factors c_i that appear in the decomposition Eq. (1.2) can be written as

$$c_i = \sum_{\tau \in S_{n-2}} W_{i\tau} c_\tau \tag{1.4}$$

where $W_{i\tau}$ is a $(2n-5)!! \times (n-2)!$ matrix that encodes the Jacobi relations among the color factors. Our notation expresses sums over permutations (as in the DDM decomposition) with τ and ω, and sums over cubic diagrams by Latin indices i, j.

Color-kinematic duality states that there exists a set of color-dual numerators n_i that obey the exact same Jacobi relations as the color factors c_i. In other words, for the same

matrix $W_{i\tau}$ defined above in Eq. (1.4), we can write

$$n_i = \sum_{\tau \in S_{n-2}} W_{i\tau} n_\tau \tag{1.5}$$

for some set of $(n-2)!$ numerators n_τ. Substituting Eq. (1.4) and Eq. (1.5) into the BCJ decomposition, we find

$$
\begin{aligned}
\mathcal{A}_n &= g^{n-2} \sum_{i=1}^{(2n-5)!!} \sum_{\tau,\omega \in S_{n-2}} \frac{c_\tau n_\omega}{D_i} W_{i\tau} W_{i\omega} \\
&= g^{n-2} \sum_{\tau,\omega \in S_{n-2}} c_\tau n_\omega F_{\tau\omega},
\end{aligned} \tag{1.6}
$$

where $F_{\tau\omega}$ is an $(n-2)! \times (n-2)!$ symmetric matrix with products of inverse propagators as entries:

$$F_{\tau\omega} \equiv \sum_{i=1}^{(2n-5)!!} \frac{W_{i\tau} W_{i\omega}}{D_i}. \tag{1.7}$$

The matrix $F_{\tau\omega}$ is a convenient way of simultaneously encoding both the color and numerator Jacobi relations in the basis of partial amplitudes.

Equating Eq. (1.6) to the DDM decomposition and matching coefficients of the c_τ, we have the identity

$$A_n\left(1, \tau\left(2\right), \ldots, \tau\left(n-1\right), n\right) = \sum_{\omega \in S_{n-2}} F_{\tau\omega} n_\omega. \tag{1.8}$$

This can be thought of in matrix notation as a system of linear equations

$$FN = A \tag{1.9}$$

in the $(n-2)!$-dimensional space of partial amplitudes spanned by Kleiss-Kuijf basis amplitudes and indexed by $\tau \in S_{n-2}$, and N is a column vector of numerators. Ideally we could invert this formula to get an expression for the numerators in terms of the partial amplitudes, but this is impossible because F is singular. This is no surprise: the invariance of the full amplitude under generalized gauge transformations as in Eq. (1.3) ensures that

6

the numerators are not unique, so F cannot be invertible.

Therefore F has a nontrivial kernel. To circumvent this problem, Ref. [35] suggested using the machinery of generalized inverses (also called pseudoinverses). A generalized inverse is a matrix F^+ satisfying $FF^+F = F$, and it can be shown that such an F^+ always exists, but is not unique. Generalized inverses are useful because of the following theorem [38]: a solution to $FN = A$ exists if and only if the consistency condition

$$FF^+A = A \tag{1.10}$$

holds for some generalized inverse F^+. The general solution is then given by

$$N = F^+A + \left(I - F^+F\right)v \tag{1.11}$$

for an arbitrary vector v that parametrizes the kernel of F.

Notice that $I - F^+F$ is a projection operator onto the kernel of F, since, by the definition of F^+, $F\left(I - F^+F\right) = F - FF^+F = 0$. The consistency condition Eq. (1.10) has been conjectured to be equivalent to the BCJ amplitude identities [35], and we prove this conjecture below. Note, however, that because the existence of color-dual numerators has been proven at tree level [39, 40], we know that the consistency condition is satisfied thanks to the "if and only if" logic. Our proof that the consistency condition Eq. (1.10) is equivalent to the BCJ amplitude identities gives an alternative proof of the existence of color dual numerators, one that will extend to the residue numerators defined in Section 1.2.

1.1.2 Equivalence of the BCJ Identities and the Consistency Condition

Our goal is to show that the equation $FF^+A = A$ is the same as the BCJ amplitude identities, which we shall write formally as $\mathcal{S}A = 0$, where $\mathcal{S}$ is a matrix that forms the linear combination of amplitudes appearing in the BCJ identities. Since we chose the A in FF^+A to be a vector of amplitudes in the Kleiss-Kuijf basis, we have to be care-

ful to choose the matrix $\mathcal{S}$ so that it acts on the same vector of Kleiss-Kuijf amplitudes to produce the BCJ amplitude identities. One particularly nice choice for $\mathcal{S}$ that accomplishes this is a matrix representation of the momentum kernel [40–43], given explicitly by $\mathcal{S}_{\tau\omega} = \mathcal{S}\left[\tau\left(2\right), \tau\left(3\right), \ldots, \tau\left(n-1\right) | \omega\left(2\right), \omega\left(3\right), \ldots, \omega\left(n-1\right)\right]$. This matrix has polynomials of Mandelstam variables as entries, and many of its properties are discussed in Ref. [40].

There are two assumptions that will go into our proof. These assumptions are both widely believed and have survived extensive low-point checks, but remain unproven for general n. The first is that the basis of $(n-3)!$ amplitudes appears to be minimal [44–46]. In other words, there are not further relations that will reduce the number of independent amplitudes below the $(n-3)!$ BCJ-independent amplitudes. The second assumption is that Eq. (1.9) only has solutions for A in the basis spanned by the $(n-3)!$ BCJ-independent amplitudes. It is known that the span of these amplitudes is sufficient for a wide class of theories, including both Yang-Mills theories and the colored trivalent scalar theories discussed in [45]. Our assumption is that this sufficiency holds for any theory that possesses color-kinematic duality, and so this sufficiency also holds for any theories for which F can be defined.

We demonstrate that the two equations $FF^{+}A = A$ and $\mathcal{S}A = 0$ impose the same constraints on the elements of A using a simple dimension counting argument. As mentioned above, the BCJ amplitude identities are known to reduce the $(n-2)!$ Kleiss-Kuijf independent amplitudes to $(n-3)!$ independent amplitudes [6, 44, 46], i.e. the rank of $\mathcal{S}$ is $(n-2)! - (n-3)!$. Our two assumptions imply that for generic momenta, the solution space of Eq. (1.9) necessarily has dimension $(n-3)!$ i.e. $\text{rank}\,F = (n-3)!$. But $\text{rank}\left(FF^{+}\right) = \text{rank}\left(F\right)$ by a theorem of linear algebra [38], so the image of FF^{+} has dimension $(n-3)!$. Then the solution space of $FF^{+}A = A$ has dimension at most $(n-3)!$, since it must be contained in the image of FF^{+}. But then by the assumption that the $(n-3)!$ basis is minimal, the solution space of $FF^{+}A = A$ must have dimension equal to $(n-3)!$. The basis vectors of this space must therefore be BCJ basis amplitudes, up to at most a linear transformation. Therefore the operators FF^{+} and $\mathcal{S} + I$ must be equal up to this linear transformation, proving the result. Explicitly, we write $Q\left(FF^{+} - I\right) = \mathcal{S}$ for some

$Q \in GL\left((n-3)!\right)$ embedded in an $(n-2)! \times (n-2)!$ matrix with all other entries zero, and I the $(n-2)! \times (n-2)!$ identity matrix.

This may be understood geometrically. If the BCJ amplitudes form the true minimal basis of color-ordered amplitudes, then the larger space spanned by Kleiss-Kuijf amplitudes must be constrained to the smaller space spanned by the BCJ amplitudes. We illustrate this for the four-point case in Figure 1.2. In this simplest example, there are $(4-2)! = 2$ amplitudes in the Kleiss-Kuijf basis, and $(4-3)! = 1$ amplitude in the BCJ basis. If the Kleiss-Kuijf basis were minimal, then the vector

$$A = (A\left(1,2,3,4\right), A\left(1,3,2,4\right)) \tag{1.12}$$

in the plane[2] $\mathbb{C}^2$ would fully determine all partial amplitudes. The four-point BCJ basis linearly relates the two elements of the vector A by

$$A\left(1,3,2,4\right) = \frac{u}{s}A\left(1,2,3,4\right) \text{ or } A\left(1,2,3,4\right) = \frac{s}{u}A\left(1,3,2,4\right) \tag{1.13}$$

where either equation is valid, and amounts to choosing either $A\left(1,2,3,4\right)$ or $A\left(1,3,2,4\right)$ as a basis amplitude. This is equivalent to projecting to one axis or the other in Figure 1.2. Since the Kleiss-Kuijf vectors A describe physically valid partial amplitudes, they cannot lie at an arbitrary point in the plane, but must instead lie on the *BCJ line*. For the four-point case, both operators FF^+ and $\mathcal{S} + I$ are rank one, and act on the Kleiss-Kuijf vector of amplitudes. This means both operators necessarily map to a point along the BCJ line. The linear transformation $Q \in GL\left((4-3)!\right)$ in this case is just a constant that translates a point along the BCJ line, but such movement does not alter the relation between the amplitudes. The next-highest-point case, $n = 5$, has $(5-2)! = 6$ amplitudes in the Kleiss-Kuijf basis and $(5-3)! = 2$ amplitudes in the BCJ basis; geometrically the $n = 5$ case corresponds to a $\mathbb{C}^6$ hyperplane for the Kleiss-Kuijf basis with all points actually lying on the $\mathbb{C}^2$ plane

---

[2]We say "plane" for $\mathbb{C}^2$ and "line" for $\mathbb{C}$ to highlight the geometry.
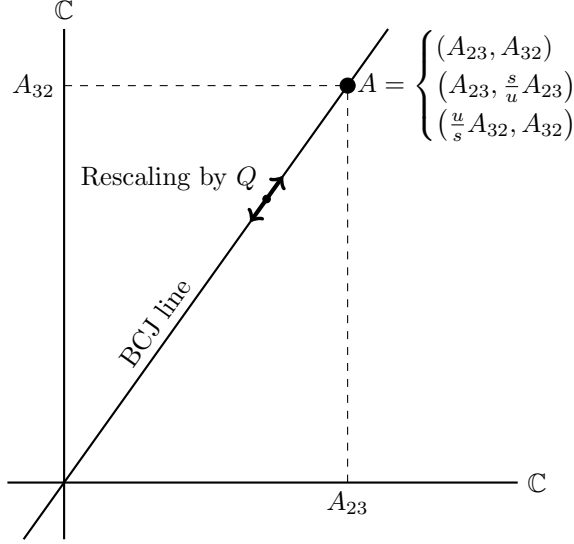
Figure 1.2: Reduction of the Kleiss-Kuijf amplitude basis to the BCJ amplitude basis for $n = 4$. In the figure, $A(1, 2, 3, 4) \equiv A_{23}$ and $A(1, 3, 2, 4) \equiv A_{32}$. Kleiss-Kuijf amplitude vectors must lie on the BCJ line. The "rescaling by Q" arrows depict the $GL(1)$ freedom that translates the point A along the BCJ line.

spanned by the BCJ basis amplitudes. This same line of geometric reasoning supports the rank-counting argument for all n.

1.1.3 RSVW Formula and Residues

As mentioned in the introduction, significant work has been done on the special case of $\mathcal{N} = 4$ super-Yang-Mills. In particular, the aforementioned RSVW formula that gives all tree level partial amplitudes is

$$
\begin{aligned}
A_n(1, 2, \ldots, n) &= \int \frac{d^{2n}\sigma}{\mathrm{vol}\, GL(2)} \frac{1}{(12)(23)\cdots(n1)} \prod_{\alpha=1}^{k} \delta^2\left(C_{\alpha a}\tilde{\lambda}_a\right) \delta^{0|4}\left(C_{\alpha a}\tilde{\eta}_a\right) \\
&\times \int d^2\rho_\alpha \prod_{b=1}^{n} \delta^2\left(\rho_\beta C_{\beta b} - \lambda_b\right),
\end{aligned} \tag{1.14}
$$

where the $C_{\alpha a}$ are $k \times n$ matrices parametrized by σ, as discussed in the Grassmannian formulations of Refs. [47–49], for particles in the R-charge sector given by k. The minors

(12), (23), etc. are minors of $C_{\alpha a}$, and are thus functions of the σ. The delta functions enforce the conditions that the spinor helicity variables λ and $\tilde{\lambda}$ (along with $\tilde{\eta}$) are appropriately orthogonal, and thus that overall supermomentum is conserved.

Notice that both the delta functions and the measure are invariant under permutations of the particle labels. This means we can write

$$A_n\left(1, \tau\left(2\right), \ldots, \tau\left(n-1\right), n\right) = \int \frac{d^{2n}\sigma}{\mathrm{vol}\, GL\left(2\right)} L_\tau \prod_{\alpha=1}^{k} \delta^2\left(C_{\alpha a}\tilde{\lambda}_a\right) \delta^{0|4}\left(C_{\alpha a}\tilde{\eta}_a\right)$$
$$\times \int d^2\rho_\alpha \prod_{b=1}^{n} \delta^2\left(\rho_\beta C_{\beta b} - \lambda_b\right), \tag{1.15}$$

where

$$L_\tau \equiv \frac{1}{\left(1\,\tau\left(2\right)\right)\cdots\left(\tau\left(n-1\right)\,n\right)\left(n\,1\right)}. \tag{1.16}$$

This representation has an important consequence. To understand the action of F on A_τ, we only need to understand how the inverse minor factor L_τ will be affected, since L_τ is the only factor in A_τ that depends on the particle label ordering. We are in particular interested in how the consistency condition $FF^+A = A$ manifests itself in this setting. By the permutation invariance discussed above, $FF^+A = A$ holds provided (in matrix notation)

$$FF^+L = L \tag{1.17}$$

on the support of the delta functions. One goal in the remainder of this section will be to establish this fact.

The proof employs two lemmas. The first lemma is the claim that $FF^+A = A$ and $\mathcal{S}A = 0$ are algebraically equivalent, which was shown in Subsection 1.1.4. The second lemma states that the BCJ amplitude identities descend to the level of residues. Mathematically, this is the statement that $\mathcal{S}A = 0$ implies $\mathcal{S}R_r = 0$ for all RSVW residues R_r (which will be defined below). This was originally noted in Ref. [33]. Because Ref. [33] proves that $\mathcal{S}L = 0$ (in our notation) on the support of the delta functions, the residue consistency condition Eq. (1.17)

11

will follow from these two lemmas. Explicitly, we can rewrite $\mathcal{S}L = 0$ as

$$Q\left(FF^+ - I\right)L = 0. \tag{1.18}$$

Multiplying by Q^{-1} and rearranging gives Eq. (1.17).

1.1.4   Proof of the BCJ Amplitude Identities for RSVW Residues

Our argument proceeds by invoking several equivalent forms of Eq. (1.15) found in Section 3.1 of Ref. [48]. We begin by noting that in supertwistor space, Eq. (1.15) is

$$A_n\left(1, \tau\left(2\right), \ldots, \tau\left(n-1\right), n\right) = \int \frac{d^{2n}\sigma}{\text{vol}\, GL\left(2\right)} L_\tau \prod_{\alpha=1}^{k} \delta^{4|4}\left(C_{\alpha a}\mathcal{W}^{\alpha a}\right), \tag{1.19}$$

with L_τ still defined as in Eq. (1.16). Here the $C_{\alpha a}$ are functions of σ as given by the Veronese map discussed in Ref. [48]. This can be cleverly rewritten as

$$A_n\left(1, \tau\left(2\right), \ldots, \tau\left(n-1\right), n\right) = \int \frac{d^{k \times n}C_{\alpha a}}{\text{vol}\, GL\left(k\right)} G_\tau\left(C\right) \prod_{\alpha=1}^{k} \delta^{4|4}\left(C_{\alpha a}\mathcal{W}^{\alpha a}\right) \tag{1.20}$$

where

$$G_\tau\left(C\right) = \int \frac{d^{2n}\sigma\, d^{k \times k}M}{\text{vol}\, GL\left(2\right)} L_\tau \prod_{\alpha=1}^{k} \prod_{a=1}^{n} \delta\left(C_{\alpha a} - M_\alpha^\beta C_{\beta a}\right), \tag{1.21}$$

with M_α^β a set of $k \times k$ matrix integration variables. This form makes the integral look more like the Grassmannian formulation of Ref. [47], but more importantly for our purposes, it allows us to recast it into the form of a contour integral. The idea is that there are $(k-2)(n-k-2)$ delta functions beyond those that fix the kinematics.[3] These extra delta functions are factors of $G_\tau\left(C\right)$. Following the discussions in Refs. [22, 48, 50], we can reinterpret integrating against one of these delta functions as instead integrating around a contour that encloses a pole located at the argument of the delta function. This is known as

---

[3]In other words, delta functions other than $\prod_{\alpha=1}^{k} \delta^{4|4}\left(C_{\alpha a}\mathcal{W}^{\alpha a}\right)$.

treating the delta functions *holomorphically*. Therefore, using the notation of Ref. [48], the integral can be recast as

$$A_n \left(1, \tau \left(2\right), \ldots, \tau \left(n - 1\right), n\right) = \int_{S_1 = \cdots = S_m = 0} \frac{d^{k \times n} C_{\alpha a}}{\text{vol}\, GL\left(k\right)} \frac{H_\tau \left(C\right)}{S_1 \left(C\right) \cdots S_m \left(C\right)}. \qquad (1.22)$$

There are $m = \left(k - 2\right)\left(n - k - 2\right)$ functions S, called Veronese operators, and these contain the locations of the poles. As the notation suggests, H_τ contains the (integrated) minor factor L_τ, since L_τ was part of G_τ. Therefore H_τ depends on τ, while none of the Veronese operators do.

A concrete example is the $n = 6$, $k = 3$ Yang-Mills amplitude. In this case, there is $m = 1$ function $S\left(C\right)$ that determines the correct contour in the complex plane. Gauge fixing in $GL\left(3\right)$ and overall momentum conservation results in only one remaining complex integration variable c, and so the calculation reduces to a standard contour integral in $\mathbb{C}$. It may be shown in this $n = 6$, $k = 3$ case, that $S\left(c\right)$ is quartic for generic momenta [22, 48]. The correct contour for calculating the amplitude must enclose the four roots c_1, c_2, c_3, and c_4 of $S\left(c\right)$, as indicated in Figure 1.3. The remaining three points $\tilde{c}_1$, $\tilde{c}_2$, $\tilde{c}_3$ in the c-plane correspond to the poles of the function $H\left(c\right)$.

For general n and k, we can then use the global residue theorem[4] to write the amplitude as a sum of residues (where we have absorbed factors of $2\pi i$):

$$A_n \left(1, \tau \left(2\right), \ldots, \tau \left(n - 1\right), n\right) = \sum_r R_r \left(1, \tau \left(2\right), \ldots, \tau \left(n - 1\right), n\right). \qquad (1.23)$$

Letting C_r denote the location of residue R_r[5], the residues have the general form (with the

---

[4]This is necessary because we are dealing with a multidimensional contour integral. See [47] for details.

[5]We cannot simply say the C_r are the zeros of the Veronese operators, due to issues at high multiplicity arising from so-called composite residues. A more complete discussions of these issues can be found in [47, 48].
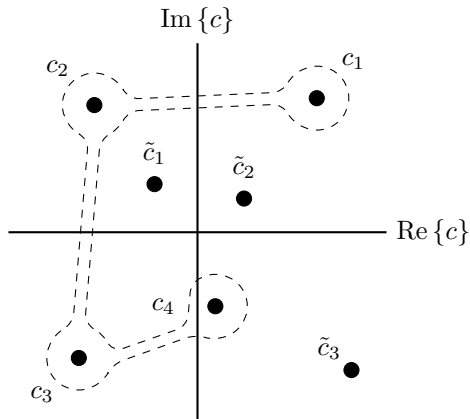
Figure 1.3: The integral for the $n = 6$, $k = 3$ Yang-Mills amplitude has one integration variable not fixed by gauge choice or momentum conservation, and so may be calculated as a standard contour integral of a complex variable $c \in \mathbb{C}$. The four poles c_1, c_2, c_3, and c_4 correspond to the four roots of $S(c)$, and the three remaining poles $\tilde{c}_1$, $\tilde{c}_2$, and $\tilde{c}_3$ match the poles of the function $H(c)$. The placement of the poles is schematic; their positions depend on the external momenta.

τ-dependence explicit)

$$R_{r,\tau} = \frac{H_\tau(C_r)}{T(C_r)}. \tag{1.24}$$

Here $T(C)$ is a function consisting of the product of the nonvanishing Veronese operators and containing the gauge fixing. Notice that T is independent of τ.

We can now apply the matrix $\mathcal{S}$ to each residue R_r. Doing so, we have

$$\mathcal{S}_{\tau\omega} R_{r,\omega} = \frac{1}{T(C_r)} \mathcal{S}_{\tau\omega} H_\omega(C_r). \tag{1.25}$$

Remembering that H_τ is precisely G_τ with some integration variables fixed by delta functions and the remaining delta functions stripped off, we see that $H_\tau(C_r)$ is proportional to L_τ evaluated on the support of all of the delta functions. But, as proved in Ref. [33], $\mathcal{S}L_\tau = 0$ on the support of the delta functions in the RSVW formula. Therefore $\mathcal{S}_{\tau\omega} H_\omega(C_r) = 0$, and so $\mathcal{S}$ annihilates the residues R_r individually, exactly as we wished to show.

14

1.1.5 Gravity

We are ultimately interested in the application of the techniques developed so far to analyze gravity. We therefore discuss how this material can be generalized to gravity.

The first concept is the double-copy formula. This states that tree level gravitational amplitudes can be written as

$$\mathcal{M}_n = \left(\frac{\kappa}{2}\right)^{n-2} \sum_{i=1}^{(2n-5)!!} \frac{n_i \tilde{n}_i}{D_i}, \tag{1.26}$$

where the n_i and $\tilde{n}_i$ are both sets of kinematic numerators, possibly from different Yang-Mills theories (such as with varying amounts of supersymmetry), at least one set of which is color-dual. The gravitational coupling constant is κ. This formula was first proposed in Ref. [9], and was proven in Ref. [17] using color-kinematic duality and the BCFW recursion relations. Our ultimate goal is to derive an analogous formula valid at the level of residues.

The second concept defines exactly what the residues look like on the gravitational side. The Cachazo-Geyer formula for gravitational amplitudes was proposed in Ref. [26]:

$$\mathcal{M}_n = \int \frac{d^{2n}\sigma}{\text{vol}\,GL\,(2)} \frac{H_n}{J_n} \prod_{\alpha=1}^{k} \delta^2 \left(C_{\alpha a}\tilde{\lambda}_a\right) \delta^{0|8} \left(C_{\alpha a}\tilde{\eta}_a\right) \int d^2\rho_\alpha \prod_{b=1}^{n} \delta^2 \left(\rho_\beta C_{\beta b} - \lambda_b\right), \tag{1.27}$$

which looks exactly the same as the RSVW formula Eq. (1.14) except for the four extra supersymmetries and the replacement of the inverse minor factor with $\frac{H_n}{J_n}$. The exact definition of $\frac{H_n}{J_n}$ is not important for our purposes, but it is also a function of the minors of $C_{\alpha a}$. All of the discussion involving writing the RSVW formula as a contour integral applies to this formula as well. Indeed, since the delta functions in both formulas are the same, the residues occur at the exact same points, and the same contours may be used. This is crucial, as it allows us to put RSVW residues in one-to-one correspondence with the residues of this formula. Explicitly, we write

$$\mathcal{M}_n = \sum_r R_r^G, \tag{1.28}$$

with the index r matching the RSVW residue index r.

The formula Eq. (1.27) was conjectured in Ref. [26]; its proof depended on the resolution of a conjecture called the KLT orthogonality conjecture. This conjecture was proven in Ref. [51]. In addition to putting Eq. (1.27) on a solid foundation, it will play an important role in proving the residue analog of Eq. (1.26). We will give a formal statement of the conjecture at that time.

1.2   Residue Numerators

The lemmas proved in the previous section have important implications. In particular Eq. 1.17, the consistency condition for residues, guarantees the existence of what we have christened *residue numerators*, defined by

$$N_r \equiv F^+ R_r + \left(I - F^+ F \right) v,\tag{1.29}$$

again for arbitrary v. These numerators obey all of the properties of full amplitude numerators, essentially by definition. In particular, $R_r = F N_r$.

Recall that the gravity amplitude $\mathcal{M}_n$ can be written in terms of Yang-Mills partial amplitudes using the KLT relations, which in our notation take the form [35]

$$\mathcal{M}_n = \left(\frac{\kappa}{2} \right)^{n-2} A^T F^+ \tilde{A}.\tag{1.30}$$

A and $\tilde{A}$ are vectors of partial amplitudes associated with two (possibly different) Yang-Mills theories. We can now address our central question: if we combine two $\mathcal{N} = 4$ super-Yang-Mills theories to get $\mathcal{N} = 8$ supergravity, can we replace everything by residues and still get an analogous result? In other words, we conjecture

$$R_r^G \stackrel{?}{=} \left(\frac{\kappa}{2} \right)^{n-2} R_r^T F^+ \tilde{R}_r.\tag{1.31}$$

To test this hypothesis, we substitute the expressions for $\mathcal{M}_n$ and A_n as sums of residues into the KLT relations Eq. (1.30). This yields

$$
\begin{aligned}
\sum_r R_r^G &= \sum_{r,\tilde{r}} R_r^T F^+ \tilde{R}_{\tilde{r}} \\
&= \sum_r R_r^T F^+ \tilde{R}_r + \sum_{r \neq \tilde{r}} R_r^T F^+ \tilde{R}_{\tilde{r}},
\end{aligned} \tag{1.32}
$$

where we have separated out the cross terms in the second line. If our conjecture is true, it must imply

$$
\sum_{r \neq \tilde{r}} R_r^T F^+ \tilde{R}_{\tilde{r}} = 0. \tag{1.33}
$$

This is the aforementioned KLT orthogonality conjecture, and it was recently proved in Ref. [51].

Now we have

$$
\sum_r R_r^G = \left(\frac{\kappa}{2}\right)^{n-2} \sum_r R_r^T F^+ \tilde{R}_r. \tag{1.34}
$$

However, this is insufficient to show the two sides are equal term-by-term. To show this stronger statement, we need to go back to the derivation of Eq. (1.27) found in Ref. [26]. In particular, the residues R_r^G and R_r are dependent only on the integrands of the RSVW and Cachazo-Geyer formulas. After inserting two copies of the RSVW formula into the KLT relations, the use of KLT orthogonality reduces the integral to an integral over a single set of the RSVW variables (rather than one set for A and one for $\tilde{A}$). Therefore the integrands, not just the integrals, are in fact equal. Since the integrands are evaluated at exactly the same set of points in determining the residues, this implies that Eq. (1.34) holds term-by-term, proving $R_r^G = (\kappa/2)^{n-2} R_r^T F^+ \tilde{R}_r$.

We can now recast this in terms of residue numerators. Specifically, we can write

$$
\begin{aligned}
R_r^G &= \left(\frac{\kappa}{2}\right)^{n-2} R_r^T F^+ \tilde{R}_r \\
&= \left(\frac{\kappa}{2}\right)^{n-2} R_r^T F^+ F F^+ \tilde{R}_r
\end{aligned}
$$

17

$$= \left(\frac{\kappa}{2}\right)^{n-2} \left(\left(F^+\right)^T R_r\right)^T F F^+ \tilde{R}_r$$
$$= \left(\frac{\kappa}{2}\right)^{n-2} N_r^T F \tilde{N}_r, \tag{1.35}$$

where in going to the second line we have used the fact that the residues obey the consistency condition $\tilde{R}_r = F F^+ \tilde{R}_r$, and in the last line we have used the fact that for F symmetric, $\left(F^+\right)^T$ is also a generalized inverse[6]. But the last line is precisely the double-copy formula with ordinary kinematic numerators replaced by residue numerators, and the gravitational amplitude replaced by the corresponding gravitational residue!

Notice that this argument holds in reverse. Assuming the double-copy formula for residue numerators, we can reverse the logic in the equations leading to Eq. (1.35) and derive the KLT relations for RSVW residues. The course of this argument uses "residue numerator orthogonality"

$$\sum_{\tilde{r} \neq r} N_r^T F \tilde{N}_{\tilde{r}} = 0, \tag{1.36}$$

which follows from the residue numerator double-copy formula, to prove KLT orthogonality. As a simple consistency check, we have numerically verified this result at six points ($n = 6$ is the smallest n for which nontrivial residues occur in the connected prescription[22]).

This equivalency between the KLT relations and the double-copy formula harks back to the equivalency at the amplitude level [35], and we expect it will be important for similar reasons. In particular, the double-copy formulation has two major advantages over the KLT relations. First, the double-copy formula is much cleaner, making the "gravity is the square of gauge theory" adage more transparent. Second, the KLT relations are restricted to tree level, while the double-copy formula is conjectured to apply to all loop orders. This suggests that the residue numerators, while only now defined at tree level, might have loop-level analogs.

---

[6]Since $\left(F^+\right)^T$ may be different than F^+, the resulting numerators may differ from those generated by F^+ by a generalized gauge transformation, but this is irrelevant for out purposes.

We have now shown that not only do the BCJ amplitude identities and the KLT relations descend from the full amplitude to their residues, but so do the concepts of kinematic numerators and the double-copy formula. In the same vein, we emphasize that it is equivalent to use residue numerators as a starting point, and derive the residue relations, much as the original BCJ amplitude identities were originally derived from numerators.

1.3   Summary of Tree-Level Results

We have introduced residue numerators. These objects give a BCJ decomposition of RSVW residues. They have the property that under replacement of a color factor by a residue numerator we obtain gravity residues, and they obey an orthogonality condition equivalent to the KLT orthogonality condition [30].

To do this, we proved two lemmas. First we proved that the consistency condition of the generalized inverse is equivalent to the BCJ amplitude identities by counting the rank of the matrices F and FF^+, largely in the spirit of the arguments suggested in Ref. [35]. By replacing amplitudes with RSVW residues, $A \to R_r$, and $N \to N_r$ in expressions for amplitudes, our proof implies that RSVW residues obey BCJ amplitude identities if and only if there exist decompositions of RSVW residues into residue numerators. It is possible to explicitly construct such residue numerator solutions [32, 52], so we only needed to verify that RSVW residues obey amplitude relations in general. We did this by demonstrating that RSVW residues contain permutation-dependent factors which vanish in the BCJ amplitude relation, as discussed in Ref. [33]. This was the second lemma that we proved.

From these two lemmas, our main result followed. We showed that the new proof of KLT orthogonality for RSVW residues implies a residue numerator orthogonality condition. Conversely, from the *ab initio* assumption that both RSVW and gravity residues could be decomposed into residue numerators, we arrived at a residue numerator orthogonality condition that implies the KLT orthogonality condition.

Most research building in the same general direction as the subjects discussed in this

chapter now works within the CHY paradigm [32, 51]. That said, we expect that residue numerators will offer insight into a variety of topics that are currently phrased in terms of amplitudes. At tree-level, the interplay of combinatorics and linear algebra that go into constructing F are suggestive of the positive Grassmannian [49] and amplituhedron [53, 54]. The numerator Jacobi relations may be relevant to lifting the theory described by the amplituhedron out of the planar limit, since numerator Jacobi identities relate planar and nonplanar diagrams. (See, for example, Ref. [10], as well as the later chapters of this dissertation.) It would also be interesting to explore the role of residue numerators in theories like ABJM, in which even the tree-level connection between color-kinematic duality and BCJ amplitude identities is less well understood [55, 56].

Numerator decompositions have proven to be a powerful way to evaluate loop-level contributions to amplitudes as well. The decomposition of residues into numerators performed here may offer insight into improved ways of constructing loop integrands. We expect that reexamining loop-level amplitudes where known color-dual numerators are available will offer insight into how residue numerators might be applied in loop calculations. There are good starting points in the literature pursuing such systematization at tree level [57], at loop level with color-dual numerators [14], and at higher-loop level without color-dual numerators [58, 59]. Recent work [8, 60] also explicitly illustrates a color-dual numerator construction for pure Yang-Mills at one loop and two loops, providing nontrivial evidence that numerator representations extend to nonsupersymmetric theories. We expect that residue numerators might be applicable to theories with less supersymmetry.

That said, the extension of the RSVW formula (and more recently the scattering equations) to loop level has been fraught with difficulties [61, 62]. It has been difficult to understand generalized gauge invariance at loop level [35], as the invariance applies at the level of the integrand, and must therefore be extended to include terms that vanish upon integration over loop momenta. Some progress has been made using ambitwistor string theory and the CHY formulation [61, 63–65], but many problems remain. We hope the algebraic simplicity of residue numerators will help these barriers be overcome.

Finally, the existence of residue numerators reemphasizes the role of numerators in color-kinematic duality. In the same way that color-kinematic duality underlies the BCJ amplitude identities, we have demonstrated that these residue numerators imply KLT and BCJ relations as well as the KLT orthogonality relations between RSVW residues.

CHAPTER 2

Singularity Structure of Loop Amplitudes in $\mathcal{N} = 4$ Super-Yang-Mills: Planar Background

We now turn to loop-level amplitudes. Since all particles of the theory will run in the loops, we must now choose a specific theory to focus on. The subject of the remainder of this dissertation will be nonplanar $\mathcal{N} = 4$ super-Yang-Mills (SYM) theory. This is based on work done with Zvi Bern, Enrico Herrmann, James Stankowicz, and Jaroslav Trnka, and includes material from Refs. [2, 3].

Recent years have seen enormous advances in our understanding of scattering amplitudes in $\mathcal{N} = 4$ super-Yang-Mills theory. Most progress has been made in the planar sector, with many calculations of new amplitudes with large numbers of loops and legs both at the integrand and integrated levels now available. Discoveries of new structures and symmetries have led to the development of deep theoretical frameworks which greatly aid new computations while also connecting to new areas of mathematics.

In the planar theory there are a number of recently discovered structures, including dual conformal symmetry [66–68], Yangian symmetry [69], integrability [70, 71], a dual interpretation in terms of Wilson loops [72–77], amplitudes at finite coupling using OPE [78–80], hexagon bootstrap [81–83], and symbols and cluster polylogarithmics [84–87], as well as a variety of other structures. More recently, scattering amplitudes were reformulated using on-shell diagrams and the positive Grassmannian [47–50, 88–90] (see related work in Ref. [91–94]). This reformulation fits nicely into the geometric concept of the amplituhedron [53] (see also Refs. [54, 95–100]), and makes connections to active areas of research in algebraic geometry and combinatorics (see e.g. Refs. [101–106]).

In the remainder of this dissertation, we investigate how some of these properties carry over to the nonplanar sector. A basic difficulty in the nonplanar sector is that it is currently unclear how to define a unique integrand, largely due to the lack of global variables with which to describe a nonplanar integrand. Such ambiguities greatly obscure the desired structures that might be hiding in the amplitude. In addition, we lose Yangian symmetry and presumably any associated integrability constraints, as well as the connection between amplitudes and Wilson loops. Naively we also lose the ability to construct amplitudes using on-shell diagrams, the positive Grassmannian, and the amplituhedron.

Nevertheless, one might suspect that many features of the planar theory can be extended to the full nonplanar theory. As discussed in 1, the conjectured duality between color and kinematics [6, 107] suggests that nonplanar integrands are obtainable directly from planar ones, and hence properties of the nonplanar theory should be related to properties of the planar sector. However, it is not *a priori* obvious which features can be carried over.

The dual formulation of planar $\mathcal{N} = 4$ super-Yang-Mills scattering amplitudes using on-shell diagrams and the positive Grassmannian makes manifest that the integrand has only logarithmic singularities, and can be written in a $d$log *form*. Furthermore, the integrand has no poles at infinity as a consequence of dual conformal symmetry. Arkani-Hamed, Bourjaily, Cachazo, and Trnka conjectured the same singularity properties hold to all loop orders for all maximally helicity violating (MHV) amplitudes in the nonplanar sector as well [108]. Refs. [2, 3] provided significant evidence in favor of this conjecture. In Ref. [2], the conjecture this was confirmed explicitly for the full three-loop four-point integrand of $\mathcal{N} = 4$ SYM by finding a basis of diagram integrands where each term manifests these properties. Studies of this amplitude, along with examination of some properties of four- and five-loop amplitudes, led to the conjecture that, to all loop orders, the singularity constraints give us the key analytic information contained in dual conformal symmetry. Ref. [3] pursued this line of reasoning further and showed that in the planar case, dual conformal invariance is equivalent to integrands with (i) no poles at infinity and (ii) special values of leading singularities (maximal codimension residues). In the MHV sector, property (ii)

and superconformal invariance imply that leading singularities are necessarily equal to ± 1 times the usual Parke-Taylor factor [109, 110]. Moreover, the existence of a dual formulation using on-shell diagrams and the positive Grassmannian implies that (iii) integrands have only logarithmic singularities. While (i) and (iii) can be directly conjectured for nonplanar amplitudes, property (ii) must be slightly modified. As proven in Ref. [111] for both planar and nonplanar cases, the leading singularities are not just individual Parke-Taylor factors, but more generally are linear combinations of Parke-Taylor factors with different orderings and with coefficients ± 1. This set of three conditions was first conjectured in [108], and Ref. [3] gave a more detailed argument as to why the content of dual conformal symmetry is exhausted by this set of conditions. It also provided direct nontrivial evidence showing they hold for the two-loop five-point amplitude and the three-loop four-point amplitude, building on the explicit analysis of Ref. [2].

All of these results provide evidence for the amplituhedron concept [53] beyond the planar limit. The amplituhedron is defined in momentum twistor variables, which intrinsically require cyclic ordering of amplitudes, making direct nonplanar tests in these variables impossible. However, we can test specific implications even for nonplanar amplitudes. In Ref. [97], it was argued that the existence of the "dual" amplituhedron implies certain positivity conditions of amplitude integrands. Indeed, these conditions were proven analytically for some simple cases and numerically in a large number of examples. (Interestingly, these conditions appear to hold even post-integration [97, 112]). The dual amplituhedron can be interpreted as a geometric region of which the amplitude is literally a volume, in contrast to the original definition where the amplitude is a differential form with logarithmic singularities on the boundaries of the amplituhedron space. This implies a very interesting property when the integrand is combined into a single rational function: its numerator represents a codimension one surface which lies outside the dual amplituhedron space. The surface is simply described as a polynomial in momentum twistor variables and therefore can be fully determined by the zeros of the polynomial, which correspond to points violating positivity conditions defining the amplituhedron. A nontrivial statement implied by the amplituhedron geometry is that

all of these zeros can be interpreted as cuts where the amplitude vanishes.

This leads to a concrete feature that can be tested even in a diagrammatic representation of a nonplanar amplitude: *The integrand should be fixed entirely by homogeneous conditions, up to an overall normalization.* Concretely, by "homogeneous conditions" we mean the conditions of no poles at infinity, only logarithmic singularities, and unitarity cuts that vanish. That is, in the unitarity method, the only required cut equations are the ones where one side of the equation is zero, as opposed to a nontrivial kinematic function of the external momenta. These zeros occur either because the amplitude vanishes on a particular branch of the cut solutions or because the cut is spurious[1]. This conjecture has exciting implications, because this feature is closely related to the underlying geometry in the planar sector, suggesting that the nonplanar contributions to amplitudes admit a similar structure.

This chapter will focus on the background material to this work, summarizing properties connected to the amplituhedron picture of amplitudes in planar $\mathcal{N} = 4$ SYM. The following chapter 3 will discuss explicit results for nonplanar amplitudes, showing in various examples that the consequences of dual conformal invariance and the logarithmic singularity condition do carry over to the nonplanar sector. It will also give evidence for a geometric interpretation of the amplitude by showing that the coefficients in the diagrammatic expansion are determined by zero conditions.

2.1   Dual Picture for Planar Integrands

In this section we summarize known properties of planar amplitudes in $\mathcal{N} = 4$ SYM theory that we wish to carry beyond the planar limit to amplitudes of the full theory. We emphasize those features associated with the amplituhedron construction. In the planar case, we strip the amplitude of color factors. Later when we deal with the nonplanar case, we restore them.

The classic representation of scattering amplitudes uses Feynman diagrams. At loop level

---

[1]A spurious cut is one that exposes a nonphysical singularity, i.e. a singularity that is not present in the full amplitude.

the diagrams can be expressed in terms of scalar and tensor integrals. We can then write the amplitude as[2]

$$\mathcal{M} = \sum_j d_j \int d\mathcal{I}^j \,, \tag{2.1}$$

where the sum is over a set of basis integrands $d\mathcal{I}^j$, and d_j are functions of the momenta of external particles, hereafter called kinematic functions. In general the integrations should be performed in $D = 4 - 2\epsilon$ dimensions as a means for regulating both infrared and ultraviolet divergences. While the integrand can contain pieces that differ between four dimensions and D dimensions, in this dissertation we ignore any potential contributions proportional to (-2ϵ) components of loop momenta. At four points we do not expect any such contribution through at least six loops [113], but they can enter at lower loop orders as the number of legs increases [114]. We will not deal with such contributions in this paper, but we expect that they can be treated systematically as corrections to any uncovered four-dimensional structure.

In $\mathcal{N} = 4$ SYM we can split off an MHV prefactor, including the supermomentum-conserving delta function $\delta^8(Q)$, from all d_j,

$$\mathrm{PT}(1234\cdots n) = \frac{\delta^8(Q)}{\langle 12\rangle\langle 23\rangle\langle 34\rangle\cdots\langle n1\rangle} \,, \tag{2.2}$$

which is called a *Parke-Taylor factor* [109, 110, 115]. Usually, we describe the $d\mathcal{I}^j$ in terms of local integrals that share the same Feynman propagators as corresponding Feynman diagrams. However, in the planar sector of the amplitude we do not need to rely on those diagrams. Instead we can choose *dual coordinates* $k_i = x_i - x_{i-1}$ to encode external kinematics, as well as analogously defined y_j for different loop momenta. The variables are associated with the faces of each diagram, are globally defined for all diagrams, and allow us to define a unique integrand by appropriately symmetrizing over the faces [90]. With these variables,

---

[2]In general we drop overall factors of $1/(2\pi)^D$ and couplings from the amplitude, since these play no role in our discussion.

we can sum all diagrams under one integration symbol and write an L-loop amplitude as

$$\mathcal{M} \sim \int d\mathcal{I}(x_i, y_j) = \int d^4y_1 \, d^4y_2 \ldots d^4y_L \, \mathcal{I}(x_i, y_j), \qquad (2.3)$$

where $d\mathcal{I}$ is the integrand form and $\mathcal{I}$ is the unique *integrand* of the scattering amplitude. The integrand form $d\mathcal{I}$ for the n-point amplitude is a unique rational form with many extraordinary properties that we will review in this chapter. Particularly effective ways of constructing the integrand are unitarity cut methods [116–118] or BCFW recursion relations [5, 90].

2.2 Dual Conformal Symmetry

A key property of $\mathcal{N} = 4$ SYM planar amplitudes is that they possess *dual conformal symmetry* [66–68]. This symmetry acts like ordinary conformal symmetry on the dual variables x_i and y_j mentioned above. This can be supersymmetrically extended to a dual *super*conformal symmetry, and closes with the ordinary superconformal symmetry into the infinite-dimensional Yangian symmetry [69]. This is a symmetry of tree-level amplitudes, and at loop level is a symmetry of quantities such as the integrand $d\mathcal{I}$ and IR safe quantities like ratio functions [68].

We are interested in understanding the implications of dual conformal symmetry on the analytic structure of the amplitude. Good variables for doing so are the momentum twistor variables Z_i, introduced in Ref. [119]. These are points in complex projective space $\mathbb{CP}^3$ and are related to the spinor helicity variables $\lambda_i \equiv |i\rangle$, $\widetilde{\lambda}_i \equiv |i]$ via

$$Z_i = \begin{pmatrix} \lambda_i \\ \mu_i \end{pmatrix} \qquad \text{where} \quad \mu_i^{\dot{a}} = x_i^{a\dot{a}} \lambda_{i,a}, \qquad (2.4)$$

where $x_i^{a\dot{a}}$ are the dual variables defined above in spinor indices. The set of n on-shell external momenta are then described by n momentum twistors Z_i, $i = 1, 2, \ldots, n$. Momentum twistors

are unconstrained variables and trivialize momentum conservation, which is a quadratic condition on the λ_i, $\widetilde{\lambda}_i$ spinors. Each off-shell loop momentum ℓ_i is equivalent to a point y_i in dual momentum space, which in turn is represented by a line $Z_{A_i} Z_{B_i}$ in momentum twistor space.

Dual conformal symmetry acts as $SL(4)$ on Z_i, and we can construct invariants from a contraction of four different Z's,

$$\langle ijkl \rangle \equiv \langle Z_i Z_j Z_k Z_l \rangle = \epsilon_{\alpha\beta\rho\sigma} Z_i^\alpha Z_j^\beta Z_k^\rho Z_l^\sigma \, , \tag{2.5}$$

where $\epsilon_{\alpha\beta\rho\sigma}$ is a totally antisymmetric Levi-Civita symbol. Any dual conformal invariant can be written using these four-brackets. The contractions of spinor helicity variables λ can be written as

$$\langle ij \rangle \equiv \epsilon_{ab} \lambda_i^a \lambda_j^b = \epsilon_{\alpha\beta\rho\sigma} Z_i^\alpha Z_j^\beta I^{\rho\sigma} \, , \tag{2.6}$$

where $I^{\rho\sigma}$ is the *infinity twistor* defined in Ref. [119]. An expression containing $I^{\rho\sigma}$ breaks dual conformal symmetry because $I^{\rho\sigma}$ does not transform as a tensor. There is a simple dictionary between momentum space and momentum twistor invariants; we refer the reader to Ref. [119] for details.

A simple example of a dual conformal invariant integrand is the zero-mass box,

$$d\mathcal{I} = \frac{d^4\ell \, (k_1 + k_2)^2 (k_2 + k_3)^2}{\ell^2 (\ell - k_1)^2 (\ell - k_1 - k_2)^2 (\ell + k_4)^2} = \frac{\langle AB \, d^2 A \rangle \langle AB \, d^2 B \rangle \langle 1234 \rangle^2}{\langle AB12 \rangle \langle AB23 \rangle \langle AB34 \rangle \langle AB41 \rangle} \, . \tag{2.7}$$

This represents the full one-loop four-point integrand form in $\mathcal{N} = 4$ SYM. Note that the integrand in Eq. (2.7) is completely projective in all variables Z, and the infinity twistor is absent in this expression. This is true for any dual conformal invariant integrand.

This brings us to a key question: what is the content of dual conformal symmetry for integrands in momentum space? In momentum twistor space the answer is obvious: the infinity twistor $I^{\rho\sigma}$ is absent. Suppose instead the infinity twistor is present. What is the implication in momentum space? The first trivial case is when the prefactor of the integrand

is not chosen properly. For example, if the factor $(k_2 + k_3)^2$ in the numerator of the zero-mass box in Eq. (2.7) is replaced with, say $(k_1 + k_2)^2$, this will introduce a dependence on I, signaling broken dual conformal invariance. In this case, the only dependence on the infinity twistor is through four-brackets $\langle ijI \rangle$ involving only external variables. The presence of these is easily avoided by correctly normalizing $d\mathcal{I}$.

The nontrivial interesting cases occur when the infinity twistor appears in combination with the line $Z_A Z_B$ that represents a loop momentum, e.g. $\langle ABI \rangle$. In this case no prefactor depending only on external kinematics can fix it, and the integrand form necessarily violates dual conformal symmetry. The factor $\langle ABI \rangle$ (or its powers) can appear either in the numerator or the denominator. If it is in the denominator, the integrand has a spurious singularity at $\langle ABI \rangle = 0$. In momentum space this corresponds to sending $\ell \to \infty$. To see this, consider a simple example: the one-loop triangle given by

$$d\mathcal{I} = \frac{d^4\ell \,(k_1 + k_2)^2}{\ell^2(\ell - k_1)^2(\ell - k_1 - k_2)^2} = \frac{\langle AB\, d^2A \rangle \langle AB\, d^2B \rangle \langle 1234 \rangle \langle 23I \rangle}{\langle AB12 \rangle \langle AB23 \rangle \langle AB34 \rangle \langle ABI \rangle} \,. \tag{2.8}$$

If we parametrize the loop momentum as $\ell = \alpha\lambda_1\widetilde{\lambda}_1 + \beta\lambda_2\widetilde{\lambda}_2 + \gamma\lambda_1\widetilde{\lambda}_2 + \delta\lambda_2\widetilde{\lambda}_1$ and send $\gamma \to \infty$ while keeping $\gamma\delta =$ finite, there is a pole which corresponds to $\ell \to \infty$. Bubble integrals even have a double pole at infinity, which corresponds to a double pole $\langle ABI \rangle^2$ when written in momentum twistor space. This sort of behavior is discussed further in Appendix B.

If the $\langle ABI \rangle$ factor is in the numerator, there is a problem with the values of leading singularities. For an L-loop integrand, these are $4L$-dimensional residues that are just rational functions of external kinematics [120]. If the integrand form is dual conformal invariant, all its leading singularities are dual conformal cross ratios (defined in Ref. [121]). A special case is when they are all ± 1, as for the box integrand in Eq. (2.7).

If the integrand has $\langle ABI \rangle$ in the numerator, the values of leading singularities, denoted $LS(\cdot)$, depend on $\langle (AB)^*I \rangle$,

$$LS(d\mathcal{I}) = \langle (AB)^*I \rangle \cdot \mathcal{F}(Z_i, \langle ab \rangle) \,, \tag{2.9}$$

where $(AB)^*$ is the position of the line AB with the leading singularity solution substituted in. The function $\mathcal{F}$ is dual conformal invariant up to some two-brackets of external twistors $\langle ab \rangle$ from normalization. For one particular leading singularity we can choose the normalization of $d\mathcal{I}$ and therefore force $\mathcal{F}$ to cancel $\langle (AB)^* I \rangle$, restoring dual conformal symmetry. However, different leading singularities – of which each integrand has at least two by the residue theorem – are located at different $(AB)^*$, so that it is not possible to simultaneously normalize all leading singularities correctly using only external data. As a result, some of the leading singularities necessarily are not dual conformal invariant. A simple example is the scalar one-loop pentagon,

$$
\begin{aligned}
d\mathcal{I} &= \frac{d^4\ell\, (k_1 + k_2)^2 (k_2 + k_3)^2 (k_3 + k_4)^2}{\ell^2 (\ell - k_1)^2 (\ell - k_1 - k_2)^2 (\ell - k_1 - k_2 - k_3)^2 (\ell + k_5)^2} \\
&= \frac{\langle AB\, d^2 A \rangle \langle AB\, d^2 B \rangle \langle ABI \rangle \langle 1234 \rangle \langle 2345 \rangle \langle 5123 \rangle}{\langle AB12 \rangle \langle AB23 \rangle \langle AB34 \rangle \langle AB45 \rangle \langle AB51 \rangle \langle 23I \rangle}\,,
\end{aligned}
\tag{2.10}
$$

which is not dual conformal invariant, as implied by the appearance of the infinity twistor. The numerator of this pentagon can be modified to a chiral version studied in Ref. [122], which restores dual conformal symmetry.

Based on these considerations, we can summarize the content of dual conformal symmetry of individual integrands in momentum space in two conditions:

1. There are no poles as $\ell \to \infty$.

2. All leading singularities are dual conformal cross ratios.

Any integrand that satisfies these properties necessarily is dual conformal invariant.

In the context of integrands for MHV amplitudes in planar $\mathcal{N} = 4$ SYM, if we strip off the MHV tree-level amplitude, i.e. the Parke-Taylor factor $\text{PT}(123 \cdots n)$ Eq. (2.2),

$$
\mathcal{M} = \text{PT}(123 \cdots n) \int d\mathcal{I}\,,
\tag{2.11}
$$

then the integrand $d\mathcal{I}$ is dual conformal invariant satisfying both properties above. There are
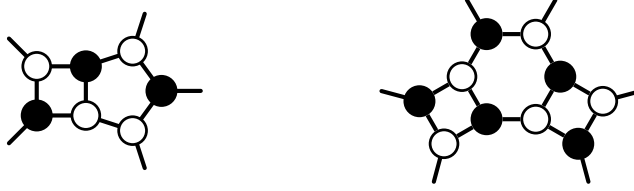
Figure 2.1: Sample on-shell diagrams. The black and white dots respectively represent MHV and $\overline{\text{MHV}}$ three-point amplitudes. Black lines are on-shell particles.

even stronger constraints: superconformal symmetry requires that all leading singularities are holomorphic functions [18] of λ_i's alone. The only functions that are holomorphic, satisfy property 2 above, and have the correct mass dimension and little-group weight are constants. In the normalization conventions adopted here, they are ± 1 or 0. While we do not have a direct formulation of dual conformal symmetry in the nonplanar sector, we shall find analogous analytic structures in the amplitudes for all the examples we study. The role of the Parke-Taylor factor will have to be modified slightly, however.

2.3 On-Shell Diagrams

On-shell diagrams provide another novel representation of the integrand [49]. These are diagrams with black and white vertices connected by lines, as illustrated in Figure 2.1. Black vertices represent MHV three-point amplitudes, white vertices $\overline{\text{MHV}}$ three-point amplitudes, and all lines, both internal and external, represent on-shell particles. There are two indices associated with any on-shell diagram: the number of external legs n and the helicity index k. The k-index is defined as

$$k = \sum_V k_V - P \,, \tag{2.12}$$

where the sum is over all vertices V, k_V is the k-count of the tree-level amplitude in a given vertex, and P is the number of on-shell internal propagators. Black and white vertices have $k_B = 2$ and $k_W = 1$, respectively. As an example, the first diagram in Figure 2.1 has $k = (2+2+2) + (1+1+1+1) - 8 = 2$. This k corresponds to the total number of external negative helicities.

31

The values of the diagrams are computed by integrating the product of tree-level amplitudes A_j over the phase space $d\Omega_i$ of on-shell internal particles for each vertex

$$d\Omega = \prod_i \int d\Omega_i \prod_j A_j \,. \tag{2.13}$$

An on-shell diagram may be interpreted as a specific generalized unitarity cut of an amplitude. In this interpretation, the internal lines of an on-shell diagram represent cut propagators. The on-shell diagram represents a nonvanishing valid cut of the amplitude only if the labels n, k of the on-shell diagram coincide with the same labels of the amplitude.

A very different way to describe and calculate planar on-shell diagrams is as cells of a positive Grassmannian $G_+(k, n)$ [49]. For each diagram we define variables α_j associated with edges or faces of the diagram. Using certain rules [49], we build a $(k \times n)$ matrix C with positive main minors – a cell in the positive Grassmannian. Then the value of the diagram is given by a logarithmic form in the variables of the diagram, multiplied by a delta function which connects the C matrix with external variables (ordinary momenta or momentum twistors),[3]

$$d\Omega = \frac{d\alpha_1}{\alpha_1}\frac{d\alpha_2}{\alpha_2}\frac{d\alpha_3}{\alpha_3}\cdots\frac{d\alpha_m}{\alpha_m}\ \delta(C \cdot Z)\,. \tag{2.14}$$

This is known as a "$d$log form" since all singularities have the structure $d\log\alpha_i \equiv d\alpha_i/\alpha_i$. For further details we refer the reader to Ref. [49], as well as to Appendix B.

Since the planar integrand can be expressed as a sum of these on-shell diagrams via recursion relations [49], all its singularities are also logarithmic. That is, if we approach a singularity of the amplitude for $\alpha_j \to 0$, the integrand develops a pole

$$d\mathcal{I} \xrightarrow{\alpha_j=0} \frac{d\alpha_j}{\alpha_j}\,d\widetilde{\mathcal{I}} \quad \text{where } d\widetilde{\mathcal{I}} \text{ does not depend on } \alpha_j. \tag{2.15}$$

This property is not at all obvious in more traditional diagrammatic representations of

---

[3]We suppress wedge notation for forms throughout: $dxdy \equiv dx \wedge dy$.

scattering amplitudes.

The on-shell diagrams are individually both dual-conformal and Yangian invariant, and therefore are good building blocks that make both symmetries manifest. On the other hand, rewriting the variables α_j in terms of momenta results in spurious poles which only cancel in the sum over all contributions, so this sort of representation obscures locality.

While Eq. (2.15) holds for all planar $\mathcal{N} = 4$ SYM integrands for all helicities, in general the variables α_j are variables of on-shell diagrams that are nontrivially related to the loop and external variables through the delta function $\delta(C \cdot Z)$. For MHV, NMHV (next-to-MHV) and N^{2}MHV (next-to-next-to-MHV) amplitudes, this change of variables implies that the integrand also has logarithmic singularities in momentum space. But for N^{m}MHV amplitudes with $m > 2$, fermionic Grassmann variables enter in the change of variables, so the integrand is no longer manifestly a $d$log form in momentum variables. In this dissertation we only deal with the case of MHV amplitudes, so that the $d$log structure is clearly visible in momentum space. As conjectured in Ref. [108], the same properties hold at the nonplanar level.

2.4 Pure Integrand Diagrams

In the MHV sector, we can check the $d$log property for individual momentum-space planar diagrams with only Feynman propagators. In this check, we consider different cuts[4] of a diagram and probe whether Eq. (2.15) is always valid in momentum space. If so, its integrand form indeed has logarithmic singularities and can in principle be written as a sum of $d$log forms

$$d\mathcal{I}^j = \sum_k b_k \, d\log f_1^{(k)} \, d\log f_2^{(k)} \dots d\log f_{4L}^{(k)} \,, \tag{2.16}$$

where $f_m^{(k)}$ are some functions of external and loop momenta. Constraining these integrands to be dual conformal invariant further enforces that the functions $d\log f_m^{(k)}$ never generate a pole if any of the loop momenta approach infinity, $\ell_i \to \infty$. In addition, for appropriately

---

[4]We use the words "cuts" and "residues" interchangeably throughout.

normalized diagrams the coefficients b_k are all equal to ± 1. A form $d\mathcal{I}^j$ with all these properties is called a *pure integrand form*. A simple example of such a form is the box integrand in Eq. (2.7), which can be expressed explicitly as a single $d$log form [49]. More complicated $d$log integrands have been used to write explicit expressions for one-loop and two-loop planar integrands for all multiplicities [123, 124]. Whenever the amplitude is built from $d\mathcal{I}^j$'s that are individually pure integrands, we will refer to such an expansion as a *pure integrand representation* of the amplitude, and to the set of $d\mathcal{I}^j$'s as a *pure integrand basis*.

We can now expand the n-point planar MHV integrand with Parke-Taylor factors factored out as a sum of pure integrands,

$$d\mathcal{I} = \sum_j a_j \, d\mathcal{I}^j \,. \tag{2.17}$$

The existence of a diagram basis of pure integrands $d\mathcal{I}^j$ with only local poles is a conjecture. There is no guarantee that we can fix the a_j coefficients of this ansatz to match the integrand of the amplitude; it might be necessary to use impure integrands where unwanted singularities cancel between diagrams. Presently, it seems that pure integrands are sufficient up to relatively high loop order. The coefficients must all be $a_j = \pm 1, 0$ based on the requirements of superconformal and dual conformal symmetry. Their precise values are determined by calculating leading singularities or other unitarity cuts, as is detailed in Chapter 3.

We note that the representation in Eq. (2.17) does not make the full Yangian symmetry manifest, as there is a tension between this symmetry and locality. However, the representation does make manifest both dual conformal symmetry and logarithmic singularities.

2.5   Zero Conditions from the Amplituhedron

With on-shell diagrams, scattering amplitudes are built from abstract mathematical objects with no reference to spacetime dynamics. This is an important step towards finding a new description of physics where locality and unitarity are not fundamental, but rather are derived from geometric properties of amplitudes. The on-shell diagrams individually have

this flavor, but the particular sum that gives the amplitude is dictated by recursion relations that are based on unitarity properties. A procedure that dictates which particular sum of on-shell diagrams gives the amplitude without reference to unitarity would therefore be an improvement on recursion relations. The amplituhedron exactly has this property [53], as it is a self-consistent geometric definition of the planar integrand. Here we will not need the details of this object, just some of its basic properties.

We focus mainly on the fact that a scattering amplitude's integrand is defined as a differential form $d\Omega$ with logarithmic singularities on the boundaries of the amplituhedron space. This space is defined as a certain map of the positive Grassmannian through the matrix of positive (bosonized) external data Z for the tree-level case, and its generalization to loops. A given representation of the amplitude by on-shell diagrams gives a triangulation of this space, but the amplituhedron's definition is independent of any particular triangulation.

The underlying assumptions in this construction are *logarithmic singularities*, in terms of which the form $d\Omega$ is defined, and *dual conformal symmetry*, which is manifest in momentum twistor space and generalizations thereof. All other properties of the integrand, including locality and unitarity, are derived from the amplituhedron geometry. This gives a complete definition of the integrand in a geometric language; yet, as mentioned in Ref. [97], it is desirable to find another formulation that calculates the integrand as a volume of an object rather than as a differential form with special properties. In search of this *dual amplituhedron*, it was conjectured in Ref. [97] and checked in a variety of cases that the integrand $\mathcal{I}$ (without the measure) is positive when evaluated inside the amplituhedron. This is exactly the property we expect to be true for a volume function. If we write $\mathcal{I}$ as a numerator divided by all local poles,

$$\mathcal{I} = \frac{N}{\prod (\text{local poles})}\,, \tag{2.18}$$

then, since N is a polynomial in the loop variables $(AB)_j$ (and for non-MHV cases also in other objects), it must be completely fixed by its zeros (roots). An interesting conjecture is that the zeros of N have two simple interpretations:

- The zeros correspond to forbidden cuts generated by the denominator; geometrically these are points outside the amplituhedron.

- The zeros cancel higher poles in the denominator to ensure that all singularities are logarithmic.

This should be true for all singularities of the integrand, both in external and loop variables. In the context of MHV amplitudes however, only the loop part is nontrivial. As an example, we can write the MHV one-loop integrand in the following way,

$$\mathcal{I} = \frac{N(AB, Z_i)}{\langle AB12 \rangle \langle AB23 \rangle \langle AB34 \rangle \ldots \langle ABn1 \rangle}, \tag{2.19}$$

where $N(AB, Z_i)$ is a degree $n - 4$ polynomial in AB with proper little group weights in Z_i. In this case the denominator generates only logarithmic poles on the cuts, and the numerator N is completely fixed (up to an overall constant) by requiring only that it vanishes on all forbidden cuts. There are two types of forbidden cut solutions for MHV amplitudes:

- *Unphysical cut solutions*: all helicity amplitudes vanish. In the on-shell diagram representation, no on-shell diagram exists.

- *Non-MHV cut solutions:* only MHV amplitudes vanish while other helicity amplitudes can be nonzero. In the on-shell diagram representation, the corresponding on-shell diagram has $k \neq 2$.

A simple example of the first case is the collinear cut $\ell = \alpha k_1$, followed by cutting another propagator $(\ell - k_1 - k_2 - k_3)^2$ of the pentagon integral in Eq. (2.10). In momentum twistor geometry this corresponds to $\langle AB12 \rangle = \langle AB23 \rangle = \langle AB45 \rangle = 0$ (as well as setting a Jacobian to zero) which localizes $Z_A = Z_2$, $Z_B = (123) \cap (45)$. This is an example of an unphysical cut that vanishes for all amplitudes, including MHV. Therefore the numerator N in Eq. (2.19) must vanish for this choice of Z_A, Z_B, and indeed one can verify that it does.

All forbidden cuts correspond to points outside the amplituhedron, and therefore we can think about N as a codimension-one surface outside the amplituhedron. The amplituhedron
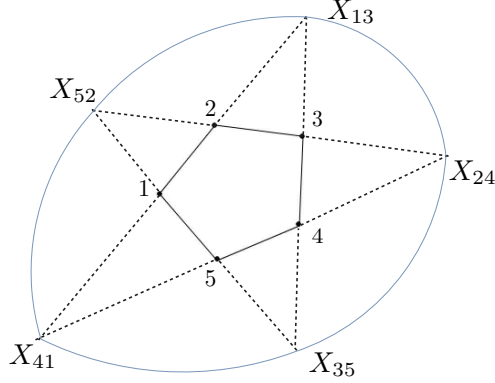
Figure 2.2: A simple amplituhedron example [97]. The area of the pentagon formed by the black solid line is the amplituhedron. The points $X_{i,i+2}$ define zeros of a numerator, so the conic given by the outer (blue) solid lines connecting the points represents the numerator.

and the surface N can only touch on lower dimensional boundaries. This is completely consistent with the picture of the amplitude being the actual volume of the dual amplituhedron, making a clear distinction between the inside and outside of the space.

Consider the simple example discussed in Ref. [97] and shown in Figure 2.2. In this case the amplituhedron is the area of the pentagon. The numerator N is given by the conic that passes through five given points cyclically labeled by the $X_{i,i+2}$. These points correspond to "unphysical" singularities of the form $d\Omega$. Knowing the positions of the $X_{i,i+2}$ fully fixes the numerator N, as there is a unique conic passing through five points. Knowing N fixes the integrand $\mathcal{I}$, per Eq. (2.18). Note that all five $X_{i,i+2}$ are outside the amplituhedron (in this case the pentagon). The existence of a zero surface outside the amplituhedron in this example directly leads to a geometric construction of the integrand. The same happens for more complicated amplituhedra, which typically lack a low-dimensional intuitive visualization.

Now let us go several steps back and consider the standard expansion for the integrand Eq. (2.17) in momentum space as the starting point, and think about the zero conditions as coming from physics (unphysical cuts) rather than geometry (forbidden boundaries). We can reformulate the conjecture about fixing N in Eq. (2.18) in terms of unknown coefficients a_j in the expansion in Eq. (2.17):

$$\mathcal{M}_4^{2-\text{loop}} = a_1 n_1 \quad \boxed{}_{\substack{2\;\;3\\1\;\;4}} \quad + \quad a_2 n_2 \quad \boxed{}_{\substack{3\;\;4\\2\;\;1}}$$

Figure 2.3: The planar two-loop four-point amplitude can be represented in terms of double-box diagrams.

All coefficients a_j are fixed by *zero conditions*, up to an overall normalization.

By zero conditions we mean both unphysical and non-MHV cuts (as defined above) for which the integrand vanishes, $d\mathcal{I}|_{\text{cuts}} = 0$. The overall normalization just means the overall scale of the amplitude is one undetermined coefficient of the a_j, which may be fixed by one inhomogeneous condition.

Assuming the integrand may be expanded as in Eq. (2.17) automatically assumes the presence of only logarithmic singularities as well as the cancelation of some unphysical cuts, viz. those which do not correspond to planar diagrams. On one hand, we can think about this conjecture as a reduced version of the one stated in Ref. [97], where both logarithmic singularities and diagram-like cuts were nontrivial conditions on the numerator N of the planar integrand Eq. (2.18). On the other hand, a (dual) amplituhedron exactly implies our conjecture about zero conditions given the diagrammatic expansion of the integrand in Eq. (2.17). And most importantly, our new conjecture is now formulated in a language which allows us to carry it over to the nonplanar sector in Chapter 3.

A simple example that illustrates our zero conditions conjecture is the planar two-loop four-point amplitude [125], which can be represented using the diagrammatic expansion in Figure 2.3. The diagrams represent the denominators of individual integrands and their unit leading singularity normalizations are $n_1 = s^2 t$, $n_2 = st^2$, where $s = (k_1 + k_2)^2$ and $t = (k_1 + k_4)^2$ are the usual Mandelstam variables. The overall planar Parke-Taylor factor PT(1234) is suppressed. We can consider a simple non-MHV cut on which the amplitude should vanish and find that the coefficients must satisfy $a_1 = a_2$, which is indeed correct. We

will elaborate on this example in the next chapter in the context of nonplanar amplitudes, where more diagrams contribute.

CHAPTER 3

Singularity Structure of Loop Amplitudes in $\mathcal{N} = 4$ Super-Yang-Mills: Nonplanar Results

Chapter 2 covered the dual formulation of amplitudes in planar $\mathcal{N} = 4$ super-Yang-Mills, and discussed the conjecture that many of these features carry over to the nonplanar sector. To test this conjecture, we use the three-loop four-point and two-loop five-point nonplanar amplitudes as nontrivial examples. A key assumption is that the desired properties can all be made manifest diagram-by-diagram [2, 3]. While it is unknown if this assumption holds for all amplitudes to all loop orders, our results confirm that this is a good hypothesis at the relatively low loop orders we work with. The three-loop four-point integrand was first obtained in Ref. [126], while the two-loop five-point integrand was first calculated in Ref. [13] in a format that makes color-kinematic duality manifest. Here we construct different representations that make manifest the facts that the amplitudes have only logarithmic singularities and no poles at infinity. These representations are then compatible with the notion that there exists a nonplanar analog of dual conformal symmetry and a geometric formulation of nonplanar amplitudes. We organize the amplitudes in terms of basis integrands that have only ± 1 leading singularities. The coefficient of these integrals in the amplitudes are then simply sums of Parke-Taylor factors, as proved in Ref. [111]. We also show that homogeneous conditions are sufficient to determine both amplitudes up to an overall factor, as expected if a nonplanar analog of the amplituhedron were to exist.

As noted previously, there is an essential difference between the planar and nonplanar sectors. In the nonplanar case, it is not known how to construct a unique integrand prior to integration. This is a direct consequence of the lack of global variables. Without those,

the choice of variables in one nonplanar diagram relative to the choice in another diagram is arbitrary. This is a nontrivial obstruction to carrying over the planar amplituhedron construction directly to the full amplitude.

Here we circumvent this problem and follow the strategy developed in Refs. [2, 3, 108], which is to consider diagrams as individual objects and to impose all desired properties diagram-by-diagram. These elements then form a basis for the complete amplitude and give us a representation in terms of a linear combination of said objects. Each integral is furthermore dressed by color factors c_j, as well as with some kinematic coefficients d_j that need to be determined,

$$\mathcal{M} = \sum_j d_j c_j \int d\mathcal{I}^j \, . \tag{3.1}$$

The individual pieces $d\mathcal{I}^j$, interpreted as integrand forms, are not really well-defined because of the arbitrariness in their choice of variables, and they become well-defined only when integrated over loop momenta. However, we can still impose nontrivial requirements on the singularity structure of individual diagrams, as was done in Refs. [2, 3, 108]. This is because unitarity cuts of the amplitude impose constraints in terms of a well-defined set of cut momenta, just as they do in the planar sector. This implies that the integrand forms $d\mathcal{I}^j$ are interesting in their own right, and that we can systematically study their properties with the tools at hand. In particular, we will see concrete examples where MHV integrands may be expanded in a pure integrand basis.

3.1 Nonplanar Conjectures

In the context of $\mathcal{N} = 4$ SYM it is natural to propose the following properties of the "integrand", even in the nonplanar case:

(i) The integrand has only logarithmic singularities.

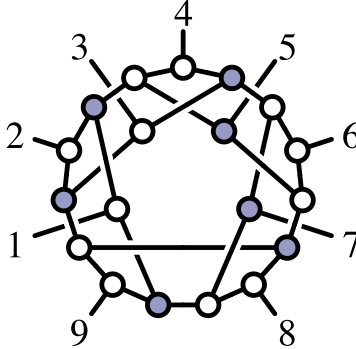(ii) The integrand has no poles at infinity.

Figure 3.1: Example of a nonplanar on-shell diagram.

(iii) The leading singularities of the integrand all take on special values.

The presence of only logarithmic singularities (i) would be an indication of the "volume" interpretation of nonplanar amplitudes. We will give more detailed evidence for such an interpretation in the next section. Demonstrating properties (ii) and (iii) would provide nontrivial evidence for the existence of an analog of dual conformal symmetry for full $\mathcal{N} = 4$ SYM amplitudes, including the nonplanar sector. Since we lack nonplanar momentum twistor variables, we cannot formulate an analogous symmetry directly, yet the basic constraints of properties (ii) and (iii) on nonplanar amplitudes would be identical to the constraints of dual conformal symmetry on planar amplitudes.

The first property (i) can be directly linked to the properties of on-shell diagrams, which are well-defined beyond the planar sector [95, 111]. Nonplanar on-shell diagrams, one of which is illustrated in Figure 3.1, are calculated following the same rules as in the planar case [49]. In particular, they are given by the same logarithmic form Eq. (2.14), where the C-matrix is now some cell in the (not necessarily positive) Grassmannian $G(k, n)$. However, the singularities are again logarithmic for MHV, NMHV, and N^{2}MHV amplitudes; this property holds directly in momentum space like in the planar case. At present it is not known whether this is a property of the full amplitude, including nonplanar contributions. Unlike the planar case, we do not currently have an on-shell diagram representation of the amplitude since it is not known how to unambiguously implement recursion relations. If such a construction

exists, then the amplitude would share the properties of the on-shell diagrams, including their singularity structure. Therefore it is very natural to conjecture that the full amplitude indeed has only logarithmic singularities [108].

Because there is no global definition for the integrand, it is reasonable to assume that there exist $d\mathcal{I}^j$ as in Eq. (3.1) such that each $d\mathcal{I}^j$ has only logarithmic singularities [2]. That is, we assume that there exists a $d$log representation Eq. (2.16) for each diagram,

$$d\mathcal{I}^j = \sum_k b_k \, d\log f_1^{(k)} \, d\log f_2^{(k)} \ldots \, d\log f_{4L}^{(k)} , \tag{3.2}$$

where $f_i^{(k)}$ are some functions of external and loop momenta, and the coefficients b_k are numerical coefficients independent of external kinematics.

In the planar sector, the other two properties (ii) and (iii) are closely related to dual conformal symmetry. As discussed in Chapter 2, the exact constraints of dual conformal symmetry on MHV amplitudes are that the amplitudes have unit leading singularities (when combined with ordinary superconformal symmetry and stripped off Parke-Taylor factor) and no poles at infinity. Property (ii) can be directly carried over to any nonplanar integrand; in particular it would imply that the $d$log forms in Eq. (3.2) never generate a pole as $\ell \to \infty$. As for property (iii), the value of leading singularities cannot be directly translated to the nonplanar case, since there is no single overall Parke-Taylor factor to strip off. Superconformal invariance only allows us to write leading singularities as any holomorphic function $\mathcal{F}_n(\lambda)$, but as proven in Ref. [111], the only allowed functions are

$$\mathcal{F}_n = \sum_\sigma a_\sigma \mathrm{PT}_\sigma , \tag{3.3}$$

where $a_\sigma = (\pm 1, 0)$ and PT stands for a Parke-Taylor factor with a given ordering,

$$\mathrm{PT}_\sigma \equiv \mathrm{PT}(\sigma_1 \sigma_2 \sigma_3 \ldots \sigma_n) = \frac{\delta^8(Q)}{\langle \sigma_1 \sigma_2 \rangle \langle \sigma_2 \sigma_3 \rangle \ldots \langle \sigma_n \sigma_1 \rangle} . \tag{3.4}$$

The sum over σ runs over the $(n-2)!$ Parke-Taylor amplitudes independent under the Kleiss-Kuijf relations [7], as in Eq. (1.1). There are additional relations between the amplitudes, the BCJ identities that played a starring role in Chapter 1, but they introduce ratios of kinematic invariants [6] — which introduce spurious poles in external kinematics because they involve $\tilde{\lambda}$ — and so we will not make use of them here.

As an example, consider the on-shell diagram from Figure 3.1 above, which is equal to the sum of seven Parke-Taylor factors (see Eq. (3.11) of Ref. [111]),

$$\mathcal{F}_6 = \text{PT}(123456) + \text{PT}(124563) + \text{PT}(142563) + \text{PT}(145623)$$
$$+ \text{PT}(146235) + \text{PT}(146253) + \text{PT}(162345) . \tag{3.5}$$

This is a nontrivial property, since there exist many holomorphic functions $\mathcal{F}_n(\lambda)$ for $n \geq 6$ which are not of the form of Eq. (3.3).

Analogously to the planar case, we can define a pure integrand to take the form Eq. (2.16), so that the integrand has unit logarithmic singularities with no poles at infinity. Putting together the results from Refs. [2, 108, 111], our conjecture is that all MHV amplitudes in $\mathcal{N} = 4$ SYM theory can be written as

$$\mathcal{M} = \sum_{k,\sigma,j} a_{\sigma,k,j}\, c_k\, \text{PT}_\sigma \int d\mathcal{I}^j \,, \tag{3.6}$$

where $a_{\sigma,k,j}$ are numerical rational coefficients and $d\mathcal{I}^j$ are pure integrands with leading singularities $(\pm 1, 0)$. The PT_σ are as in Eq. (3.4), and c_k are color factors. For contributions with the maximum number of propagators, the unique color factors can be read off directly from the corresponding diagrams, but contact term contributions may have multiple contributing color factors. The $a_{\sigma,k,j}$ coefficients are such that, up to sums of Parke-Taylor factors, the leading singularities of the amplitude are normalized to be $(\pm 1, 0)$, reflecting a known property of the amplitude.

3.1.1 Uniqueness and Total Derivatives

There is an important question about the uniqueness of our result. The standard wisdom is that the final amplitude $\mathcal{M}$ is a unique object while the planar integrand $d\mathcal{I}$ is ambiguous, as we can add any total derivative $d\mathcal{I}^{\text{tot}}$,

$$\int d\mathcal{I}^{\text{tot}} = 0 \,, \tag{3.7}$$

that leaves $\mathcal{M}$ invariant. Note that this is not true in our way of constructing the integrand, which relies on matching the cuts of the amplitude. This was sharply stated in Ref. [90]: there is only one function which satisfies all constraints (logarithmic singularities, dual conformal symmetry) and cut conditions. Any total derivative $d\mathcal{I}^{\text{tot}}$ would violate one or the other. In other words, if we demand dual conformal invariance and logarithmic singularities, then any integrand would necessarily contribute to some of the cuts; the integrand therefore cannot be left undetected by all cuts. It does not matter if it integrates to zero or not, its coefficient is completely fixed by cut conditions.

The same is true in the case of nonplanar amplitudes in general. In practice, our bases of pure integrands for all examples in the following sections are complete. The pure integrand representation does not distinguish between forms that do integrate to zero and those that do not. Therefore, once the cuts are matched, the pure integrand basis does not miss any total derivatives that satisfy our constraints, and thus we cannot add any terms like $\int d\mathcal{I}^{\text{tot}}$ to our amplitude. In fact, some linear combination of the basis elements $d\mathcal{I}^j$ in Eq. (3.6) might be total derivatives, but the linear combination must contribute to the amplitude prior to integration with fixed coefficients to match all cuts. There is no freedom to change this coefficient to some other value. As a result, like in the planar sector, the nonplanar result is unique once we impose all constraints.

In the remainder of this chapter, we explicitly demonstrate that the two-loop four-point, three-loop four-point, and two-loop five-point amplitudes may be written in this pure integrand expansion. In 3.5, we furthermore demonstrate that the coefficients $a_{\sigma,k,j}$ are all
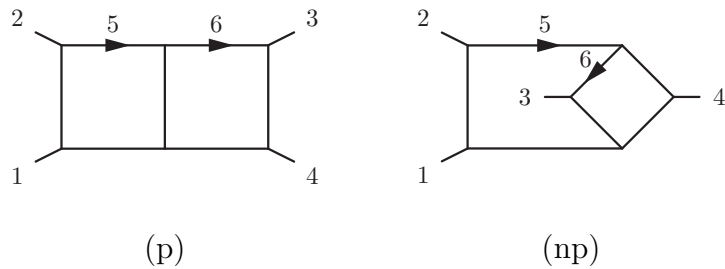
Figure 3.2: The integrals appearing in the two-loop four-point amplitude of $\mathcal{N} = 4$ SYM theory.

determined from homogeneous information.

3.2 Two-Loop Four-Point Amplitude

The simplest multi-loop example is the two-loop four-point amplitude, which was first obtained in Refs. [125, 127]. In Ref. [108] these results were reorganized in terms of individual integrals with only logarithmic singularities and no poles at infinity. There are two topologies: the planar and nonplanar double boxes, as illustrated in Figure 3.2. Using our convention that all external momenta are outgoing, the numerators for the planar and nonplanar double box integrals with these properties are

$$\widetilde{N}^{(\mathrm{p})} = s \,, \qquad \widetilde{N}^{(\mathrm{np})} = (\ell_5 - k_3)^2 + (\ell_5 - k_4)^2 \,, \tag{3.8}$$

up to overall factors independent of loop momentum. The integrand $d\mathcal{I}^{\mathrm{np}}$ with this numerator has logarithmic singularities and no poles at infinity, but it is not a pure integrand. That is, the leading singularities are not all ± 1, but also contain ratios of the form $\pm u/t$. The kinematic invariants $s = (k_1 + k_2)^2$, $t = (k_1 + k_4)^2$ and $u = (k_1 + k_3)^2$ are the usual Mandelstam invariants.

Here we want to decompose the $\widetilde{N}$ numerators so that the resulting integrands $d\mathcal{I}^j$ are pure, and express the amplitude in terms of the resulting pure integrand basis. In practice, we do this by retaining (with respect to Ref. [108]) the permutation invariant function

46

$\mathcal{K} = st\mathrm{PT}(1234) = su\mathrm{PT}(1243)$, and by requiring each basis integrand to have correct mass dimension — six in this case — and unit leading singularities ± 1. This gives us three basis elements:

$$N^{(\mathrm{p})} = s^2 t\,, \qquad N_1^{(\mathrm{np})} = su(\ell_5 - k_3)^2\,, \qquad N_2^{(\mathrm{np})} = st(\ell_5 - k_4)^2\,. \tag{3.9}$$

The two nonplanar basis integrals are related by the symmetry of the diagram, but to maintain unit leading singularities we keep the terms distinct. The corresponding pure integrand forms $d\mathcal{I}^{(\mathrm{p})}$, $d\mathcal{I}_1^{(\mathrm{np})}$, $d\mathcal{I}_2^{(\mathrm{np})}$ are obtained by including the integration measure and the appropriate propagators that can be read off from Figure 3.2

We note that for the planar double box, an explicit $d$log form is known [108],

$$\begin{aligned}
d\mathcal{I}^{(\mathrm{p})} = {}&d\log\frac{\ell_5^2}{(\ell_5 - \ell_5^*)^2}\, d\log\frac{(\ell_5 + k_2)^2}{(\ell_5 - \ell_5^*)^2}\, d\log\frac{(\ell_5 + k_1 + k_2)^2}{(\ell_5 - \ell_5^*)^2}\, d\log\frac{(\ell_5 - k_3)^2}{(\ell_5 - \ell_5^*)^2}\\
&\times d\log\frac{(\ell_5 - \ell_6)^2}{(\ell_6 - \ell_6^*)^2}\, d\log\frac{\ell_6^2}{(\ell_6 - \ell_6^*)^2}\, d\log\frac{(\ell_6 - k_3)^2}{(\ell_6 - \ell_6^*)^2}\, d\log\frac{(\ell_6 - k_3 - k_4)^2}{(\ell_6 - \ell_6^*)^2}\,,
\end{aligned} \tag{3.10}$$

where

$$\ell_5^* = -\frac{\langle 12 \rangle}{\langle 13 \rangle}\lambda_3 \widetilde{\lambda}_2\,, \qquad \ell_6^* = k_3 + \frac{(\ell_5 - k_3)^2}{\langle 4|\ell_5|3]}\lambda_4 \widetilde{\lambda}_3\,, \tag{3.11}$$

each denote solutions to the on-shell conditions. Ref. [108] gave the $d$log form for the nonplanar double box with numerators as in Eq. (3.9) as a sum of four $d$log forms with prefactors (leading to different Parke-Taylor factors). This representation has the advantage that it naturally separates parity even and odd pieces. In Ref. [2] this was rewritten in a way that manifestly splits into unit leading singularity pieces, so that there are single $d$log forms corresponding to each of the nonplanar numerators $N_1^{(\mathrm{np})}$ and $N_2^{(\mathrm{np})}$. As usual, we suppress the wedge notation and write,

$$d\mathcal{I}_1^{(\mathrm{np})} = d\Omega_1\, d\Omega_{2,(1)}, \qquad d\mathcal{I}_2^{(\mathrm{np})} = d\Omega_1\, d\Omega_{2,(2)}\,. \tag{3.12}$$

More explicitly, these forms are

$$
\begin{aligned}
d\Omega_1 &= d\log\frac{\ell_6^2}{(\ell_6 - \ell_6^*)^2}\, d\log\frac{(\ell_6 - k_3)^2}{(\ell_6 - \ell_6^*)^2}\, d\log\frac{(\ell_6 - \ell_5)^2}{(\ell_6 - \ell_6^*)^2}\, d\log\frac{(\ell_6 - \ell_5 + k_4)^2}{(\ell_6 - \ell_6^*)^2}\,, \\
d\Omega_{2,(1)} &= d\log\frac{\ell_5^2}{\langle 4|\ell_5|3]}\, d\log\frac{(\ell_5 + k_2)^2}{\langle 4|\ell_5|3]}\, d\log\frac{(\ell_5 + k_1 + k_2)^2}{\langle 3|\ell_5|4]}\, d\log\frac{(\ell_5 - \ell_{5,1}^*)^2}{\langle 3|\ell_5|4]}\,, \\
d\Omega_{2,(2)} &= d\log\frac{\ell_5^2}{\langle 3|\ell_5|4]}\, d\log\frac{(\ell_5 + k_2)^2}{\langle 3|\ell_5|4]}\, d\log\frac{(\ell_5 + k_1 + k_2)^2}{\langle 4|\ell_5|3]}\, d\log\frac{(\ell_5 - \ell_{5,2}^*)^2}{\langle 4|\ell_5|3]}\,.
\end{aligned}
\tag{3.13}
$$

where the cut solutions read

$$
\ell_6^* = -\frac{\lambda_3\,\ell_5 \cdot \lambda_4}{\langle 34 \rangle}\,, \qquad
\ell_{5,1}^* = -\frac{\langle 34 \rangle}{\langle 31 \rangle}\lambda_1\widetilde{\lambda}_4 - k_1 - k_2\,, \qquad
\ell_{5,2}^* = -\frac{\langle 43 \rangle}{\langle 41 \rangle}\lambda_1\widetilde{\lambda}_3 - k_1 - k_2\,.
\tag{3.14}
$$

Using these basis integrals, the full two-loop four-point amplitude can be written as a linear combination dressed with the appropriate color and Parke-Taylor factors,

$$
\begin{aligned}
\mathcal{M}_4^{\text{2-loop}} = \frac{1}{4}\sum_{S_4}\Big[&c_{1234}^{(\mathrm{p})}\, a^{(\mathrm{p})}\mathrm{PT}(1234)\int d\mathcal{I}^{(\mathrm{p})} \\
&+ c_{1234}^{(\mathrm{np})}\left(a_1^{(\mathrm{np})}\mathrm{PT}(1243)\int d\mathcal{I}_1^{(\mathrm{np})} + a_2^{(\mathrm{np})}\mathrm{PT}(1234)\int d\mathcal{I}_2^{(\mathrm{np})}\right)\Big],
\end{aligned}
\tag{3.15}
$$

where we sum over all 24 permutations of the external legs S_4. The overall $1/4$ divides out the symmetry factor for each diagram to remove the overcount from the permutation sum. The planar and nonplanar double-box color factors are

$$
\begin{aligned}
c_{1234}^{(\mathrm{p})} &= \tilde{f}^{a_1 a_7 a_9}\,\tilde{f}^{a_2 a_5 a_7}\,\tilde{f}^{a_5 a_6 a_8}\,\tilde{f}^{a_9 a_8 a_{10}}\,\tilde{f}^{a_3 a_{11} a_6}\,\tilde{f}^{a_4 a_{10} a_{11}}\,, \\
c_{1234}^{(\mathrm{np})} &= \tilde{f}^{a_1 a_7 a_8}\,\tilde{f}^{a_2 a_5 a_7}\,\tilde{f}^{a_5 a_{11} a_6}\,\tilde{f}^{a_8 a_9 a_{10}}\,\tilde{f}^{a_3 a_6 a_9}\,\tilde{f}^{a_4 a_{10} a_{11}}\,,
\end{aligned}
\tag{3.16}
$$

where the $\tilde{f}^{abc} = i\sqrt{2}f^{abc}$ are appropriately normalized color structure constants.

Matching the amplitude on unitarity cuts determines the coefficients to be

$$
a^{(\mathrm{p})} = 1\,, \qquad a_1^{(\mathrm{np})} = -1\,, \qquad a_2^{(\mathrm{np})} = -1\,,
\tag{3.17}
$$

so that the amplitude in Eq. (3.15) is equivalent to the one presented in Ref. [108]. The trivial difference is that there the two pieces $d\mathcal{I}_1^{(\text{np})}$ and $d\mathcal{I}_2^{(\text{np})}$ are combined into one numerator.

3.3 Three-Loop Four-Point Amplitude

Now consider the three-loop four-point amplitude. This amplitude has been discussed already in various papers [2, 107, 126, 128]. Here we will express the amplitude in a pure integrand basis. In order to find such a basis, we follow the strategy of Ref. [2], wherein integrands with only logarithmic singularities were identified. We proceed in the same way, but at the end impose the additional requirement that the leading singularities be ± 1 or 0. The construction of diagram numerators which lead to pure integrands is very similar to the previous representation of Ref. [2], so we will only summarize the construction here. Details on direct construction of the amplitude can be found in Appendix C.

The construction starts from a general $\mathcal{N} = 4$ SYM power counting of loop momenta. For a given loop variable, we require the overall scaling of a given integrand to behave like a box in that variable. For example, if there is a pentagon subdiagram for loop variable ℓ, we allow a nontrivial numerator in ℓ, $N \sim \rho_1 \ell^2 + \rho_2 (\ell \cdot Q) + \rho_3$, where Q is some complex momentum (not necessarily massless). Similarly, if there is a hexagon subdiagram in loop variable ℓ, we allow $N \sim \rho_1 (\ell^2)^2 + \rho_2 (\ell^2)(\ell \cdot Q) + \rho_3 (\ell \cdot Q_1)(\ell \cdot Q_2) + \ldots$, and so on. Our conventions require that the overall mass dimension of $d\mathcal{I}_j$ is zero[1], which fixes the mass dimension of the ρ_j.

In Ref. [2], we then directly constructed the amplitude by constraining the ansatz numerators to obey the symmetry of the diagrams and to vanish on poles at infinity and double (or multiple) poles. We now take a slightly different approach: instead of constructing the amplitude directly, focus on constructing the pure integrand basis. The approach of Ref. [2] is followed in Appendix C.

---

[1]This mass dimension is different than in Ref. [2], where we factored out the totally crossing-symmetric $\mathcal{K} = st\text{PT}(1234) = su\text{PT}(1243) = tu\text{PT}(1324)$.

3.3.1 Basis of Unit Leading Singularity Numerators

The next step in constructing the pure integrand basis is to require the elements have unit leading singularities. We write each basis element as an ansatz that has the same power counting as the diagram numerators. We then constrain the elements so that *any* leading singularity — codimension $4L$ residue — is either ± 1 or 0.

The resulting basis elements differ slightly from those of Ref. [2]. Terms that were originally grouped so that the numerator obeyed diagram symmetry are now split to make the unit leading singularity property manifest. This is exactly the same reason we rewrote Eq. (3.8) as Eq. (3.9) in the two-loop four-point example. Additionally, the basis elements are scaled by products st, su, or tu to account for differing normalizations. The results of our construction of basis numerators yielding pure integrands are summarized in Table 3.1.

In Table 3.1 we use the relabeling convention $N\big|_{i\leftrightarrow j}$: "redraw the graph associated with numerator N with the indicated exchanges of external momenta i,j and also relabel loop momenta accordingly." As a simple example look at $N_1^{(i)}\big|_{1\leftrightarrow 3}$,

$$N_1^{(i)} = tu(\ell_6 + k_4)^2(\ell_5 - k_1 - k_2)^2 \,, \qquad\qquad N_2^{(i)} = N_1^{(i)}\big|_{1\leftrightarrow 3}\,. \qquad (3.18)$$

Under this relabeling, the Mandelstam variables s and t transform into one another $s = (k_1 + k_2)^2 \leftrightarrow (k_3 + k_2)^2 = t$ and u stays invariant. Besides changing the external labels, we are instructed to relabel the loop momenta as well. In the chosen example, this corresponds to interchanging $\ell_5 \leftrightarrow \ell_6$, so that

$$N_2^{(i)} = N_1^{(i)}\big|_{1\leftrightarrow 3} = su(\ell_5 + k_4)^2(\ell_6 - k_3 - k_2)^2 \,. \qquad (3.19)$$

Diagram	Numerators

(a) $\quad N_1^{(a)} = s^3 t\,,$

(b) $\quad N_1^{(b)} = s^2 u (\ell_6 - k_3)^2\,, \qquad N_2^{(b)} = N_1^{(b)}\big|_{3\leftrightarrow 4}\,,$

(c) $\quad N_1^{(c)} = s^2 u (\ell_5 - \ell_7)^2\,, \qquad N_2^{(c)} = N_1^{(c)}\big|_{1\leftrightarrow 2}\,,$

(d) $\quad N_1^{(d)} = su\Big[(\ell_6 - k_1)^2 (\ell_6 + k_3)^2 - \ell_6^2 (\ell_6 - k_1 - k_2)^2\Big]\,,$

$N_2^{(d)} = N_1^{(d)}\big|_{3\leftrightarrow 4}\,, \qquad N_3^{(d)} = N_1^{(d)}\big|_{1\leftrightarrow 2}\,, \qquad N_4^{(d)} = N_1^{(d)}\big|_{\substack{1\leftrightarrow 2 \\ 3\leftrightarrow 4}}\,,$

(e) $\quad N_1^{(e)} = s^2 t (\ell_5 + k_4)^2\,,$

(f) $\quad N_1^{(f)} = st(\ell_5 + k_4)^2 (\ell_5 + k_3)^2\,, \qquad N_2^{(f)} = su(\ell_5 + k_4)^2 (\ell_5 + k_4)^2\,,$

(g) $\quad N_1^{(g)} = s^2 t (\ell_5 + \ell_6 + k_3)^2\,,$

$N_2^{(g)} = st(\ell_5 + k_3)^2 (\ell_6 + k_1 + k_2)^2\,, \quad N_3^{(g)} = N_2^{(g)}\big|_{3\leftrightarrow 4}\,,$

(h)

$N_1^{(h)} = st\Big[(\ell_6 + \ell_7)^2 (\ell_5 + k_2 + k_3)^2 - \ell_5^2 (\ell_6 + \ell_7 - k_1 - k_2)^2$
$\qquad - (\ell_5 + \ell_6)^2 (\ell_7 + k_2 + k_3)^2 - (\ell_5 + \ell_6 + k_2 + k_3)^2 \ell_7^2$
$\qquad - (\ell_6 + k_1 + k_4)^2 (\ell_5 - \ell_7)^2 - (\ell_5 - \ell_7 + k_2 + k_3)^2 \ell_6^2\Big]\,,$

$N_2^{(h)} = tu\Big[[(\ell_5 - k_1)^2 + (\ell_5 - k_4)^2][(\ell_6 + \ell_7 - k_1)^2 + (\ell_6 + \ell_7 - k_2)^2]$
$\qquad - 4\,\ell_5^2 (\ell_6 + \ell_7 - k_1 - k_2)^2$
$\qquad - (\ell_7 + k_4)^2 (\ell_5 + \ell_6 - k_1)^2 - (\ell_7 + k_3)^2 (\ell_5 + \ell_6 - k_2)^2$
$\qquad - (\ell_6 + k_4)^2 (\ell_5 - \ell_7 + k_1)^2 - (\ell_6 + k_3)^2 (\ell_5 - \ell_7 + k_2)^2\Big]\,,$

$N_3^{(h)} = N_1^{(h)}\big|_{2\leftrightarrow 4}\,, \qquad N_4^{(h)} = N_2^{(h)}\big|_{2\leftrightarrow 4}\,,$

(i) $\quad N_1^{(i)} = tu(\ell_6 + k_4)^2 (\ell_5 - k_1 - k_2)^2\,, \qquad\qquad N_2^{(i)} = N_1^{(i)}\big|_{1\leftrightarrow 3}$

$N_3^{(i)} = st\big[(\ell_6 + k_4)^2 (\ell_5 - k_1 - k_3)^2 - \ell_5^2 (\ell_6 - k_2)^2\big]\,, \quad N_4^{(i)} = N_3^{(i)}\big|_{1\leftrightarrow 3}$

(j) $\quad N^{(j)} = stu\,.$

(k) $\quad N^{(k)} = su\,,$

Table 3.1: The basis of numerators for pure integrands for the three-loop four-point amplitude. The notation $N\big|_{i\leftrightarrow j}$ is defined in the text.

3.3.2 Matching the Amplitude

The three-loop four-point amplitude is assembled from the basis numerators as

$$\mathcal{M}_4^{\text{3-loop}} = \sum_{S_4} \sum_x \frac{1}{\mathcal{S}_x} \int d^4\ell_5 d^4\ell_6 d^4\ell_7 \frac{\mathcal{N}^{(x)}}{\prod_{\alpha_x} p_{\alpha_x}^2} \,, \tag{3.20}$$

analogously to Eq. (3.15). Now the sum over x runs over all diagrams in the basis listed in Table 3.1, the sum over S_4 is a sum over all 24 permutations of the external legs, and $\mathcal{S}_x$ is the symmetry factor of diagram x determined by counting the number of the diagram's graph automorphisms. The product over α_x indicates the product of Feynman propagators $p_{\alpha_x}^2$ of diagram x, as read from the graphs in Table 3.1. The Parke-Taylor factors, color factors, and coefficients are absorbed in $\mathcal{N}^{(x)}$, which we list in Table 3.2.

For four external particles, there are only two independent Parke-Taylor factors. We abbreviate these as

$$\text{PT}_1 = \text{PT}(1234) \,, \qquad \text{PT}_2 = \text{PT}(1243) \,. \tag{3.21}$$

The third possible factor (after imposing cyclic symmetry), $\text{PT}(1423)$, is related to the other two by a $U(1)$ decoupling identity or dual Ward identity [129]:

$$\text{PT}(1423) = -\text{PT}(1234) - \text{PT}(1243) \,, \tag{3.22}$$

and is therefore linearly dependent on PT_1 and PT_2.

When checking cuts of the amplitude, certain cuts may combine contributions from different terms in the permutation sum of Eq. (3.20), resulting in a cut expression that involves diagrams that are relabelings of those in Table 3.1. In that case, the procedure is to relabel the numerators, propagators, Parke-Taylor factors, and color factors given in the tables into the cut labels. The resulting Parke-Taylor factors may not be in the original basis of Parke-Taylor factors; however every Parke-Taylor in the relabeled expression can be expanded in the original Parke-Taylor basis.

The diagrams with 10 propagators contain only three-point vertices and therefore have unique color factors included in $\mathcal{N}^{(x)}$. For the two diagrams with fewer than 10 propagators, we include in our ansatz for $\mathcal{N}$ all independent color factors from all 10-propagator diagrams that are related to the lower-propagator diagrams by collapsing internal legs. For example, three 10-propagator diagrams are related to diagram (j) in this way, with color factors $c_{1234}^{(i)}$, $c_{1243}^{(i)}$ and $c_{3241}^{(i)}$, where

$$c_{1234}^{(i)} = \tilde{f}^{a_1 a_8 a_5} \tilde{f}^{a_6 a_2 a_9} \tilde{f}^{a_3 a_{11} a_{10}} \tilde{f}^{a_{12} a_4 a_{13}} \tilde{f}^{a_9 a_{10} a_8} \tilde{f}^{a_{11} a_{12} a_{14}} \tilde{f}^{a_{13} a_5 a_7} \tilde{f}^{a_{14} a_7 a_6} \tag{3.23}$$

is the standard color factor in terms of appropriately normalized structure constants, and the others c's are relabelings of 1234 of this color factor. The Jacobi relation between the three color factors allows us to eliminate, say $c_{1243}^{(i)}$. This is exactly what we do for diagram (j). In diagram (k), there are nine contributing parent diagrams. Typically there are four independent color factors in the solution to the set of six Jacobi relations, but in this case two of the color factors that contribute happen to be identical up to a sign, and thus there are only three independent color factors.

In Ref. [2], the final representation of the amplitude contained arbitrary free parameters associated with the color Jacobi identity that allowed contact terms to be moved between parent diagrams without altering the amplitude. Here we removed this freedom by assigning the contact terms to their own diagrams and keeping only a basis of independent color factors for each. See Appendix C for more details on how this works.

One advantage of the Parke-Taylor expansion of the amplitude is that we can compactly express the solution to the cut equations in the set of matrices listed on the right hand side of Table 3.2. For example, $\mathcal{N}^{(i)}$ can be read off from the table as

$$\mathcal{N}^{(i)} = c_{1234}^{(i)}(-1)\big(N_1^{(i)}(\mathrm{PT}_1 + \mathrm{PT}_2) + N_2^{(i)}\mathrm{PT}_2 - N_3^{(i)}\mathrm{PT}_1 + N_4^{(i)}\mathrm{PT}_1\big). \tag{3.24}$$

This expression supplies the Parke-Taylor and color dependence required for Eq. (3.20), in agreement with the general form of Eq. (3.6).

Color Dressed Numerators	PT Matrices

$$\mathcal{N}^{(a)} = c^{(a)}_{1234} \sum_{1 \leq \sigma \leq 2} N^{(a)}_1 \mathsf{a}^{(a)}_{1\sigma} \mathrm{PT}_\sigma \,, \qquad \mathsf{a}^{(a)}_{1\sigma} = \begin{pmatrix} 1 & 0 \end{pmatrix} \,,$$

$$\mathcal{N}^{(b)} = c^{(b)}_{1234} \sum_{\substack{1 \leq \nu \leq 2 \\ 1 \leq \sigma \leq 2}} N^{(b)}_\nu \mathsf{a}^{(b)}_{\nu\sigma} \mathrm{PT}_\sigma \,, \qquad \mathsf{a}^{(b)}_{\nu\sigma} = (-1)\begin{pmatrix} 0 & 1 \\ 1 & 0 \end{pmatrix} \,,$$

$$\mathcal{N}^{(c)} = c^{(c)}_{1234} \sum_{\substack{1 \leq \nu \leq 2 \\ 1 \leq \sigma \leq 2}} N^{(c)}_\nu \mathsf{a}^{(c)}_{\nu\sigma} \mathrm{PT}_\sigma \,, \qquad \mathsf{a}^{(c)}_{\nu\sigma} = (-1)\begin{pmatrix} 0 & 1 \\ 1 & 0 \end{pmatrix} \,,$$

$$\mathcal{N}^{(d)} = c^{(d)}_{1234} \sum_{\substack{1 \leq \nu \leq 4 \\ 1 \leq \sigma \leq 2}} N^{(d)}_\nu \mathsf{a}^{(d)}_{\nu\sigma} \mathrm{PT}_\sigma \,, \qquad \mathsf{a}^{(d)}_{\nu\sigma} = \begin{pmatrix} 0 & 1 & 1 & 0 \\ 1 & 0 & 0 & 1 \end{pmatrix}^T \,,$$

$$\mathcal{N}^{(e)} = c^{(e)}_{1234} \sum_{1 \leq \sigma \leq 2} N^{(e)}_1 \mathsf{a}^{(e)}_{1\sigma} \mathrm{PT}_\sigma \,, \qquad \mathsf{a}^{(e)}_{1\sigma} = \begin{pmatrix} 1 & 0 \end{pmatrix} \,,$$

$$\mathcal{N}^{(f)} = c^{(f)}_{1234} \sum_{\substack{1 \leq \nu \leq 2 \\ 1 \leq \sigma \leq 2}} N^{(f)}_\nu \mathsf{a}^{(f)}_{\nu\sigma} \mathrm{PT}_\sigma \,, \qquad \mathsf{a}^{(f)}_{\nu\sigma} = (-1)\begin{pmatrix} 1 & 0 \\ 0 & 1 \end{pmatrix} \,,$$

$$\mathcal{N}^{(g)} = c^{(g)}_{1234} \sum_{\substack{1 \leq \nu \leq 3 \\ 1 \leq \sigma \leq 2}} N^{(g)}_\nu \mathsf{a}^{(g)}_{\nu\sigma} \mathrm{PT}_\sigma \,, \qquad \mathsf{a}^{(g)}_{\nu\sigma} = \begin{pmatrix} -1 & 1 & 0 \\ 0 & 0 & 1 \end{pmatrix}^T \,,$$

$$\mathcal{N}^{(h)} = c^{(h)}_{1234} \sum_{\substack{1 \leq \nu \leq 4 \\ 1 \leq \sigma \leq 2}} N^{(h)}_\nu \mathsf{a}^{(h)}_{\nu\sigma} \mathrm{PT}_\sigma \,, \qquad \mathsf{a}^{(h)}_{\nu\sigma} = \frac{1}{2}\begin{pmatrix} 1 & 1 & 1 & 0 \\ 0 & 1 & 0 & -1 \end{pmatrix}^T \,,$$

$$\mathcal{N}^{(i)} = c^{(i)}_{1234} \sum_{\substack{1 \leq \nu \leq 4 \\ 1 \leq \sigma \leq 2}} N^{(i)}_\nu \mathsf{a}^{(i)}_{\nu\sigma} \mathrm{PT}_\sigma \,, \qquad \mathsf{a}^{(i)}_{\nu\sigma} = (-1)\begin{pmatrix} 1 & 0 & -1 & 1 \\ 1 & 1 & 0 & 0 \end{pmatrix}^T \,,$$

$$\mathcal{N}^{(j)} = c^{(i)}_{1234} \sum_{1 \leq \sigma \leq 2} N^{(j)}_1 \mathsf{a}^{(j)}_{1\sigma,(1234)} \mathrm{PT}_\sigma \qquad \mathsf{a}^{(j)}_{1\sigma,(1234)} = \begin{pmatrix} 1 & 1 \end{pmatrix} \,,$$
$$+ c^{(i)}_{3241} \sum_{1 \leq \sigma \leq 2} N^{(j)}_1 \mathsf{a}^{(j)}_{1\sigma,(3241)} \mathrm{PT}_\sigma \,, \qquad \mathsf{a}^{(j)}_{1\sigma,(3241)} = \begin{pmatrix} -1 & 0 \end{pmatrix} \,,$$

$$\mathcal{N}^{(k)} = c^{(g)}_{1234} \sum_{1 \leq \sigma \leq 2} N^{(k)}_1 \mathsf{a}^{(k)}_{1\sigma,(1234)} \mathrm{PT}_\sigma \qquad \mathsf{a}^{(k)}_{1\sigma,(1234)} = \begin{pmatrix} -2 & 0 \end{pmatrix} \,,$$
$$+ c^{(g)}_{4312} \sum_{1 \leq \sigma \leq 2} N^{(k)}_1 \mathsf{a}^{(k)}_{1\sigma,(4312)} \mathrm{PT}_\sigma \qquad \mathsf{a}^{(k)}_{1\sigma,(4312)} = 0 \,,$$
$$+ c^{(f)}_{2431} \sum_{1 \leq \sigma \leq 2} N^{(k)}_1 \mathsf{a}^{(k)}_{1\sigma,(2431)} \mathrm{PT}_\sigma \,. \qquad \mathsf{a}^{(k)}_{1\sigma,(2431)} = 0 \,.$$

Table 3.2: The three-loop four-point numerators that contribute to the amplitude. The $N^{(x)}_\nu$ are listed in Table 3.1. The four-point Parke-Taylor factors PT_σ are listed in Eq. (3.21). The numerators including color factors are denoted as $\mathcal{N}^{(x)}$. The symbol T denotes a transpose.

3.4 Two-Loop Five-Point Amplitude

The integrand for the two-loop five-point amplitude was first obtained in Ref. [13] in a format that makes color-kinematic duality manifest. Here we find a pure integrand representation. An additional feature of our representation is that it is manifestly free of spurious poles in external kinematics.

3.4.1 Basis of Unit Leading Singularity Numerators

Following the three-loop four-point case, our first step is to construct a pure integrand basis. Constructing this basis is similar to constructing the three-loop four-point amplitude in Ref. [2] and summarized in Sec. 3.3. Although deriving the numerators for the two-loop five-point case is in principle straightforward, it does require a nontrivial amount of algebra, which we suppress. We again split the basis elements according to diagram topologies and distinguish between parent diagrams and contact diagrams. The numerators of each pure integrand are given in Table 3.3.

Table 3.4 contains an additional pure integrand. However we do not include it in our basis because it is linearly dependent on two other basis elements: $N_1^{(h)} - N_2^{(h)} + N_1^{(j)}(\ell_6 - k_1)^2 = 0$. In our result, we choose $N_1^{(h)}$ and $N_2^{(h)}$ as our linearly independent pure integrands, and only mention $N_1^{(j)}$ because it might be an interesting object in future studies.

In contrast to the three-loop four-point basis, in the two-loop five-point case it is useful to allow spinor-helicity variables associated with external momenta. Specifically, several of the expressions in Table 3.3 have the structure $(\ell + \alpha \lambda_i \widetilde{\lambda}_j)^2$, where α is such that both mass dimension and little group weights are consistent. For example, the penta-box numerator

$$N_1^{(b)} \sim \left(\ell_6 + \frac{Q_{45} \cdot \widetilde{\lambda}_3 \, \widetilde{\lambda}_1}{[13]} \right)^2 = (\ell_6 - \ell_6^*)^2 \,, \tag{3.25}$$

is a "chiral" numerator that manifestly vanishes on the $\overline{\text{MHV}}$ solution $\ell_6 = \ell_6^*$ [122]. As a

shorthand notation, we use $Q_{ij} = k_i + k_j$. Therefore we have, in this example,

$$Q_{45} \cdot \widetilde{\lambda}_3 = (\lambda_4 \widetilde{\lambda}_4 + \lambda_5 \widetilde{\lambda}_5) \cdot \widetilde{\lambda}_3 = [43]\lambda_4 + [53]\lambda_5. \tag{3.26}$$

3.4.2   Matching the Amplitude

Following the construction of the pure integrand basis in Subsection 3.4.1, we are ready to build up the amplitude. In complete analogy to Eq. (3.20), the two-loop five-point amplitude is assembled from the basis numerators as,

$$\mathcal{M}_5^{\text{2-loop}} = \sum_{S_5} \sum_x \frac{1}{\mathcal{S}_x} \int d^4\ell_6 d^4\ell_7 \frac{\mathcal{N}^{(x)}}{\prod_{\alpha_x} p_{\alpha_x}^2}, \tag{3.27}$$

where the sum over x runs over all diagrams in the basis listed in Table 3.3, the sum over S_5 is a sum over all 120 permutations of the external legs, and $\mathcal{S}_x$ is the symmetry factor of diagram x. The product over α_x indicates the product of Feynman propagators $p_{\alpha_x}^2$ of diagram x, as read from the graphs in Table 3.3.

We refer the reader to the discussion in Subsection 3.3.2 for explicit examples on how to read Table 3.5. We choose the following set of independent five-point Parke-Taylor basis elements:

$$\begin{aligned}
\text{PT}_1 &= \text{PT}(12345), & \text{PT}_2 &= \text{PT}(12354), & \text{PT}_3 &= \text{PT}(12453), \\
\text{PT}_4 &= \text{PT}(12534), & \text{PT}_5 &= \text{PT}(13425), & \text{PT}_6 &= \text{PT}(15423).
\end{aligned} \tag{3.28}$$

The basis elements $\overline{N}^{(x)}$ in Table 3.5 do not contribute to the MHV amplitude, so that data is omitted from the $\mathsf{a}_{\nu\sigma}^{(x)}$.

Diagram	Numerators

(a)

$$N_1^{(a)} = \langle 13\rangle\langle 24\rangle\Big[[24][13]\Big(\ell_7 + \tfrac{[45]}{[24]}\lambda_5\widetilde\lambda_2\Big)^2\Big(\ell_6 - \tfrac{Q_{12}\cdot\widetilde\lambda_3\,\widetilde\lambda_1}{[13]}\Big)^2$$
$$-[14][23]\Big(\ell_7 + \tfrac{[45]}{[14]}\lambda_5\widetilde\lambda_1\Big)^2\Big(\ell_6 - \tfrac{Q_{12}\cdot\widetilde\lambda_3\,\widetilde\lambda_2}{[23]}\Big)^2\Big]\,,$$

$$N_2^{(a)} = N_1^{(a)}\big|_{\substack{1\leftrightarrow 2\\4\leftrightarrow 5}}\,,\qquad N_3^{(a)} = N_1^{(a)}\big|_{\substack{2\leftrightarrow 4\\1\leftrightarrow 5}}\,,\qquad N_4^{(a)} = N_1^{(a)}\big|_{\substack{1\leftrightarrow 4\\2\leftrightarrow 5}}\,,$$

$$N_5^{(a)} = \overline{N}_1^{(a)}\,,\quad N_6^{(a)} = \overline{N}_2^{(a)}\,,\quad N_7^{(a)} = \overline{N}_3^{(a)}\,,\quad N_8^{(a)} = \overline{N}_4^{(a)}\,,$$

(b)

$$N_1^{(b)} = \langle 15\rangle[45]\langle 43\rangle s_{45}[13]\Big(\ell_6 + \tfrac{Q_{45}\cdot\widetilde\lambda_3\,\widetilde\lambda_1}{[13]}\Big)^2\,,$$
$$N_2^{(b)} = \overline{N}_1^{(b)}\,,$$

(c)

$$N_1^{(c)} = [13]\Big(\ell_6 + \tfrac{Q_{45}\cdot\widetilde\lambda_3\,\widetilde\lambda_1}{[13]}\Big)^2\langle 15\rangle[54]\langle 43\rangle(\ell_6 + k_4)^2\,,$$
$$N_2^{(c)} = N_1^{(c)}\big|_{4\leftrightarrow 5}\,,\qquad N_3^{(c)} = \overline{N}_1^{(c)}\,,\qquad N_4^{(c)} = \overline{N}_2^{(c)}\,,$$

(d)

$$N_1^{(d)} = s_{34}(s_{34} + s_{35})\Big(\ell_7 - k_5 + \tfrac{\langle 35\rangle}{\langle 34\rangle}\lambda_4\widetilde\lambda_5\Big)^2\,,$$
$$N_2^{(d)} = N_1^{(d)}\big|_{4\leftrightarrow 5}\,,\qquad N_3^{(d)} = \overline{N}_1^{(d)}\,,\qquad N_4^{(d)} = \overline{N}_2^{(d)}\,,$$

(e)

$$N_1^{(e)} = s_{15}s_{45}^2\,,$$

(f)

$$N_1^{(f)} = s_{14}s_{45}(\ell_6 + k_5)^2\,,\qquad N_2^{(f)} = N_1^{(f)}\big|_{4\leftrightarrow 5}\,,$$

(g)

$$N_1^{(g)} = s_{12}s_{45}s_{24}\,,$$

(h)

$$N_1^{(h)} = \langle 15\rangle[35]\langle 23\rangle[12]\Big(\ell_6 - \tfrac{\langle 12\rangle}{\langle 32\rangle}\lambda_3\widetilde\lambda_1\Big)^2\,,\qquad N_2^{(h)} = N_1^{(h)}\big|_{3\leftrightarrow 5}\,,$$
$$N_3^{(h)} = s_{12}\langle 13\rangle[15]\langle 5|\ell_6|3]\,,\qquad N_4^{(h)} = s_{12}[13]\langle 15\rangle\langle 3|\ell_6|5]\,,$$
$$N_5^{(h)} = \overline{N}_1^{(h)}\,,\qquad N_6^{(h)} = \overline{N}_2^{(h)}\,,$$

(i)

$$N_1^{(i)} = \langle 2|4|3]\langle 3|5|2] - \langle 3|4|2]\langle 2|5|3]\,.$$

Table 3.3: The parent diagram numerators that give pure integrands for the two-loop five-point amplitude. Each basis diagram is consistent with requiring logarithmic singularities and no poles at infinity. The overline notation means $[\cdot]\leftrightarrow\langle\cdot\rangle$.
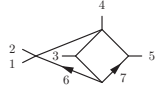
Diagram	Numerators

(j) $\quad$ $\quad N_1^{(j)} = s_{12}s_{35} = (N_2^{(h)} - N_1^{(h)})/(\ell_6 - k_1)^2 \,,$

Table 3.4: A diagram and numerator that gives a pure integrand. However, as indicated in the table and explained in the text, it is not a an independent basis element.

Color Dressed Numerators	PT Matrices

$$\mathcal{N}^{(a)} = c_{12345}^{(a)} \sum_{\substack{1\leq\nu\leq4 \\ 1\leq\sigma\leq6}} N_\nu^{(a)} \mathsf{a}_{\nu\sigma}^{(a)} \mathrm{PT}_\sigma \,, \qquad \mathsf{a}_{\nu\sigma}^{(a)} = \frac{1}{4}\begin{pmatrix} -1 & 0 & 1 & 0 & 0 & 2 \\ 1 & 0 & -1 & 0 & 0 & 2 \\ -3 & 0 & -1 & 0 & 0 & 2 \\ -1 & 0 & -3 & 0 & 0 & 2 \end{pmatrix},$$

$$\mathcal{N}^{(b)} = c_{12345}^{(b)} \sum_{1\leq\sigma\leq6} N_1^{(b)} \mathsf{a}_{1\sigma}^{(b)} \mathrm{PT}_\sigma \,, \qquad \mathsf{a}_{1\nu}^{(b)} = \begin{pmatrix} -1 & 0 & 0 & 0 & 0 & 0 \end{pmatrix},$$

$$\mathcal{N}^{(c)} = c_{12345}^{(c)} \sum_{\substack{1\leq\nu\leq2 \\ 1\leq\sigma\leq6}} N_\nu^{(c)} \mathsf{a}_{\nu\sigma}^{(c)} \mathrm{PT}_\sigma \,, \qquad \mathsf{a}_{\nu\sigma}^{(c)} = \begin{pmatrix} -1 & 0 & 0 & 0 & 0 & 0 \\ 0 & -1 & 0 & 0 & 0 & 0 \end{pmatrix},$$

$$\mathcal{N}^{(d)} = \mathcal{N}^{(e)} = \mathcal{N}^{(f)} = 0 \,,$$

$$\mathcal{N}^{(g)} = c_{12345}^{(a)} \sum_{1\leq\sigma\leq6} N_1^{(g)} \mathsf{a}_{1\sigma,(12345)}^{(g)} \mathrm{PT}_\sigma \qquad \mathsf{a}_{1\sigma,(12345)}^{(g)} = \frac{1}{4}\begin{pmatrix} 1 & 0 & 3 & 0 & 0 & -2 \end{pmatrix},$$

$$+ c_{31245}^{(b)} \sum_{1\leq\sigma\leq6} N_1^{(g)} \mathsf{a}_{1\sigma,(31245)}^{(g)} \mathrm{PT}_\sigma \,, \qquad \mathsf{a}_{1\sigma,(31245)}^{(g)} = \begin{pmatrix} 0 & 0 & -1 & 0 & 0 & 0 \end{pmatrix},$$

$$\mathcal{N}^{(h)} = c_{12345}^{(a)} \sum_{\substack{1\leq\nu\leq4 \\ 1\leq\sigma\leq6}} N_\nu^{(h)} \mathsf{a}_{\nu\sigma,(12345)}^{(h)} \mathrm{PT}_\sigma \qquad \mathsf{a}_{\nu\sigma,(12345)}^{(h)} = \frac{1}{4}\begin{pmatrix} 4 & 0 & 4 & 0 & 0 & -4 \\ 2 & 0 & 3 & 0 & 1 & -2 \\ -2 & 0 & -3 & 0 & -1 & 2 \\ 4 & 0 & 4 & 0 & 0 & -4 \end{pmatrix},$$

$$+ c_{12543}^{(a)} \sum_{\substack{1\leq\nu\leq4 \\ 1\leq\sigma\leq6}} N_\nu^{(h)} \mathsf{a}_{\nu\sigma,(12543)}^{(h)} \mathrm{PT}_\sigma \,, \qquad \mathsf{a}_{\nu\sigma,(12543)}^{(h)} = \mathsf{a}_{\nu\sigma,(12345)}^{(h)} \,,$$

$$\mathcal{N}^{(i)} = c_{12345}^{(a)} \sum_{1\leq\sigma\leq6} N_1^{(i)} \mathsf{a}_{1\sigma,(12345)}^{(i)} \mathrm{PT}_\sigma \qquad \mathsf{a}_{1\sigma,(12345)}^{(i)} = 2\begin{pmatrix} 0 & 0 & -1 & 0 & 0 & 1 \end{pmatrix},$$

$$+ c_{13245}^{(a)} \sum_{1\leq\sigma\leq6} N_1^{(i)} \mathsf{a}_{1\sigma,(13245)}^{(i)} \mathrm{PT}_\sigma \qquad \mathsf{a}_{1\sigma,(13245)}^{(i)} = 2\begin{pmatrix} 0 & 0 & 0 & 0 & 0 & 1 \end{pmatrix},$$

$$+ c_{12543}^{(a)} \sum_{1\leq\sigma\leq6} N_1^{(i)} \mathsf{a}_{1\sigma,(12543)}^{(i)} \mathrm{PT}_\sigma \qquad \mathsf{a}_{1\sigma,(12543)}^{(i)} = 2\begin{pmatrix} 1 & 0 & 1 & 0 & 1 & -1 \end{pmatrix},$$

$$+ c_{15243}^{(a)} \sum_{1\leq\sigma\leq6} N_1^{(i)} \mathsf{a}_{1\sigma,(15243)}^{(i)} \mathrm{PT}_\sigma \,, \qquad \mathsf{a}_{1\sigma,(15243)}^{(i)} = 2\begin{pmatrix} 0 & 0 & 0 & 0 & -1 & 0 \end{pmatrix}.$$

Table 3.5: The two-loop five-point numerators that contribute to the amplitude. The $N_\nu^{(x)}$ are listed in Table 3.3. The five-point PT_σ are listed in Eq. (3.28). We denote the numerators including color information as $\mathcal{N}^{(x)}$.

3.5 Zeros of the Integrand

In the previous section we gave explicit examples of the expansion of the amplitude, Eq. (3.1), in terms of a basis of pure integrands, giving new nontrivial evidence that the analytic consequences of dual conformal symmetry hold beyond the planar sector. In this section we take a further step and present evidence that the amplituhedron concept, which is a complete and self-contained geometric definition of the integrand, may exist beyond the planar sector as well.

As already mentioned in previous sections, beyond the planar limit we currently have no alternative other than to use diagrams representing local integrals, Eq. (3.1), as a starting point for defining nonplanar integrands. The lack of global variables makes it unclear how to directly test for a geometric construction analogous to the amplituhedron in the nonplanar sector. However, as discussed in Chapter 2, in the planar sector the (dual) amplituhedron construction implies that all coefficients in the expansion in Eq. (2.17) are determined by zero conditions, up to an overall normalization. We expect that if an analogous geometric construction exists in the nonplanar sector, then zero conditions should also determine the amplitude. This can be tested directly. Indeed, we conjecture that for the representation in Eq. (3.1):

All coefficients d_j are fixed by *zero* conditions, up to overall normalization.

This is the direct analog of the corresponding planar statement in Chapter 2. In the MHV case, which we consider here, the coefficients d_j are linear combinations of Parke-Taylor factors, so that only numerical coefficients $a_{\sigma,k,j}$ in Eq. (3.6) need to be determined. The above conjecture is a statement that we can obtain these coefficients using only zero conditions, up to an overall constant. Here we confirm this proposal for all amplitudes constructed in the previous section.

As a simple first example, consider the two-loop four-point amplitude. The integrand is given as a linear combination of planar and nonplanar double boxes, c.f. Section 3.2. The
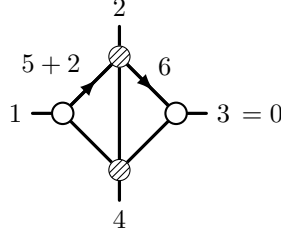
Figure 3.3: The two-loop four-point MHV amplitude vanishes on this cut. The four-point trees in the diagram have $k = 2$, so the overall helicity counting is $k = 1$.

Figure 3.4: The two-loop four-point amplitude evaluated on the cut of Figure 3.3. In each diagram the two shaded propagators are uncut, and every other propagator is cut. Eq. (3.35) gives the value of the cut.

only required condition to determine the unknown conditions is the cut in Figure 3.3.

In the full amplitude, we have contributions from the planar and nonplanar double boxes in Figure 3.2 and their permutations of external legs. All permutations of diagrams that contribute to the cut in Figure 3.3 are shown in Figure 3.4, along with their numerators and color factors. For convenience, we indicate the permutation labels of external legs of the seven contributing diagrams. There are only seven diagrams rather than nine because two of the nine diagrams have triangle subdiagrams, and so have vanishing numerators in $\mathcal{N} = 4$ SYM.

For the cut in Figure 3.3, five propagators are put on-shell so that the cut solution

60

depends on α, γ, and δ, three unfixed parameters of the loop momenta. Explicitly, the cut solution is given by

$$\ell_5^* + k_2 = \lambda_1 \left[\alpha \widetilde{\lambda}_1 + \frac{1}{\delta \langle 13 \rangle [23]} \left(\delta t - \alpha (s + \delta u + \gamma \langle 13 \rangle [12]) \right) \widetilde{\lambda}_2 \right],$$
$$\ell_6^* = \lambda_3 \left[\delta \widetilde{\lambda}_3 + \gamma \widetilde{\lambda}_2 \right]. \tag{3.29}$$

On this $k = 1$ cut, the MHV amplitude vanishes for any values of α, γ, δ. By cutting the Jacobian

$$J = \gamma \left(\delta t - \alpha (s + \delta u + \gamma \langle 13 \rangle [12]) \right), \tag{3.30}$$

the amplitude remains zero, and this condition simplifies. Specifically, this allows us to localize $\ell_5 + k_2$ to be collinear with k_1 and to localize ℓ_6 to be collinear with k_3. This is equivalent to taking further residues of the already-cut integrand at $\gamma = 0$, $\alpha = \delta t/(s + \delta u)$. On this cut, the solution for the loop momenta simplifies,

$$\ell_5^* + k_2 = \frac{\delta t}{s + \delta u} \lambda_1 \widetilde{\lambda}_1, \qquad \ell_6^* = \delta \lambda_3 \widetilde{\lambda}_3, \tag{3.31}$$

with the overall Jacobian $J' = s + u\delta$. Even in this simplified setting with one parameter δ left, the single zero cut condition Figure 3.3 is sufficient to fix the integrand up to an overall constant.

The numerators for the pure integrands, using the labels in Figure 3.2, are given in Eq. (3.9). Including labels for the external legs to help us track relabelings, these are

$$N_{1234}^{(\mathrm{p},1)} = s^2 t, \quad N_{1234}^{(\mathrm{np},1)} = su \left(\ell_5 - k_3 \right)^2, \quad N_{1234}^{(\mathrm{np},2)} = st \left(\ell_5 - k_4 \right)^2. \tag{3.32}$$

As noted near Eq. (3.21), there are only two Parke-Taylor factors independent under the $U(1)$-decoupling relations for four-particle scattering, namely $\mathrm{PT}_1 = \mathrm{PT}\,(1234)$ and $\mathrm{PT}_2 =$

PT (1243). Therefore the numerator ansatz for the planar diagram is

$$N^{(\mathrm{p})}_{1234} = \left(a^{(\mathrm{p})}_{1,1}\,\mathrm{PT}_1 + a^{(\mathrm{p})}_{1,2}\,\mathrm{PT}_2\right) N^{(\mathrm{p},1)}_{1234}. \tag{3.33}$$

For the nonplanar diagram, there are two pure integrands, each of which gets decorated with the two independent Parke-Taylor factors, so that the ansatz takes the form

$$\begin{aligned}
N^{(\mathrm{np})}_{1234} = \Big[&\left(a^{(\mathrm{np})}_{1,1}\,\mathrm{PT}_1 + a^{(\mathrm{np})}_{1,2}\,\mathrm{PT}_2\right) N^{(\mathrm{np},1)}_{1234} \\
&+ \left(a^{(\mathrm{np})}_{2,1}\,\mathrm{PT}_1 + a^{(\mathrm{np})}_{2,2}\,\mathrm{PT}_2\right) N^{(\mathrm{np},2)}_{1234} \Big],
\end{aligned} \tag{3.34}$$

and both numerators are then decorated with corresponding color factors $c^{(\mathrm{p})}_{1234}$, $c^{(\mathrm{np})}_{1234}$ and propagators. The $a^{(x)}_{i,j}$ coefficients are determined by demanding the integrand vanishes on the cut solution in Eq. (3.31).

Explicitly, the zero condition from the cut corresponding to Figure 3.4 is:

$$\begin{aligned}
0 = \Bigg(& \frac{c^{(\mathrm{p})}_{1234} N^{(\mathrm{p})}_{1234}}{\ell_5^2 \,(\ell_6 - k_3 - k_4)^2} + \frac{c^{(\mathrm{p})}_{4123} N^{(\mathrm{p})}_{4123}}{(\ell_5 - k_3)^2 \,(\ell_6 + k_2)^2} + \frac{c^{(\mathrm{np})}_{1234} N^{(\mathrm{np})}_{1234}}{\ell_5^2 \,(\ell_5 - \ell_6 - k_4)^2} \\
& + \frac{c^{(\mathrm{np})}_{4123} N^{(\mathrm{np})}_{4123}}{(\ell_5 - k_3)^2 \,(\ell_5 - \ell_6 + k_2)^2} + \frac{c^{(\mathrm{np})}_{3214} N^{(\mathrm{np})}_{3214}}{(\ell_6 + k_2)^2 \,(\ell_5 - \ell_6 - k_4)^2} \\
& + \frac{c^{(\mathrm{np})}_{3412} N^{(\mathrm{np})}_{3412}}{(\ell_6 - k_3 - k_4)^2 \,(\ell_5 - \ell_6 + k_2)^2} + \frac{c^{(\mathrm{np})}_{4213} N^{(\mathrm{np})}_{4213}}{(\ell_5 - \ell_6 + k_2)^2 \,(\ell_5 - \ell_6 - k_4)^2} \Bigg)\Bigg|_{\ell_5^*,\ell_6^*}. \tag{3.35}
\end{aligned}$$

The sum runs over the seven contributing diagrams, following the order displayed in Figure 3.4. The denominators are the two propagators that are left uncut in each diagram when performing this cut. One of the terms in the cut equation, for example the fifth term, is

$$\begin{aligned}
\frac{N^{(\mathrm{np})}_{3214}}{(\ell_6 + k_2)^2 \,(\ell_5 - \ell_6 - k_4)^2} = \; & \frac{1}{(\ell_6 + k_2)^2 \,(\ell_5 - \ell_6 - k_4)^2} \\
& \times \Big[\left(a^{(\mathrm{np})}_{1,1}\mathrm{PT}\,(3214) + a^{(\mathrm{np})}_{1,2}\mathrm{PT}\,(4213)\right) tu\,(\ell_6 + k_1 + k_2)^2 \\
& + \left(a^{(\mathrm{np})}_{2,1}\mathrm{PT}\,(3214) + a^{(\mathrm{np})}_{2,2}\mathrm{PT}\,(4213)\right) st\,(\ell_6 + k_2 + k_4)^2 \Big].
\end{aligned} \tag{3.36}$$

This has been relabeled from the master labels of Eq. (3.32) to the labels of the third nonplanar diagram in Figure 3.4, including the two uncut propagators. Specifically $\ell_5 \mapsto -\ell_6 - k_2$ and $\ell_6 \mapsto -\ell_5 - k_1$ is the relabeling for this diagram. A key simplifying feature is that the $a_{i,j}^{(x)}$ coefficients do not change under this relabeling so as to maintain crossing symmetry; the same four coefficients contribute to all five of the nonplanar double boxes that appear, for example. As discussed in Subsection 3.3.2, the Parke-Taylor factors that appear in Eq. (3.36) do not necessarily need to be in the chosen basis, although here $\text{PT}(3214) = \text{PT}_1$ and $\text{PT}(4213) = \text{PT}_2$.

The single zero condition Eq. (3.35) determines five of the six $a_{ij}^{(x)}$ parameters. This is, consistent with our conjecture above, the maximum amount of information that we can extract from all zero conditions. To do so in this example, we reduce to the two-member Parke-Taylor basis mentioned before, and also use Jacobi identities to reduce the seven contributing color factors to a basis of four. Since the remaining Parke-Taylor and color factors are independent, setting the coefficients of $\text{PT} \cdot c$ to zero yields eight potentially independent equations for the six coefficients. It turns out only five are independent:

$$a_{1,2}^{(p)} = a_{1,1}^{(p)} + 3a_{1,1}^{(np)} + a_{2,1}^{(np)} = a_{1,1}^{(p)} + a_{1,1}^{(np)} + a_{2,1}^{(np)} = 0, \qquad (3.37)$$
$$2a_{1,2}^{(p)} - a_{1,1}^{(np)} + a_{1,2}^{(np)} - a_{2,1}^{(np)} + a_{2,2}^{(np)} = a_{1,2}^{(p)} + a_{1,1}^{(np)} + a_{1,2}^{(np)} - a_{2,1}^{(np)} + 3a_{2,2}^{(np)} = 0.$$

The solution for this system is

$$a_{1,2}^{(p)} = a_{1,1}^{(np)} = a_{2,2}^{(np)} = 0, \qquad a_{1,2}^{(np)} = a_{2,1}^{(np)} = -a_{1,1}^{(p)}, \qquad (3.38)$$

and any of $a_{1,2}^{(np)}$, $a_{2,1}^{(np)}$, or $a_{1,1}^{(p)}$ is the overall undetermined parameter. This matches the result in Eq. (3.17), if we take $a_{1,1}^{(p)} = 1$. This last condition is exactly the overall scale that the zero conditions cannot determine, and must fixed by matching to an inhomogeneous cut.

Finally, we confirmed that the three-loop four-point and two-loop five-point amplitudes can also be uniquely determined via a zero cut condition up to a single overall constant.
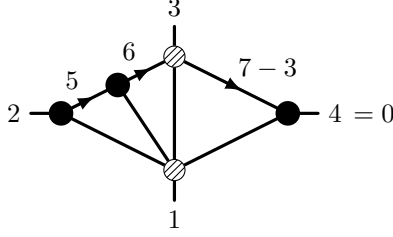
Figure 3.5: The three-loop four-point MHV amplitude vanishes on this cut. The five-point tree at the bottom of the diagram has $k = 2$ or $k = 3$, so the overall helicity counting is $k = 3$ or $k = 4$.
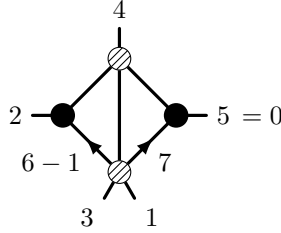
Figure 3.6: The two-loop five-point MHV amplitude vanishes on this cut. The five-point tree at the bottom of the diagram has $k = 2$ or $k = 3$, so the overall helicity counting is $k = 3$ or $k = 4$.

We used the cut in Figure 3.5 to determine the arbitrary parameters in the three-loop four-point amplitude, and we used the cut in Figure 3.6 to determine the parameters of the two-loop five-point amplitude. We also confirmed in both cases that using one cut where the amplitude does not vanish is sufficient to determine the overall unfixed parameter to the correct value. To confirm that the so-constructed amplitudes are correct, we verified a complete set of unitarity cuts needed to fully determine the amplitudes, matching to the corresponding cuts of previously known results in Refs. [13, 107, 126].

We thus conclude that in all three examples that we analyzed, the coefficients in the expansion Eq. (3.6) are determined up to one constant by zero conditions. The set of relations is more complicated in the three-loop four-point and two-loop five-point examples than in the two-loop four-point example, but in all cases all coefficients are determined as simple rational numbers without any kinematic dependence, leaving one overall coefficient free.

While far from a proof, these results point to the existence of an amplituhedron-like construction in the nonplanar sector of the theory. As discussed in Chapter 2, in the planar sector the existence of such a construction implies that homogeneous conditions determine the amplitudes up to an overall normalization. This is indeed what we have found in the various nonplanar examples studied above: the homogeneous requirements of only logarithmic singularities, no poles at infinity, and vanishing of unphysical cuts do determine the amplitudes. In any case, the notion that homogeneous conditions fully determine amplitudes opens a door to applying these ideas to other theories where no geometric properties are expected. Of course, we ultimately would like a direct amplituhedron-like geometric formulation of $\mathcal{N} = 4$ SYM amplitudes, including the nonplanar contributions. As a next step, we would need sensible global variables that allow us to define a unique integrand, generalizing the power of momentum twistors in the planar sector.

3.6 Summary of Loop-Level Results

In this chapter, we found evidence that an amplituhedron-like construction of nonplanar $\mathcal{N} = 4$ SYM theory scattering amplitudes may exist. We did so by checking the expected consequences of such a construction: that the integrand should be determined by homogeneous conditions, such as vanishing on certain cut solutions. We also gave additional nontrivial evidence for the conjecture that only logarithmic singularities appear in nonplanar amplitudes [2, 108], which is another characteristic feature of planar amplitudes resulting from the amplituhedron construction.

An important complication is that unlike in the planar sector, there is no unique integrand of scattering amplitudes which can be directly interpreted as a volume of some space. This forced us to chop up the amplitude into local diagrams containing only Feynman propagators. As pointed out in Ref. [108] and further developed in Ref. [2], analytic properties that follow from dual conformal invariance can be imposed on such local diagrams. We developed the notion of a pure integrand basis: a basis of integrands with only logarithmic singularities,

no poles at infinity, and only unit leading singularities. The first property is motivated by the analogous statement for on-shell diagrams in $\mathcal{N} = 4$ SYM. If, like in the planar case, we understood how to formulate nonplanar recursion relations, we expect that it would then be possible to express nonplanar amplitudes directly as sums of on-shell diagrams [49, 111, 130] and manifestly expose their $d$log structure. The latter two properties lift the exact content of the planar sector's dual conformal symmetry to the nonplanar one.

We constructed a pure integrand basis for each of the two-loop four-point, three-loop four-point and two-loop five-point amplitudes, and showed that the amplitudes could be expanded in their respective bases. This confirmed that the three example amplitudes share the three properties of the pure integrands. Our pure integrand representations here are closely related to Refs. [2, 108] for four-point amplitudes at two- and three-loops, while our representation of the two-loop five-point amplitude, first published in Ref. [3], has completely novel properties compared to the result in Ref. [13]. The fact that we exposed analytic properties in the nonplanar sector similar to those connected to dual conformal symmetry in the planar sector suggests that an analog of dual conformal symmetry may exist in the nonplanar sector. (For Yangian symmetry a similar statement is less clear, although there has been some recent work in this direction in Ref. [131].)

One particularly bold future goal is to lift the amplituhedron [53] paradigm from the planar sector to the nonplanar sector of $\mathcal{N} = 4$ SYM. The amplituhedron provides a geometric picture of the planar integrand where all standard physical principles like locality and unitarity are derived. In such a picture, traditional ways of organizing amplitudes, be it via Feynman diagrams, unitarity cuts, or even on-shell diagrams, are consequences of amplituhedron geometry, rather than *a priori* organizational principles. The amplituhedron reverses traditional logic, as logarithmic singularities and dual conformal symmetry, rather than locality and unitarity, are fundamental inputs into the definition of the amplituhedron. The definition then invokes intuitive geometric ideas about the inside of a projective triangle, generalized to the more complicated setting of Grassmannian geometry.

We would like to carry this geometric picture over to the nonplanar sector. However, a

66

lack of global variables limits us to demanding that the amplitude be a sum of local integrals. This already imposes locality and some unitarity constraints. Nevertheless, after imposing special analytic structures on the basis integrals — unit logarithmic singularities with no poles at infinity — one can extract the "remaining" geometric information. Motivated by the discussion in Ref. [97], we conjecture that this remaining information is a set of *zero conditions*, i.e. cuts on which the amplitude vanishes. This is exactly the statement which we successfully carried over to the nonplanar sector and tested in examples in Section 3.5. Here we propose that after constructing a pure integrand basis, zero conditions are sufficient for finding the complete amplitude, up to normalization.

This provides nontrivial evidence that an amplituhedron-like construction might very well exist beyond the planar limit for amplitudes in $\mathcal{N} = 4$ SYM theory. However there are still many obstacles including, among other things, a choice of good variables and a geometric space in which nonplanar scattering amplitudes are defined as volumes. If such a nonplanar amplituhedron really exists, it would be phrased in terms of very interesting mathematical structures going beyond those of the planar amplituhedron.

If our zero condition conjecture indeed holds, how might it extend to other theories? The most naive possibility is that $\mathcal{N} = 4$ SYM amplitudes are the most constrained amplitudes and so need no inhomogeneous conditions except for overall normalization, while amplitudes in other theories, with less supersymmetry for example, do need additional inhomogeneous information. Even in such theories the zero conditions would still constrain the amplitudes, and it would be interesting to see which and how many additional inhomogeneous conditions are required to completely determine the amplitudes.

It may be possible to link the $\mathcal{N} = 4$ SYM results we presented here directly to identical helicity amplitudes in quantum chromodynamics (QCD) via dimension shifting relations [132, 133]. These relations were recently employed to aid in the construction of a representation of the two-loop five-point identical helicity QCD amplitude where the duality between color and kinematics holds [134]. It should also be possible to find a new representation of the identical helicity QCD amplitude in terms of the $\mathcal{N} = 4$ SYM representation

we gave here.

Another line of research is to concentrate on individual integrals rather than on the full amplitude. After integration, integrands with only logarithmic singularities are expected to have uniform maximum transcendental weight at the loop order of the integrand [135]. This provides a nice connection between properties of the integrand and conjectured properties of final integrated amplitudes. On the practical level, having a good basis of master integrals under integral reduction is important for many problems, including applications to phenomenology. As explained in Refs. [136, 137], uniformly transcendental integrals obey relatively simple differential equations, making them easy to work with [138, 139]. This also makes our basis of pure integrands useful for five-point scattering in NNLO QCD. For a recent discussion of the planar case see Ref. [140].

As already noted in Ref. [2], the types of gauge-theory results described here can have a direct bearing on issues in quantum gravity, through the double-copy relation of Yang-Mills theories to gravity [107]. We expect that developing a better understanding of the nonplanar sector of $\mathcal{N} = 4$ SYM will aid our ability to construct corresponding gravity amplitudes, where no natural separation of planar and nonplanar contributions exists.

In summary, we have presented evidence that nonplanar integrands of $\mathcal{N} = 4$ SYM share important analytic structure with planar ones. We have also presented evidence for a geometric structure similar to the amplituhedron [53], based on the idea that such a structure implies that zero conditions are sufficient to fix the amplitude, up to an overall normalization. While there is much more to do, these results suggest that the full theory has structure at least as rich as the planar theory.

APPENDIX A

Logarithmic Singularities and Poles at Infinity

APPENDIX B

Logarithmic Singularities and Poles at Infinity

B.1   Logarithmic Singularities and $d\log$ Forms

In this appendix, we give a thorough review of the concept of $d\log$ forms in the context of ordinary momentum-space variables. This serves to clarify the mathematics, as well as strip away any confusion that may result from the use of momentum twistors and notational conveniences. It is natural to define an integrand form $\Omega(x_1, \ldots, x_m)$ of the integral F by stripping off the integration symbol

$$F = \int \Omega(x_1, \ldots, x_m) \,, \tag{B.1}$$

and to study its singularity structure. There is a special class of forms that we are interested in here: those that have only *logarithmic singularities*. As defined in Eq. (2.15), a form has only logarithmic singularities if near any pole $x_i \to a$ it behaves as

$$\Omega(x_1, \ldots, x_m) \to \frac{dx_i}{x_i - a} \wedge \hat{\Omega}(x_1, \ldots, \hat{x}_i, \ldots, x_m) \,, \tag{B.2}$$

where $\hat{\Omega}(x_1, \ldots, \hat{x}_i, \ldots x_m)$ is an $(m-1)$-form[1] in all variables except $\hat{x}_i$. An equivalent terminology is that there are only simple poles. That is, we are interested in integrands

---

[1] The signs from the wedge products will not play a role because at the end we will construct basis elements whose normalization in the amplitude is fixed from unitarity cuts.

where we can change variables $x_i \to g_i(x_j)$ such that the form becomes

$$\Omega = d\log g_1 \wedge d\log g_2 \wedge \cdots \wedge d\log g_m \, , \tag{B.3}$$

where we denote

$$d\log x \equiv \frac{dx}{x} \, . \tag{B.4}$$

We refer to this representation as a "$d$log form".

A simple example of such a form is $\Omega(x) = dx/x \equiv d\log x$, while $\Omega(x) = dx$ or $\Omega(x) = dx/x^2$ are examples of forms which do not have this property. A trivial two-form with logarithmic singularities is $\Omega(x, y) = dx \wedge dy/(xy) = d\log x \wedge d\log y$. A less trivial example of a $d$log form is

$$\Omega(x, y) = \frac{dx \wedge dy}{xy(x + y + 1)} = d\log\frac{x}{x + y + 1} \wedge d\log\frac{y}{x + y + 1} \, . \tag{B.5}$$

In this case, the property of only logarithmic singularities is not obvious from the first expression, but a change of variables resulting in the second expression makes the fact that Ω is a $d$log form manifest. This may be contrasted with the form

$$\Omega(x, y) = \frac{dx \wedge dy}{xy(x + y)} \, , \tag{B.6}$$

which is not logarithmic because near the pole $x = 0$ it behaves as dy/y^2; this form cannot be written as a $d$log form. In general, the nontrivial changes of variables required can make it difficult to find explicit $d$log forms even where they exist.

In a bit more detail, consider the behavior of a form near $x = 0$. If the integrand scales as dx/x^m for integer m, we consider two different regimes where integrands can fail to have logarithmic singularities. The first is when $m \geq 2$, which results in double or higher poles at $x = 0$. The second is when $m \leq 0$, which results in a pole at infinity. Avoiding unwanted singularities, either at finite or infinite values of x, leads to tight constraints on our integrands, as is covered in Section 2.4. Since we take the denominators to be the standard
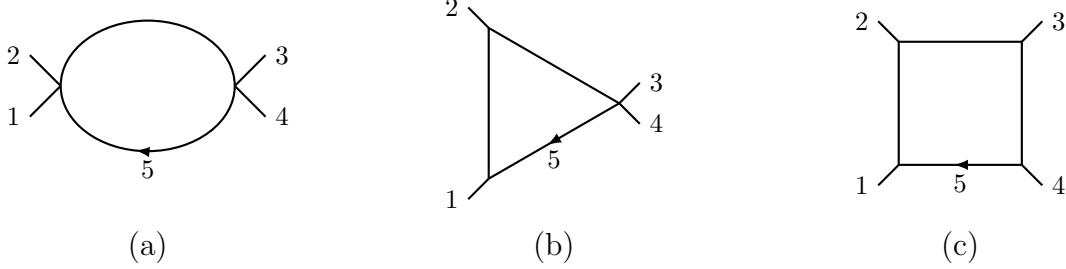
Figure B.1: The (a) bubble, (b) triangle and (c) box one-loop diagrams.

Feynman propagators associated to a given diagram, in our expansion of the amplitude the only available freedom is to adjust the kinematic numerators. As a simple toy example, consider the form

$$\Omega(x, y) = \frac{dx \wedge dy \; N(x, y)}{xy(x + y)} \; . \tag{B.7}$$

As noted above, for a constant numerator $N(x, y) = 1$ the form develops a double pole at $x = 0$. Similarly, for $N(x, y) = x^2 + y^2$ the form behaves like dy for $x = 0$ and again it is not logarithmic. There is only one class of numerators that make the form logarithmic near $x = 0$ and $y = 0 : N(x, y) = a_1 x + a_2 y$ for arbitrary a_1 and a_2.

Our discussion of loop integrands in Chapter 3 follows this pattern: constant numerators (i.e. those independent of loop momenta) are dangerous, for they may allow double or higher poles located at finite values of loop momenta, while a numerator with too many powers of loop momentum can develop higher poles at infinity. It turns out that the first case is generally the problem in gauge theory, whereas the second case usually arises for gravity amplitudes, because the power counting of numerators is boosted relative to the gauge-theory case. For $\mathcal{N} = 4$ SYM integrands, we carefully tune numerators so that only logarithmic singularities are present. The desired numerators live exactly on the boundary between too many and too few powers of loop momenta.

B.2 Loop Integrands and Poles at Infinity

Now consider the special class of four-forms that correspond to one-loop integrands. Standard integral reduction methods [141, 142] reduce any massless one-loop amplitude to a linear combination of box, triangle and bubble integrals. In nonsupersymmetric theories, there are additional rational terms arising from loop momenta outside of $D = 4$; these are not relevant for our discussion of $\mathcal{N} = 4$ SYM theory. While it will eventually be necessary to include the (-2ϵ) dimensional components of loop momenta, since these are in general required by dimensional regularization, for the purposes of studying the singularities of the integrand we simply put this matter aside. In any case, direct checks reveal that these (-2ϵ) dimensional pieces do not lead to extra contributions through at least six loops in $\mathcal{N} = 4$ SYM four-point amplitudes [113]. That is, the naive continuation of the four-dimensional integrand into D dimensions yields the correct results. As usual, infrared singularities are regularized using dimensional regularization. (See for example, Refs. [126, 128, 143].) We focus here on the four-point case, but a similar analysis can be performed for larger numbers of external legs as well, although in this case we expect nontrivial corrections from (-2ϵ) components of the loop momenta.

Consider the bubble, triangle and box integrals in Fig. B.1, taking all external legs as outgoing. The explicit forms in $D = 4$ are

$$d\mathcal{I}_2 = d^4\ell_5 \frac{1}{\ell_5^2(\ell_5 - k_1 - k_2)^2} \,,$$

$$d\mathcal{I}_3 = d^4\ell_5 \frac{s}{\ell_5^2(\ell_5 - k_1)^2(\ell_5 - k_1 - k_2)^2} \,, \tag{B.8}$$

$$d\mathcal{I}_4 = d^4\ell_5 \frac{st}{\ell_5^2(\ell_5 - k_1)^2(\ell_5 - k_1 - k_2)^2(\ell_5 + k_4)^2} \,,$$

where we have chosen a convenient normalization. (Note this matches Eq. (2.7).) The variables $s = (k_1 + k_2)^2$ and $t = (k_2 + k_3)^2$ are the usual Mandelstam invariants, depending only on external momenta. Under integration, these forms are infrared or ultraviolet divergent and need to be regularized, but as mentioned above we set this aside and work directly in

four dimensions.

In $D = 4$, we can parametrize the loop momentum in terms of four independent vectors constructed from the spinor-helicity variables associated with the external momenta $k_1 = \lambda_1 \tilde{\lambda}_1$ and $k_2 = \lambda_2 \tilde{\lambda}_2$. A clean choice for the four degrees of freedom of the loop momentum is

$$\ell_5 = \alpha_1 \lambda_1 \tilde{\lambda}_1 + \alpha_2 \lambda_2 \tilde{\lambda}_2 + \alpha_3 \lambda_1 \tilde{\lambda}_2 + \alpha_4 \lambda_2 \tilde{\lambda}_1 , \qquad (B.9)$$

where the α_i are now the independent variables. Writing $d\mathcal{I}_2$ in this parametrization we obtain

$$d\mathcal{I}_2 = \frac{d\alpha_1 \wedge d\alpha_2 \wedge d\alpha_3 \wedge d\alpha_4}{(\alpha_1 \alpha_2 - \alpha_3 \alpha_4)(\alpha_1 \alpha_2 - \alpha_3 \alpha_4 - \alpha_1 - \alpha_2 + 1)} . \qquad (B.10)$$

In general, since we are not integrating the expressions, we ignore Feynman's $i\epsilon$ prescription and any factors of i from Wick rotation.

To study the singularity structure, we can focus on subregions of the integrand by imposing on-shell or cut conditions. As an example, the cut condition $\ell_5^2 = 0$ can be computed in these variables by setting

$$0 = \ell_5^2 = (\alpha_1 \alpha_2 - \alpha_3 \alpha_4)s . \qquad (B.11)$$

We can then eliminate one of the α_i, say α_4, by computing the residue on the pole located at $\alpha_4 = \alpha_1 \alpha_2 / \alpha_3$. This results in a residue,

$$\operatorname*{Res}_{\ell_5^2 = 0} d\mathcal{I}_2 = \frac{d\alpha_3}{\alpha_3} \wedge \frac{d\alpha_2}{(\alpha_2 + \alpha_1 - 1)} \wedge d\alpha_1 . \qquad (B.12)$$

Changing variables to $\alpha_\pm = \alpha_1 \pm \alpha_2$, this becomes

$$\operatorname*{Res}_{\ell_5^2 = 0} d\mathcal{I}_2 = \frac{d\alpha_3}{\alpha_3} \wedge \frac{d\alpha_+}{(\alpha_+ - 1)} \wedge d\alpha_- . \qquad (B.13)$$

We can immediately see that the form $d\mathcal{I}_2$ is non-logarithmic in α_-, and thus the bubble integrand has a nonlogarithmic singularity in this region.

Carrying out a similar exercise for the triangle $d\mathcal{I}_3$ using the parametrization in Eq. (B.9),

we obtain

$$d\mathcal{I}_3 = \frac{d\alpha_1 \wedge d\alpha_2 \wedge d\alpha_3 \wedge d\alpha_4}{(\alpha_1\alpha_2 - \alpha_3\alpha_4)(\alpha_1\alpha_2 - \alpha_3\alpha_4 - \alpha_2)(\alpha_1\alpha_2 - \alpha_3\alpha_4 - \alpha_1 - \alpha_2 + 1)}\,. \tag{B.14}$$

We can make a change of variables and rewrite it in the manifest $d$log form,

$$d\mathcal{I}_3 = d\log\left(\alpha_1\alpha_2 - \alpha_3\alpha_4\right) \wedge d\log\left(\alpha_1\alpha_2 - \alpha_3\alpha_4 - \alpha_2\right) \wedge d\log(\alpha_1\alpha_2 - \alpha_3\alpha_4 - \alpha_1 - \alpha_2 + 1) \wedge d\log\alpha_3\,. \tag{B.15}$$

Translating this back into momentum space:

$$d\mathcal{I}_3 = d\log\ell_5^2 \wedge d\log(\ell_5 - k_1)^2 \wedge d\log(\ell_5 - k_1 - k_2)^2 \wedge d\log(\ell_5 - k_1) \cdot (\ell_5^* - k_1)\,, \tag{B.16}$$

where $\ell_5^* \equiv \beta\lambda_2\widetilde{\lambda}_1 + \lambda_1\widetilde{\lambda}_1$ is one of the two solutions to the triple cut. The parameter β is arbitrary in the triple cut solution, and the $d$log form is independent of it. For the box integral, a similar process followed in Ref. [49] results in

$$d\mathcal{I}_4 = d\log\frac{\ell_5^2}{(\ell_5 - \ell_5^*)^2} \wedge d\log\frac{(\ell_5 - k_1)^2}{(\ell_5 - \ell_5^*)^2} \wedge d\log\frac{(\ell_5 - k_1 - k_2)^2}{(\ell_5 - \ell_5^*)^2} \wedge d\log\frac{(\ell_5 + k_4)^2}{(\ell_5 - \ell_5^*)^2}\,, \tag{B.17}$$

where $\ell_5^* \equiv -\frac{\langle 14\rangle}{\langle 24\rangle}\lambda_2\widetilde{\lambda}_1 + \lambda_1\widetilde{\lambda}_1$.

While both triangle and box integrands can be written in $d$log form, there is an important distinction between the triangle form $d\mathcal{I}_3$ and the box form $d\mathcal{I}_4$. On the cut $\alpha_4 = \alpha_1\alpha_2/\alpha_3$, one $d$log-factor in $d\mathcal{I}_3$ depends only on α_3 and develops a singularity in the limit $\alpha_3 \to \infty$ (which implies $\ell_5 \to \infty$); this does not occur with $d\mathcal{I}_4$. We refer to any singularity that develops as a loop momentum approaches infinity (in our example, $\ell_5 \to \infty$) at any step in the cut structure as a *pole at infinity*. To be more specific, even if a $d$log form has no pole at infinity before imposing any cut conditions, it is possible to generate such poles upon taking residues, as we saw in the example of the triangle integrand above. In this sense, the pole at infinity property is more refined than simple power counting, which only considers the overall scaling of an integrand before taking any cuts.
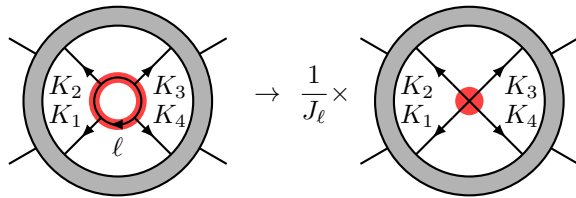
75

Figure B.2: The left diagram is a generic L-loop contribution to the four-point $\mathcal{N} = 4$ SYM amplitude. The thick (red) highlighting indicates propagators replaced by on-shell conditions. After this replacement, the highlighted propagators leave behind the simplified diagram on the right multiplied by an inverse Jacobian, Eq. (B.20). The four momenta $K_1, \ldots, K_4$ can correspond either to external legs or propagators of the higher-loop diagram.

The issue of poles at infinity is important for both $\mathcal{N} = 4$ SYM and $\mathcal{N} = 8$ supergravity amplitudes. While a lack of poles at infinity implies ultraviolet finiteness, having poles at infinity does not necessarily mean that there are divergences. For example, the triangle integral contains such a pole in the cut structure but is ultraviolet finite. In principle, there can also be nontrivial cancelations between different contributions.

To find numerators that do not allow these poles at infinity and also ensure only logarithmic singularities, it is not necessary to compute every residue of the integrand. This is because cutting box subdiagrams from a higher loop diagram, as on the left in Fig. B.2, can only increase the order of remaining poles in the integrand. To see this, consider computing the four residues that correspond to cutting the four highlighted propagators in Fig. B.2,

$$\ell^2 = (\ell - K_1)^2 = (\ell - K_1 - K_2)^2 = (\ell + K_4)^2 = 0 \,. \tag{B.18}$$

This residue is equivalent to computing the Jacobian obtained by replacing the box propagator with on-shell delta functions. This Jacobian is then

$$J_\ell = |\partial P_i / \partial \ell^\mu| \,, \tag{B.19}$$

where the P_i correspond to the four inverse propagators placed on shell in Eq. (B.18). (See, for example, Ref. [120] for more details.) Another way to obtain this Jacobian is by reading

off the rational factors appearing in front of the box integrals—see appendix I of Ref. [142].

In the generic case, J_ℓ contains square roots, making it difficult to work with. In special cases it simplifies. For example for $K_1 = k_1$ massless, the three-mass normalization is

$$J_\ell = (k_1 + K_2)^2 (K_4 + k_1)^2 - K_2^2 K_4^2 . \tag{B.20}$$

If in addition $K_3 = k_3$ is massless, the so-called "two-mass-easy" case, the numerator factorizes into a product of two factors, a feature that is important in many calculations. Specifically,

$$J_\ell = (K_2 + k_1)^2 (K_4 + k_1)^2 - K_2^2 K_4^2 = (K_2 \cdot q)(K_2 \cdot \bar{q}), \tag{B.21}$$

where $q = \lambda_1 \widetilde{\lambda}_3$ and $\bar{q} = \lambda_3 \widetilde{\lambda}_1$. If instead both $K_1 = k_1$ and $K_2 = k_2$ are massless, we get the "two-mass-hard" normalization

$$J_\ell = (k_1 + k_2)^2 (K_3 + k_2)^2 . \tag{B.22}$$

These formulas are useful at higher loops, where the K_j depend on other loop momenta.

Notice that these Jacobians go into the denominator of the integrand after a box-cut is applied. Therefore they can only raise the order of the remaining poles in the integrand. Our basic approach utilizes this fact: we cut embedded box subdiagrams from diagrams of interest and update the integrand by dividing by the obtained Jacobian (B.19). Then we identify all kinematic regions that can result in a double pole in the integrand.

It would be cumbersome to write out all cut equations for every such sequence of cuts, so we introduce a compact notation:

$$\text{cut} = \{\ldots, (\ell - K_i)^2, \ldots, B(\ell), \ldots, B(\ell', (\ell' - Q)), \ldots\} . \tag{B.23}$$

Here:

- Cuts are applied in the order listed.

- A propagator listed by itself, as $(\ell - K_i)^2$ is, means: "Cut just this propagator."

- $B(\ell)$ means: "Cut the four propagators that depend on ℓ." This exactly corresponds to cutting the box propagators as in Eq. (B.18) and Fig. B.2.

- $B(\ell', (\ell' - Q))$ means: "Cut the three standard propagators depending on ℓ', as well as a fourth $1/(\ell' - Q)^2$ resulting from a previously obtained Jacobian." The momentum Q depends on other momenta besides ℓ'. The four cut propagators form a box.

We use this notation in Appendix C.

APPENDIX C

Direct Construction of the Amplitude

In this appendix, we discuss how to directly construct the two-loop and three-loop four-point amplitudes in $\mathcal{N} = 4$ super-Yang-Mills without first constructing a pure integrand basis. This was the approach followed in Ref. [2], and this appendix is based largely on the discussion therein. While very similar to the methods of Chapter 3, there are some differences. In particular, there is some additional material on freedom in the final expression for the amplitude due to color Jacobi relations, a feature which does not exist when a pure integrand basis is used.

C.1   Strategy for Nonplanar Amplitudes

As discussed in Chapter 3, instead of trying to define a nonplanar global integrand, we subdivide the amplitude into diagrams with their own momentum labels and analyze them one by one. In Ref. [108], the $\mathcal{N} = 4$ SYM two-loop four-point amplitude was rewritten in a form with no logarithmic singularities and no poles at infinity. In this section, we develop a strategy for doing the same at higher loop orders. We emphasize that we are working at the level of the amplitude integrand prior to integration. In particular, we do not allow for any manipulations that involve the integration symbol (e.g. integration-by-parts identities) to shuffle singularities between contributions; this is discussed further in Subsection 3.1.1.

Our general procedure has four steps:

1. Define a set of parent diagrams whose propagators are the standard Feynman ones. The parent diagrams are defined to have only cubic vertices and loop momentum flowing

through all propagators.

2. Construct *d*log *numerators*. These are a basis set of numerators constructed so that each diagram has only logarithmic singularities and no poles at infinity. These numerators also respect diagram symmetries, including color signs. There is no requirement that these numerators give unit leading singularity integrands. Each *d*log numerator, together with the diagram propagators, forms a basis diagram.

3. Use simple unitarity cuts to determine the linear combination of basis diagrams that gives the amplitude.

4. Confirm that the amplitude so constructed is correct and complete. We use the method of maximal cuts [118] for this task.

There is no *a priori* guarantee that this will succeed. In principle, requiring *d*log numerators could make it impossible to expand the amplitude in terms of independent diagrams with Feynman propagators. Indeed, at a sufficiently high loop order we expect that even in the planar sector it may not be possible to find a covariant diagrammatic representation manifesting the desired properties; in such circumstances we would expect that unwanted singularities cancel between diagrams. This may happen even earlier in the nonplanar sector. As in many amplitude calculations, we simply assume that we can construct a basis with the desired properties, and then, once we have an ansatz, we check that it is correct by computing a complete set of cuts.

In this section, we illustrate the process of finding diagram integrands with the desired properties and explain the steps in some detail. For simplicity, we focus on the four-point amplitude, but we expect that a similar strategy is applicable for higher-point amplitudes in the MHV and NMHV sectors as well.

We use the one- and two-loop contributions to the four-point amplitudes to illustrate the procedure, before turning to three loops in Section C.2. We find that the canonical one-loop numerator is already a *d*log numerator, while the two-loop result illustrates the issues that
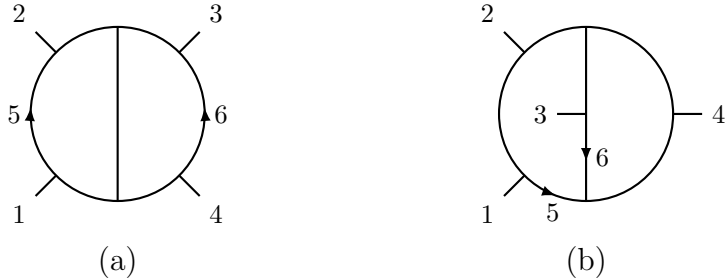
Figure C.1: Two-loop four-point parent diagrams for $\mathcal{N} = 4$ SYM theory. These are the same diagrams as appear in Figure 3.2.

we face at higher loops. The two-loop amplitude was first obtained in [125], but in a form that does not make the singularity structure clear. In Ref. [108], the two-loop amplitude was rewritten in a form that makes these properties manifest by rearranging contact terms in the amplitude by using a color Jacobi identities. In this section, we replicate this result by following our strategy of systematically constructing a basis of integrands with the desired properties. In subsequent sections, we apply our strategy to higher loops.

C.1.1 Constructing a Basis

The construction of a basis of integrands starts from a set of parent diagrams. We focus on graphs with only cubic vertices. Furthermore, we restrict to diagrams that do not have triangle or bubble subdiagrams, since these are not necessary for the $\mathcal{N} = 4$ amplitudes that we study. We also exclude any diagrams in which a propagator does not carry loop momentum, because such contributions can be absorbed into diagrams in which all propagators contain loop momenta. At the end, we confirm this basis of diagrams is sufficient by verifying a set of unitarity cuts that fully determine the amplitude.

At one loop, the parent diagrams are the three independent box integrals, one of which is displayed in Figure B.1(c), and the other two of which are cyclic permutations of the external legs k_2, k_3 and k_4 of this one. At two loops, the four-point amplitude of $\mathcal{N} = 4$ SYM theory has twelve parent diagrams, two of which are displayed in Figure C.1; the others are again just given by relabelings of external legs.

Unlike the planar case, there is no global, canonical way to label loop momenta in all diagrams. In each parent diagram, we label L independent loop momenta as $\ell_5, \ldots, \ell_{4+L}$. By conserving momentum at each vertex, all other propagators have sums of the loop and external momenta flowing in them. We define the L-loop *integrand* $\mathcal{I}^{(x)}$ of a diagram labeled by (x) by combining the kinematic part of the numerator with the Feynman propagators of the diagram as

$$\mathcal{I}^{(x)} \equiv \frac{N^{(x)}}{\prod_{\alpha_{(x)}} p_{\alpha_{(x)}}^2} \,. \tag{C.1}$$

The product in the denominator in Eq. (C.1) runs over all propagators $p_{\alpha_{(x)}}^2$ of diagram (x), and the kinematic numerator $N^{(x)}$ generally depends on loop momenta. From this we define an *integrand form*

$$d\mathcal{I}^{(x)} \equiv \prod_{l=5}^{4+L} d^4\ell_l \, \mathcal{I}^{(x)} \,. \tag{C.2}$$

This integrand form is a $4L$ form in the L independent loop momenta $\ell_5, \ldots, \ell_{4+L}$. We have passed factors of i, 2π, and coupling constants into the definition of the amplitude, Eq. (C.21). As mentioned previously, we focus on $D = 4$.

We define an expansion of the numerator

$$N^{(x)} = \sum_i a_i^{(x)} N_i^{(x)} \,, \tag{C.3}$$

where the $N_i^{(x)}$ are the $d$log numerators we aim to construct, and the $a_i^{(x)}$ are coefficients. We put off a detailed discussion of how to fix these coefficients until Subsection C.1.2, and here just mention that the coefficients can be obtained by matching an expansion of the amplitude in $d$log numerators to unitarity cuts or other physical constraints, such as leading singularities.

Starting from a generic numerator $N_i^{(x)}$, we impose the following constraints:

1. *Overall dimensionality.* $N_i^{(x)}$ must be a local polynomial of momentum invariants (i.e. $k_a \cdot k_b$, $k_a \cdot \ell_b$, or $\ell_a \cdot \ell_b$) with dimensionality $N_i^{(x)} \sim (p^2)^K$, where $K = P - 2L - 2$,

and P is the number of propagators in the integrand. We forbid numerators with $K < 0$.

2. *Asymptotic scaling.* For each loop momentum ℓ_l, the integrand $\mathcal{I}^{(x)}$ must not scale less than $1/(\ell_l^2)^4$ for $\ell_l \to \infty$ in all possible labelings.

3. *No double/higher poles.* The integrand $\mathcal{I}^{(x)}$ must be free of poles of order two or more in all kinematic regions.

4. *No poles at infinity.* The integrand $\mathcal{I}^{(x)}$ must be free of poles of any order at infinity in all kinematic regions.

The overall dimensionality and asymptotic scaling give us power counting constraints on the subdiagrams. In practice, these two constraints dictate the initial form of an ansatz for the numerator, while the last two conditions of no higher degree poles and no poles at infinity constrain that ansatz to select "$d$log numerators". The constraint on overall dimensionality is the requirement that the overall mass dimension of the integrand is $-4L-4$;[1] in $D = 4$ this matches the dimensionality of gauge-theory integrands. The asymptotic scaling constraint includes a generalization of the absence of bubble and triangle integrals at one-loop order in $\mathcal{N} = 4$ SYM theory and $\mathcal{N} = 8$ supergravity [144, 145]. This constraint is a necessary, but not a sufficient, condition for having only logarithmic singularities and no poles at infinity.

Notice that there is no requirement that the numerators lead to integrands with unit leading singularity; compare to the crieteria listed in Section 3.1. Indeed, relaxing this requirement will allow us to combine integrands with different leading singularities to respect diagram symmetries. It will also allow for additional freedom in our expression of the amplitude itself, due to color Jacobi identities discussed in Subsection C.2.3.

At one loop, the asymptotic scaling constraint implies that only Figure B.1(c), the box diagram, appears; coupling that with the overall dimensionality constraint implies that the

---

[1] The -4 in the mass dimension originates from factoring out a dimensionful quantity from the final amplitude in Eq. (C.21).

numerator is independent of loop momentum. The box numerator must then be a single basis element which we can normalize to be unity:

$$N_1^{(B)} = 1 \, . \tag{C.4}$$

In the one-loop integrand, neither higher-degree poles nor poles at infinity arise. Thus everything at one loop is consistent and manifestly exhibits only logarithmic singularities. A more thorough treatment of the one-loop box, including the sense in which logarithmic singularities are manifest in a box, is found in the context of $d$log forms in Ref. [2].

Next consider two loops. The analysis here will largely resemble that of Section 3.2, but the result for the nonplanar double box will be a symmetrized combination of the two pure integrands found there. First, notice that the asymptotic scaling constraint implies that only the planar and nonplanar double box diagrams in Figure C.1 appear, since the constraint forbids triangle or bubble subdiagrams. We now wish to construct the numerators $N^{(P)}$ and $N^{(NP)}$ for the planar (Figure C.1(a)) and nonplanar (Figure C.1(b)) diagrams respectively. There are different ways of labeling the two graphs. As already mentioned, we prefer labels in Figure C.1, where the individual loop momenta appear in the fewest possible number of propagators. This leads to the tightest power counting constraints in the sense of our general strategy outlined above. We consider the planar and nonplanar diagrams separately.

For the planar diagram in Figure C.1, only four propagators contain either loop momentum ℓ_5 or ℓ_6. By the asymptotic scaling constraint, the numerator must be independent of both loop momenta: $N^{(P)} \sim \mathcal{O}((\ell_5)^0, (\ell_6)^0)$. Since overall dimensionality restricts $N^{(P)}$ to be quadratic in momentum, we can write down two independent numerator basis elements:

$$N_1^{(P)} = s \, , \qquad N_2^{(P)} = t \, . \tag{C.5}$$

The resulting numerator is then a linear combination of these two basis elements:

$$N^{(P)} = a_1^{(P)} s + a_2^{(P)} t \, , \tag{C.6}$$

where the $a_j^{(P)}$ are constants, labeled as discussed after Eq. (C.3). Again, as in the one-loop case, there are no hidden double poles or poles at infinity from which nontrivial constraints could arise.

The nonplanar two-loop integrand $\mathcal{I}^{(NP)}$ is the first instance where nontrivial constraints result from requiring logarithmic singularities and the absence of poles at infinity, so we discuss this example in more detail. The choice of labels in Figure C.1(b) results in five propagators with momentum ℓ_5 but only four with momentum ℓ_6, so $N^{(NP)}$ is at most quadratic in ℓ_5 and independent of ℓ_6: $N^{(NP)} \sim \mathcal{O}((\ell_5)^2, (\ell_6)^0)$. Overall dimensionality again restricts $N^{(NP)}$ to be quadratic in momentum. This dictates the form of the numerator to be

$$N^{(NP)} = c_1 \ell_5^2 + c_2 (\ell_5 \cdot Q) + c_3 s + c_4 t \,, \tag{C.7}$$

where Q is some vector and the c_i are coefficients independent of loop momenta.

Now we search the integrand

$$\mathcal{I}^{(NP)} = \frac{c_1 \ell_5^2 + c_2 (\ell_5 \cdot Q) + c_3 s + c_4 t}{\ell_5^2 (\ell_5 + k_1)^2 (\ell_5 - k_3 - k_4)^2 \ell_6^2 (\ell_5 + \ell_6)^2 (\ell_5 + \ell_6 - k_4)^2 (\ell_6 + k_3)^2} \tag{C.8}$$

for double poles as well as poles at infinity, and impose conditions on the c_i and Q such that any such poles vanish. For the nonplanar double box, we apply the following cut on the four propagators carrying momentum ℓ_6,

$$\ell_6^2 = (\ell_5 + \ell_6)^2 = (\ell_5 + \ell_6 - k_4)^2 = (\ell_6 + k_3)^2 = 0 \,. \tag{C.9}$$

The Jacobian for this cut is

$$J_6 = (\ell_5 - k_3)^2 (\ell_5 - k_4)^2 - (\ell_5 - k_3 - k_4)^2 \ell_5^2 = (\ell_5 \cdot q)(\ell_5 \cdot \bar{q}) \,, \tag{C.10}$$

where $q = \lambda_3 \widetilde{\lambda}_4$, $\bar{q} = \lambda_4 \widetilde{\lambda}_3$.

After imposing the quadruple cut conditions in Eq. (C.9), the remaining integrand, in-

cluding the Jacobian (C.10), is

$$\operatorname*{Res}_{\ell_6\text{-cut}} \left[\mathcal{I}^{(NP)}\right] \equiv \widetilde{\mathcal{I}}^{(NP)} = \frac{c_1\ell_5^2 + c_2(\ell_5 \cdot Q) + c_3 s + c_4 t}{\ell_5^2(\ell_5 + k_1)^2(\ell_5 - k_3 - k_4)^2(\ell_5 \cdot q)(\ell_5 \cdot \bar{q})}, \tag{C.11}$$

where the integrand evaluated on the cut is denoted by a new symbol $\widetilde{\mathcal{I}}^{(NP)}$ for brevity.

To make the potentially problematic singularities visible, we write the four-dimensional part of the remaining loop momentum as

$$\ell_5 = \alpha\lambda_3\widetilde{\lambda}_3 + \beta\lambda_4\widetilde{\lambda}_4 + \gamma\lambda_3\widetilde{\lambda}_4 + \delta\lambda_4\widetilde{\lambda}_3. \tag{C.12}$$

This gives us

$$\widetilde{\mathcal{I}}^{(NP)} = \Big(c_1(\alpha\beta - \gamma\delta)s + c_2\left[\alpha(Q \cdot k_3) + \beta(Q \cdot k_4) + \gamma\langle 3|Q|4] + \delta\langle 4|Q|3]\right] + c_3 s + c_4 t\Big)$$
$$\times \Big[s^2(\alpha\beta - \gamma\delta)(\alpha\beta - \gamma\delta - \alpha - \beta + 1)$$
$$\times \Big((\alpha\beta - \gamma\delta)s + \alpha u + \beta t - \gamma\langle 13\rangle[14] - \delta\langle 14\rangle[13]\Big)\gamma\delta\Big]^{-1}, \tag{C.13}$$

where we use the convention $2k_i \cdot k_j = \langle ij\rangle[ij]$ and $\langle i|k_m|j] \equiv \langle im\rangle[mj]$. Our goal is to identify double- or higher-order poles. To expose these, we take residues in a certain order. For example, taking consecutive residues at $\gamma = 0$ and $\delta = 0$, followed by $\beta = 0$, gives

$$\operatorname*{Res}_{\substack{\gamma=\delta=0 \\ \beta=0}} \left[\widetilde{\mathcal{I}}^{(NP)}\right] = \frac{c_2\alpha(Q \cdot k_3) + c_3 s + c_4 t}{s^2 u\alpha^2(1 - \alpha)}. \tag{C.14}$$

Similarly, taking consecutive residues first at $\gamma = \delta = 0$, followed by $\beta = 1$, we get

$$\operatorname*{Res}_{\substack{\gamma=\delta=0 \\ \beta=1}} \left[\widetilde{\mathcal{I}}^{(NP)}\right] = -\frac{c_1\alpha s + c_2\left[\alpha(Q \cdot k_3) + (Q \cdot k_4)\right] + c_3 s + c_4 t}{s^2 t\alpha(1 - \alpha)^2}. \tag{C.15}$$

In both cases we see that there are unwanted double poles in α. The absence of double poles forces us to choose the c_i in the numerator such that the integrand reduces to at most a single pole in α. Canceling the double pole at $\alpha = 0$ in Eq. (C.14) requires $c_3 = c_4 = 0$.

86

Similarly, the second residue in Eq. (C.15) enforces $c_1 s + c_2(Q \cdot (k_3 + k_4)) = 0$ to cancel the double pole at $\alpha = 1$. Thus the solution that ensures $N^{(NP)}$ is a $d$log numerator is

$$N^{(NP)} = \frac{c_1}{s} \left[\ell_5^2 (Q \cdot (k_3 + k_4)) - (k_3 + k_4)^2 (\ell_5 \cdot Q) \right]. \tag{C.16}$$

The integrand is now free of the uncovered double poles, but requiring the absence of poles at infinity imposes further constraints on the numerator. If any of the parameters α, β, γ or δ grow large, the loop momentum ℓ_5, given by Eq. (C.12), also becomes large. Indeed, such a pole can be accessed by first taking the residue at $\delta = 0$, followed by taking the residues at $\alpha = 0$ and $\beta = 0$:

$$\operatorname*{Res}_{\substack{\delta=0 \\ \alpha=\beta=0}} \left[\widetilde{\mathcal{I}}^{(NP)} \right] = \frac{\langle 3|Q|4]}{\gamma s^2 \langle 13 \rangle [14]}. \tag{C.17}$$

The resulting form $d\gamma/\gamma$ has a pole for $\gamma \to \infty$. Similarly, taking a residue at $\gamma = 0$, followed by residues at $\alpha = 0$ and $\beta = 0$ results in a single pole as $\delta \to \infty$. To prevent such poles at infinity from appearing requires $\langle 3|Q|4] = \langle 4|Q|3] = 0$, which in turn requires that $Q = \sigma_1 k_3 + \sigma_2 k_4$, with the σ_i arbitrary constants. This is enough to determine the numerator, up to two arbitrary coefficients.

To illustrate a second approach, we could also consider the cut sequence $\{B(\ell_6)\}$, following the notation defined at the end of Section B.2. The resulting Jacobian is

$$J_6 = (\ell_5 - k_4)^2 (\ell_5 - k_3)^2 - (\ell_5 + k_1 + k_2)^2 \ell_5^2. \tag{C.18}$$

The two terms on the right already appear as propagators in the integrand, and so to avoid double poles, the $d$log numerator must scale as $N^{(NP)} \sim (\ell_5 + k_1 + k_2)^2 \ell_5^2$ in the kinematic regions where $(\ell_5 - k_4)^2 (\ell_5 - k_3)^2 = 0$. This constraint is sufficient to fix the ansatz Eq. (C.7) for $N^{(NP)}$.

In both approaches, the constraints of having only logarithmic singularities and no poles

at infinity results in a numerator for the nonplanar double box of the form,

$$N^{(NP)} = a_1^{(NP)}(\ell_5 - k_3)^2 + a_2^{(NP)}(\ell_5 - k_4)^2 \,, \tag{C.19}$$

where $a_1^{(NP)}$ and $a_2^{(NP)}$ are numerical coefficients. Finally, we impose the requirement that the numerator should respect the symmetries of the diagram. Because the nonplanar double box is symmetric under $k_3 \leftrightarrow k_4$, this forces $a_2^{(NP)} = a_1^{(NP)}$, resulting in a unique numerator up to an overall constant:

$$N_1^{(NP)} = (\ell_5 - k_3)^2 + (\ell_5 - k_4)^2 \,. \tag{C.20}$$

Compare this numerator to Eq. (3.9). Note that it combines the two nonplanar numerators found there, and that it therefore respects the automorphism symmetry of the nonplanar double box. The difference in Mandelstam factors results from the overall $\mathcal{K}$ that will be factored out of the amplitude in Eq. (C.21), as defined in Eq. (C.22), compared to Eq. (3.6).

C.1.2 Expansion of the Amplitude

In the previous subsection, we outlined a procedure to construct a basis of integrands where each element has only logarithmic singularities and no pole at infinity. The next step is to actually expand the amplitude in terms of this basis. As mentioned before, we primarily focus on the L-loop contribution to the $\mathcal{N} = 4$ SYM theory, four-point amplitudes. Following the normalization conventions of Ref. [128], these can be written in a diagrammatic representation (compare to Eq. (3.6))

$$\mathcal{A}_4^{L-\mathrm{loop}} = g^{2+2L} \frac{i^L \mathcal{K}}{(2\pi)^{DL}} \sum_{\mathcal{S}_4} \sum_x \frac{1}{S^{(x)}} c^{(x)} \int d\mathcal{I}^{(x)}(\ell_5, \ldots, \ell_{4+L}) \,, \tag{C.21}$$

where $d\mathcal{I}^{(x)}$ is the integrand form defined in Eq. (C.2), and we have implicitly analytically continued the expression to D dimensions to be consistent with dimensional regularization. In Eq. (C.21) the sum labeled by x runs over the set of distinct, non-isomorphic diagrams

with only cubic vertices, and the sum over $\mathcal{S}_4$ is over all $4! = 24$ permutations of external legs. The symmetry factor $S^{(x)}$ then removes overcounting that arises from automorphisms of the diagrams. The color factor $c^{(x)}$ of diagram (x) is given by dressing every three-vertex with a group-theory structure constant, $\tilde{f}^{abc} = i\sqrt{2}f^{abc}$. In the sum over permutations in Eq. (C.21), any given $d\mathcal{I}^{(x')}$ is a momentum relabeling of $d\mathcal{I}^{(x)}$ in Eq. (C.2).

For the cases we consider, the prefactor is proportional to the color-ordered tree amplitude,

$$\mathcal{K} = st A_4^{tree}(1,2,3,4) \,. \tag{C.22}$$

Furthermore $\mathcal{K}$ has a crossing symmetry, so it can also be expressed in terms of the tree amplitude with different color orderings,

$$\mathcal{K} = su A_4^{tree}(1,2,4,3) = tu A_4^{tree}(1,3,2,4) \,. \tag{C.23}$$

The explicit values of the tree amplitudes are

$$A_4^{tree}(1,2,3,4) = i\frac{\delta^8(\mathcal{Q})}{\langle 12\rangle\langle 23\rangle\langle 34\rangle\langle 41\rangle} \,, \tag{C.24}$$

where the other two orderings are just relabelings of the first. This is (up to an i) the Parke-Taylor factor defined in Eq. (3.4), but since we are not constructing a pure integrand basis, we are free to factor out a common $\mathcal{K}$ for the full amplitude, and not have to use Eq. (C.23) to distribute it among the basis integrands as in Chapter 3. The factor $\delta^8(\mathcal{Q})$ is the supermomentum-conserving delta function, as described in e.g. Ref. [146]. For external gluons with helicities $1^-, 2^-, 3^+, 4^+$ it is just $\langle 12\rangle^4$, up to Grassmann parameters.

A simple method for expanding the amplitude in terms of $d$log numerators is to use previously constructed representations of the amplitude as reference data, rather than sew together lower-loop amplitudes directly. Especially at higher loops, this drastically simplifies the process of determining the coefficients $a_i^{(x)}$. To ensure that the constructed amplitude is complete and correct, we also check a complete set of unitarity cuts via the method of

maximal cuts [147].

As an illustration of the procedure for determining the coefficients, consider the two-loop amplitude. A representation of the two-loop four-point amplitude is [125] Eqs. (C.21) and (C.3) with numerators

$$N_{old}^{(P)} = s\,, \qquad\qquad N_{old}^{(NP)} = s\,, \tag{C.25}$$

where we follow the normalization conventions of Ref. [128]. Following our strategy, we demand that the numerators are linear combinations of the basis elements constructed in Eqs. (C.6) and (C.19):

$$N^{(P)} = a_1^{(P)} s + a_2^{(P)} t\,, \qquad\qquad N^{(NP)} = a^{(NP)}((\ell_5 - k_3)^2 + (\ell_5 - k_4)^2)\,, \tag{C.26}$$

where, for comparison to $N_{old}^{(NP)}$, it is useful to rewrite the nonplanar numerator as

$$N^{(NP)} = a^{(NP)}(-s + (\ell_5 - k_3 - k_4)^2 + \ell_5^2)\,. \tag{C.27}$$

We can determine the coefficients by comparing the new and old expressions on the maximal cuts. By "maximal cuts" we mean replacing all propagators with on-shell conditions $p_{\alpha_{(x)}}^2 = 0$, defined in Eq. (C.1). The planar double-box numerator is unchanged on the maximal cut, since it is independent of all loop momenta. Comparing the two expressions in Eqs. (C.25) and (C.26) gives

$$a_1^{(P)} = 1\,, \qquad\qquad a_2^{(P)} = 0\,. \tag{C.28}$$

For the nonplanar numerator, we note that under the maximal cut conditions $\ell_5^2 = (\ell_5 - k_3 - k_4)^2 = 0$. Comparing the two forms of the nonplanar numerator in Eqs. (C.25) and (C.27) after imposing these conditions means

$$a_1^{(NP)} = -1\,, \tag{C.29}$$

so that the final numerators are

$$N^{(P)} = s \,, \qquad\qquad N^{(NP)} = -((\ell_5 - k_3)^2 + (\ell_5 - k_4)^2) \,. \qquad (C.30)$$

Although this fixes all coefficients in our basis, it does not prove that our construction gives the correct SYM amplitude. At two loops this was already proven in Ref. [108], where the difference between amplitudes in the old and the new representation was shown to vanish via the color Jacobi identity. More generally, we can appeal to the method of maximal cuts, since it offers a systematic and complete means of ensuring that our constructed nonplanar amplitudes are correct. Notice that our result for the full amplitude matches the coefficients in Eq. (3.17).

C.1.3   Amplitudes and Sums of $d\log$ Forms

At any loop order, assuming the four-point $\mathcal{N} = 4$ SYM amplitudes have only logarithmic singularities, we can write integrand forms as a sum of $d\log$ forms. At the relatively low loop orders that we are working, we can do this diagram by diagram, using the expansion of the diagrams given in Eq. (C.21). We then take each diagram form in Eq. (C.21) and expand it as a linear combination of $d\log$ forms,

$$d\mathcal{I}^{(x)} = \sum_{j=1}^{3} C_j \, d\mathcal{I}_j^{(x),d\log} \,, \qquad (C.31)$$

where the $d\mathcal{I}_j^{(x),d\log}$ are (potentially sums of) $d\log$ $4L$ forms. As discussed in Ref. [111], for MHV amplitudes the coefficients C_j are Park-Taylor factors with different orderings. This follows from super-conformal symmetry of $\mathcal{N} = 4$ SYM theory, which fixes the coefficients C_j to be holomorphic functions of spinor variables λ and normalizes $d\mathcal{I}^{(x)}$ to be a $d\log$ form. In the four-point nonplanar case this means that there are only three different coefficients

we can get,

$$C_1 = A_4^{tree}(1,2,3,4)\,, \qquad C_2 = A_4^{tree}(1,2,4,3)\,, \qquad C_3 = A_4^{tree}(1,3,2,4)\,, \qquad \text{(C.32)}$$

where the explicit form of the tree amplitudes are given in Eq. (C.24). The three coefficients are not independent, as they satisfy $C_1 + C_2 + C_3 = 0$. Suppose that the basis elements in Eq. (C.21) are chosen such that they have only logarithmic singularities. Then it was shown in Ref. [2] that we can indeed write the diagram as $d$log forms with coefficients given by the C_j.

C.2   Three-Loop Amplitude

In this section, we follow the recipe of the previous section to find a basis of three-loop diagram integrands that have only logarithmic singularities and no poles at infinity. The three-loop four-point parent diagrams are shown in Figure C.2; this matches the ten-propagator diagrams of 3.1. These have been classified in Ref. [126, 148], where an unintegrated representation of the three-loop four-point amplitude of $\mathcal{N} = 4$ SYM theory, including nonplanar contributions, was first obtained. As mentioned in Subsection C.1.1, we restrict to parent diagrams where no bubble or triangle diagrams appear as subdiagrams; otherwise we would find a pole at infinity that cannot be removed. A key difference with the analysis in Chapter 3 is that diagrams with contact terms will be incorporated into a parent diagram by including inverse propagators in the numerator that cancel propagators. This procedure wreaks havok with the unit leading singularities necessary for pure integrand forms, but is a useful simplification valid for the procedure followed in this appendix.

Next, we assign power counting of the numerator for each parent diagram. Applying the power-counting rules in Subsection C.1.1, we find that the maximum powers of allowed loop momenta for each parent diagram are

$$N^{(a)} = \mathcal{O}(1)\,, \qquad N^{(b)} = \mathcal{O}(\ell_6^2)\,, \qquad N^{(c)} = \mathcal{O}(\ell_5^2, (\ell_5 \cdot \ell_7), \ell_7^2)\,,$$
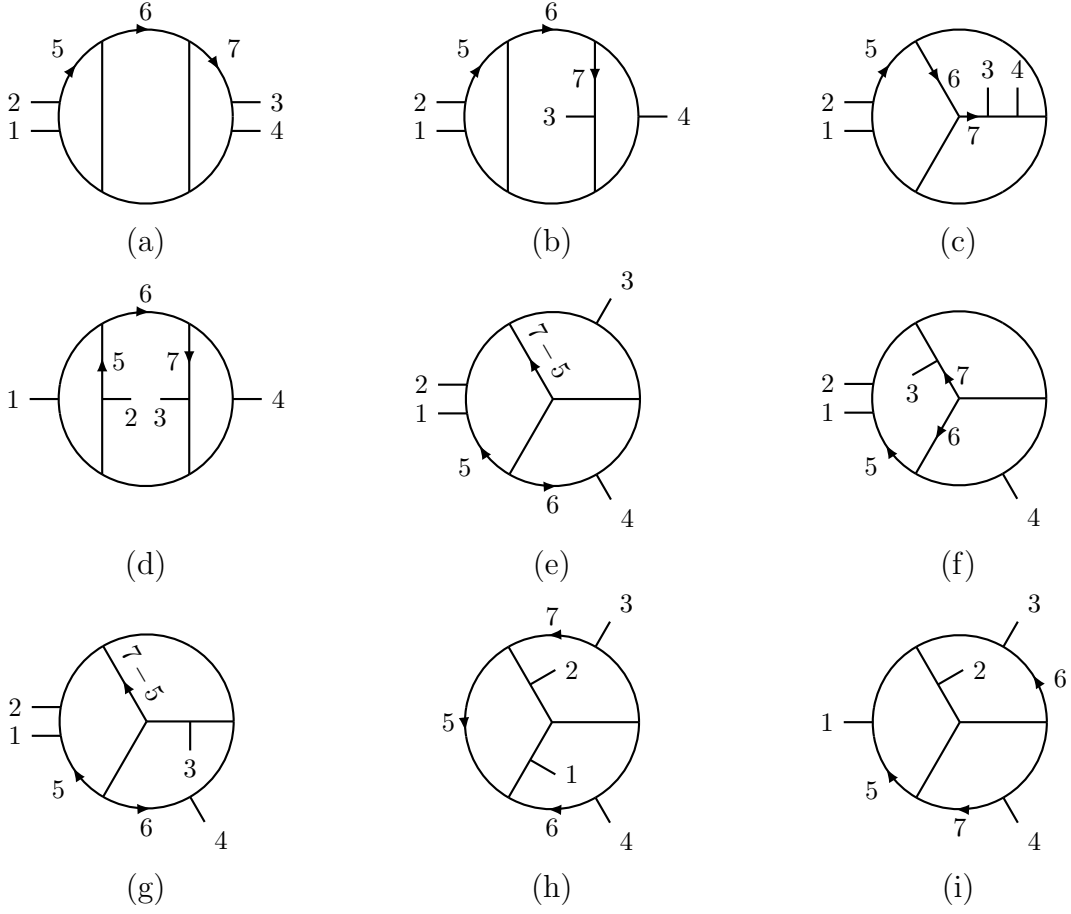
Figure C.2: The distinct parent diagrams for three-loop four-point amplitudes. The remaining parent diagrams are obtained by relabeling external legs. These are the first nine diagrams of Table 3.1.

$$N^{(d)} = \mathcal{O}(\ell_6^4)\,, \qquad N^{(e)} = \mathcal{O}(\ell_5^2)\,, \qquad N^{(f)} = \mathcal{O}(\ell_5^4)\,, \qquad N^{(g)} = \mathcal{O}(\ell_5^2\ell_6^2)\,,$$

$$N^{(h)} = \mathcal{O}(\ell_5^2\ell_6^2, \ell_5^2\ell_7^2,\ \ell_5^2(\ell_6 \cdot \ell_7))\,, \qquad\qquad N^{(i)} = \mathcal{O}(\ell_5^2\ell_6^2)\,, \qquad\qquad\qquad (C.33)$$

where we use the labels in Figure C.2, since these give the most stringent power counts. For diagram (h) we need to combine restrictions from a variety of labelings to arrive at this stringent power count. Ignoring the overall prefactor of $\mathcal{K}$, the overall dimension of each numerator is $\mathcal{O}(p^4)$, including external momenta.

C.2.1 Diagram Numerators

The next step is to write down the most general diagram numerators that are consistent with the power counting in Eq. (C.33), respect diagram symmetry, are built only from Lorentz dot products of the loop and external momenta, have only logarithmic singularities, and have no poles at infinity. Although the construction is straightforward, the complete list of conditions is lengthy, so here we only present a few examples and then write down a table of numerators satisfying the constraints.

We start with diagram (a) in Figure C.2. The required numerators are simple to write down if we follow the same logic as in the two-loop example in Subsection C.1.1. Since the numerator of diagram (a) is independent of all loop momenta as noted in Eq. (C.33), we can only write numerators that depend on the Mandelstam invariants s and t. There are three numerators that are consistent with the overall dimension,

$$N_1^{(a)} = s^2 \,, \qquad N_2^{(a)} = st \,, \qquad N_3^{(a)} = t^2 \,. \qquad (C.34)$$

Following similar logic as at two loops, it is straightforward to check that there are no double poles or poles at infinity.

The numerator for diagram (b) is also easy to obtain, this time by following the logic of the two-loop nonplanar diagram. From Eq. (C.33), we see that the only momentum dependence of the numerator must be on ℓ_6. The two-loop subdiagram on the right side of diagram (b) in Figure C.2 containing ℓ_6 is just the two-loop nonplanar double box we already analyzed in Subsection C.1.1. Repeating the earlier nonplanar box procedure for this subdiagram gives us the most general possible numerator for diagram (b),

$$N_1^{(b)} = s\big((\ell_6 - k_3)^2 + (\ell_6 - k_4)^2\big) \,. \qquad (C.35)$$

This is just the two-loop nonplanar numerator with an extra factor of s. A factor of t instead of s is disallowed because it violates the $k_3 \leftrightarrow k_4$ symmetry of diagram (b).

As a somewhat more complicated example, consider diagram (e) in Figure C.2. Because this diagram is planar we could use dual conformal invariance to find the desired numerator, although this would give a unit leading singularity numerator after normalization, as discussed in Chapter 3. (It turns out for this diagram that we'll end up with such a numerator anyway.) Instead, for illustrative purposes we choose to obtain it only from the requirements of having logarithmic singularities and no poles at infinity, without invoking dual conformal invariance. The relation to dual conformal symmetry is discussed further in Ref. [2].

From Eq. (C.33), we see that the numerator depends on the loop momentum ℓ_5 at most quadratically. Therefore we may start with the ansatz

$$N^{(e)} = (c_1 s + c_2 t)\left(\ell_5^2 + d_1(\ell_5 \cdot Q) + d_2 s + d_3 t\right),\tag{C.36}$$

where Q is a vector independent of all loop momenta and the c_i and d_i are numerical constants. We have included an overall factor depending on s and t so that the numerator has the correct overall dimensions, but this factor does not play a role in canceling unwanted singularities of the integrand.

In order to extract conditions on the numerator ansatz Eq. (C.36), we need to find any hidden double poles or poles at infinity in the integrand. The starting integrand is

$$\mathcal{I}^{(e)} = \frac{N^{(e)}}{\ell_6^2(\ell_6 + \ell_5)^2(\ell_6 + \ell_7)^2(\ell_6 + k_4)^2(\ell_7 - \ell_5)^2(\ell_7 - k_1 - k_2)^2(\ell_7 + k_4)^2}$$
$$\times \frac{1}{\ell_5^2(\ell_5 - k_1)^2(\ell_5 - k_1 - k_2)^2}\,.\tag{C.37}$$

Since our numerator ansatz (C.36) is a function of ℓ_5, we seek double poles only in the regions of momentum space that we can reach by choosing convenient on-shell values for ℓ_6 and ℓ_7. This leaves the numerator ansatz unaltered, making it straightforward to determine all coefficients.

To locate a double pole, consider the cut sequence

$$\text{cut} = \{B(\ell_6), B(\ell_7, \ell_7)\}, \tag{C.38}$$

where we follow the notation defined at the end of Section B.2. Here $B(\ell_7, \ell_7)$ indicates that we cut the $1/\ell_7^2$ propagator produced by the Jacobian of the $B(\ell_6)$ cut. This produces an overall Jacobian

$$J_{6,7} = s \left[(\ell_5 + k_4)^2 \right]^2. \tag{C.39}$$

After this sequence of cuts, the integrand of Eq. (C.37) becomes:

$$\underset{\substack{\ell_6-cut \\ \ell_7-cut}}{\text{Res}} \left[\mathcal{I}^{(e)} \right] = \frac{N^{(e)}}{\ell_5^2 (\ell_5 - k_1)^2 (\ell_5 - k_1 - k_2)^2 \left[(\ell_5 + k_4)^2 \right]^2 s}, \tag{C.40}$$

exposing a double pole at $(\ell_5 + k_4)^2 = 0$.

To impose our desired constraints on the integrand, we need to cancel the double pole in the denominator with an appropriate numerator. We see that choosing the ansatz in Eq. (C.36) to have $Q = k_4$, $d_1 = 2$, $d_2 = 0$, $d_3 = 0$ gives us the final form of the allowed numerator,

$$N^{(e)} = (c_1 s + c_2 t)(\ell_5 + k_4)^2, \tag{C.41}$$

so we have two basis numerators,

$$N_1^{(e)} = s(\ell_5 + k_4)^2, \qquad N_2^{(e)} = t(\ell_5 + k_4)^2. \tag{C.42}$$

We have also checked that this numerator passes all other double-pole constraints coming from different regions of momentum space. In addition, we have checked that it has no poles at infinity. It is interesting that, up to a factor depending only on external momenta, these are precisely the numerators consistent with dual conformal symmetry. As is discussed in Ref. [2], this is no accident.

Next, consider diagram (d) in Figure C.2. From the power counting arguments sum-

marized in Eq. (C.33), we see that the numerator for this diagram is a quartic function of momentum ℓ_6, but that it depends on neither ℓ_5 nor ℓ_7. When constructing numerators algorithmically we begin with a general ansatz, but to more easily illustrate the role of contact terms, we start from the natural guess that diagram (d) is closely related to a product of two two-loop nonplanar double boxes. Thus our initial guess is that the desired numerator is the product of numerators corresponding to the two-loop nonplanar subdiagrams:

$$\widetilde{N}^{(d)} = \left[(\ell_6 + k_1)^2 + (\ell_6 + k_2)^2\right] \left[(\ell_6 - k_3)^2 + (\ell_6 - k_4)^2\right] . \tag{C.43}$$

We label this numerator $\widetilde{N}^{(d)}$ because, as we see below, it is not quite the numerator $N^{(d)}$ that satisfies our pole constraints. As always, note that we have required the numerator to satisfy the symmetries of the diagram.

Although we do not do so here, one can show that this ansatz satisfies nearly all constraints on double poles and poles at infinity. The double pole not removed by the numerator is in the kinematic region:

$$\text{cut} = \{\ell_5^2, (\ell_5 + k_2)^2, \ell_7^2, (\ell_7 - k_3)^2, B(\ell_6)\} . \tag{C.44}$$

Before imposing the final box cut, we solve the first four cut conditions in terms of two parameters α and β:

$$\ell_5 = \alpha k_2 , \qquad \ell_7 = -\beta k_3 . \tag{C.45}$$

The final $B(\ell_6)$ represents a box-cut of four of the six remaining propagators that depend on α and β:

$$(\ell_6 - \alpha k_2)^2 = (\ell_6 - \alpha k_2 + k_1)^2 = (\ell_6 + \beta k_3)^2 = (\ell_6 + \beta k_3 - k_4)^2 = 0 . \tag{C.46}$$

97

Before cutting the $B(\ell_6)$ propagators, the integrand is

$$\operatorname*{Res}_{\substack{\ell_5-cut \\ \ell_7-cut}} \widetilde{\mathcal{I}}^{(d)} = \frac{\widetilde{N}^{(d)}}{\ell_6^2(\ell_6 + k_1 + k_2)^2(\ell_6 - \alpha k_2)^2(\ell_6 - \alpha k_2 + k_1)^2(\ell_6 + \beta k_3)^2(\ell_6 + \beta k_3 - k_4)^2} \,.$$

(C.47)

Localizing further to the $B(\ell_6)$ cuts produces a Jacobian

$$J_6 = su(\alpha - \beta)^2 \,,$$

(C.48)

while a solution to the box-cut conditions of Eq. (C.46),

$$\ell_6^* = \alpha \lambda_4 \widetilde{\lambda}_2 \frac{\langle 12 \rangle}{\langle 14 \rangle} - \beta \lambda_1 \widetilde{\lambda}_3 \frac{\langle 34 \rangle}{\langle 14 \rangle} \,,$$

(C.49)

turns the remaining uncut propagators of Eq. (C.47) into

$$\ell_6^2 = s\alpha\beta \,, \qquad\qquad (\ell_6 + k_1 + k_2)^2 = s(1 + \alpha)(1 + \beta) \,.$$

(C.50)

The result of completely localizing all momenta in this way is

$$\operatorname*{Res}_{cuts} \widetilde{\mathcal{I}}^{(d)} = -\frac{s^2(\alpha(1 + \beta) + \beta(1 + \alpha))^2}{s^3 u\alpha\beta(1 + \alpha)(1 + \beta)(\alpha - \beta)^2} \,.$$

(C.51)

We see that there is a double pole located at $\alpha - \beta = 0$. To cancel this double pole, we are forced to add an extra term to the numerator. A natural choice is a term that collapses both propagators connecting the two two-loop nonplanar subdiagrams: $\ell_6^2(\ell_6 + k_1 + k_2)^2$. On the support of the cut solutions Eq. (C.49), this becomes $s^2\alpha\beta(\alpha + 1)(\beta + 1)$. We can cancel the double pole at $\alpha - \beta = 0$ in Eq. (C.51) by choosing the linear combination

$$N_1^{(d)} = \left[(\ell_6 + k_1)^2 + (\ell_6 + k_2)^2 \right] \left[(\ell_6 - k_3)^2 + (\ell_6 - k_4)^2 \right] - 4\ell_6^2(\ell_6 + k_1 + k_2)^2 \,.$$

(C.52)

Indeed, with this numerator the diagram lacks even a single pole at $\alpha - \beta = 0$.

It is interesting to note that if we relax the condition that the numerator respects the

diagram symmetry $k_1 \leftrightarrow k_2$ and $k_3 \leftrightarrow k_4$, there are four independent numerators with no double pole. For example,

$$\tilde{N}^{(d)} = (\ell_6 + k_1)^2(\ell_6 - k_3)^2 - \ell_6^2(\ell_6 + k_1 + k_2)^2 \,, \tag{C.53}$$

is a $d$log numerator. These are precisely the four numerators that appear for diagram (d) in Table 3.1. When we require that $N^{(d)}$ respect diagram symmetry, we need the first four terms in Eq. (C.52), each with its own "correction" term $-\ell_6^2(\ell_6 + k_1 + k_2)^2$. This accounts for the factor of four on the last term in Eq. (C.52).

We have carried out detailed checks of all potentially dangerous regions of the integrand of diagram (d), showing that the numerator of Eq. (C.52) results in a diagram with only logarithmic singularities and no poles at infinity. In fact, the numerator (C.52) is the only one respecting the symmetries of diagram (d) with these properties. We showed this by starting with a general ansatz subject to the power counting constraint in Eq. (C.33) and demonstrating that no other solution exists other than the one in Eq. (C.52).

We have gone through the diagrams in Figure C.2 in great detail, finding the numerators that respect diagram symmetry (including color signs), and that have only logarithmic singularities and no poles at infinity. This gives us a set of basis $d$log numerators associated with each diagram. For the diagrams where numerator factors do not cancel any propagators, the set of numerators is collected in Table C.1. In addition, there are also diagrams where numerators do cancel propagators. For the purpose of constructing amplitudes, it is convenient to absorb these contact contributions into the parent diagrams of Figure C.2 to make color assignments manifest. This allows us to treat all contributions on an equal footing, such that we can read off the color factors directly from the associated parent diagram by dressing each trivalent vertex with an $\tilde{f}^{abc}$. This distributes the contact term diagrams in Table C.3 among the parent diagrams, listed in Table C.2. When distributing the contact terms to the parent diagrams, we change the momentum labels to those of each parent diagram and then multiply and divide by the missing propagator(s). The reason the

numerators in Table C.2 appear more complicated than those in Table C.3 is that a single term from Table C.3 can appear with multiple momentum relabelings in order to enforce the symmetries of the parent diagrams on the numerators. This process is not done in Chapter 3, as diagrams (j) and (k) are associated with pure integrands. Merging them with parent diagrams in this manner would lead to integrands that are not pure, as they would have leading singularities that are not unit.

As an example of the correspondence between the numerators in Table C.2 and Table C.3, consider diagram (j) and the associated numerators, $N_1^{(j)}$ and $N_2^{(j)}$, in Table C.3. To convert this into a contribution to diagram (i) in Table C.2, we multiply and divide by the missing propagator $1/(\ell_5+\ell_6+k_4)^2$. Then we need to take the appropriate linear combination so that the diagram (i) antisymmetry (including the color sign) under $\{k_1 \leftrightarrow k_3, \ell_5 \leftrightarrow \ell_6, \ell_7 \leftrightarrow -\ell_7\}$ is satisfied. This gives,

$$N_2^{(i)} = \frac{1}{3}(\ell_5 + \ell_6 + k_4)^2 \left[t - s\right] . \tag{C.54}$$

In fact, there are three alternative propagators that can be inserted instead of $1/(\ell_5+\ell_6+k_4)^2$; these are all equivalent to the three relabelings of external lines for diagram (i). We have absorbed a combinatorial factor of $\frac{1}{3}$ into the definition of the numerator because of the differing symmetries between diagram (i) in Table C.2 and diagram (j) in Table C.3.

As a second example, consider diagram (k) in Table C.3, corresponding to the basis element $N_1^{(k)}$. If we put back the two missing propagators by multiplying and dividing by the appropriate inverse propagators, diagram (k) contributes to the to numerators $N_2^{(c)}$, $N_2^{(f)}$, $N_5^{(g)}$, $N_6^{(g)}$, $N_2^{(h)}$ and $N_3^{(i)}$ in Table C.2.

In summary, the diagrams and numerators in Table C.1 and C.2 are a complete set with the desired power counting, have only logarithmic singularities, and lack poles at infinity. They are also constructed to satisfy diagram symmetries, including color signs.

Diagram	Numerators

(a) $N_1^{(a)} = s^2$, $\quad N_2^{(a)} = st$, $\quad N_3^{(a)} = t^2$,

(b) $N_1^{(b)} = s\left[(\ell_6 - k_3)^2 + (\ell_6 - k_4)^2\right]$,

(c) $N_1^{(c)} = s\left[(\ell_5 - \ell_7)^2 + (\ell_5 + \ell_7 + k_1 + k_2)^2\right]$,

(d) $N_1^{(d)} = \left[(\ell_6 + k_1)^2 + (\ell_6 + k_2)^2\right]^2 - 4\ell_6^2(\ell_6 + k_1 + k_2)^2$,

(e) $N_1^{(e)} = s(\ell_5 + k_4)^2$, $\quad N_2^{(e)} = t(\ell_5 + k_4)^2$,

(f) $N_1^{(f)} = (\ell_5 + k_4)^2\left[(\ell_5 + k_3)^2 + (\ell_5 + k_4)^2\right]$,

(g)
$N_1^{(g)} = s(\ell_5 + \ell_6 + k_3)^2$, $\qquad\qquad N_2^{(g)} = t(\ell_5 + \ell_6 + k_3)^2$,
$N_3^{(g)} = (\ell_5 + k_3)^2(\ell_6 + k_1 + k_2)^2$, $\qquad N_4^{(g)} = (\ell_5 + k_4)^2(\ell_6 + k_1 + k_2)^2$,

(h)
$$\begin{aligned}
N_1^{(h)} = & \Big[(\ell_6 + \ell_7)^2(\ell_5 + k_2 + k_3)^2 - \ell_5^2(\ell_6 + \ell_7 - k_1 - k_2)^2 \\
& - (\ell_5 + \ell_6)^2(\ell_7 + k_2 + k_3)^2 - (\ell_5 + \ell_6 + k_2 + k_3)^2\ell_7^2 \\
& - (\ell_6 + k_1 + k_4)^2(\ell_5 - \ell_7)^2 - (\ell_5 - \ell_7 + k_2 + k_3)^2\ell_6^2\Big] \\
& - \Big[[(\ell_5 - k_1)^2 + (\ell_5 - k_4)^2][(\ell_6 + \ell_7 - k_1)^2 + (\ell_6 + \ell_7 - k_2)^2] \\
& - 4 \times \ell_5^2(\ell_6 + \ell_7 - k_1 - k_2)^2 \\
& - (\ell_7 + k_4)^2(\ell_5 + \ell_6 - k_1)^2 - (\ell_7 + k_3)^2(\ell_5 + \ell_6 - k_2)^2 \\
& - (\ell_6 + k_4)^2(\ell_5 - \ell_7 + k_1)^2 - (\ell_6 + k_3)^2(\ell_5 - \ell_7 + k_2)^2\Big],
\end{aligned}$$

(i)
$$\begin{aligned}
N_1^{(i)} = & (\ell_6 + k_4)^2\left[(\ell_5 - k_1 - k_2)^2 + (\ell_5 - k_1 - k_3)^2\right] \\
& - (\ell_5 + k_4)^2\left[(\ell_6 + k_1 + k_4)^2 + (\ell_6 + k_2 + k_4)^2\right] \\
& - \ell_5^2(\ell_6 - k_2)^2 + \ell_6^2(\ell_5 - k_2)^2.
\end{aligned}$$

Table C.1: The parent numerator basis elements corresponding to the labels of the diagrams in Figure C.2. The basis elements respect the symmetries of the diagrams. Compare to the first nine diagrams of Table 3.1.

Diagram	Numerator

(c) $\quad N_2^{(c)} = (\ell_5)^2 (\ell_7)^2 + (\ell_5 + k_1 + k_2)^2 (\ell_7)^2 + (\ell_5)^2 (\ell_7 + k_1 + k_2)^2$
$\qquad\qquad + (\ell_5 + k_1 + k_2)^2 (\ell_7 + k_1 + k_2)^2 \,,$

(f) $\quad N_2^{(f)} = \ell_5^2 (\ell_5 - k_1 - k_2)^2 \,,$

(g) $\quad N_5^{(g)} = (\ell_5 - k_1 - k_2)^2 (\ell_6 - k_4)^2 \,,$
$\qquad\quad N_6^{(g)} = \ell_5^2 (\ell_6 - k_4)^2 \,,$

(h) $\quad N_2^{(h)} = \ell_6^2 (\ell_5 - \ell_7)^2 + \ell_7^2 (\ell_5 + \ell_6)^2 + (\ell_6 + k_4)^2 (\ell_5 - \ell_7 + k_2)^2$
$\qquad\qquad + (\ell_5 + \ell_6 - k_1)^2 (\ell_7 + k_3)^2 \,,$

(i) $\quad N_2^{(i)} = \tfrac{1}{3} (\ell_5 + \ell_6 + k_4)^2 [t - s] \,,$
$\qquad\quad N_3^{(i)} = (\ell_6)^2 (\ell_5 - k_1)^2 - (\ell_5)^2 (\ell_6 - k_3)^2 \,.$

Table C.2: The parent diagram numerator basis elements where a numerator factor cancels a propagator. Each term in brackets does not cancel a propagator, while the remaining factors each cancel a propagator. Each basis numerator maintains the symmetries of the associated diagram, including color signs. The associated color factor can be read off from each diagram. There is no analog of these in Table 3.1, as these pieces are in diagrams (j) and (k).

Diagram	Numerator

(j) $\quad N_1^{(j)} = s \,, \qquad N_2^{(j)} = t \,,$

(k) $\quad N_1^{(k)} = 1 \,.$

Table C.3: The numerator basis elements corresponding to the contact term diagrams. Black dots indicate contact terms. Written this way, the numerators are simple, but the color factors cannot be read off from the diagrams. Compare to the final two diagrams of Table 3.1.

C.2.2 Determining the Coefficients

We now express the three-loop four-point $\mathcal{N} = 4$ SYM amplitude in terms of our constructed basis. We write the numerator in Eq. (C.21) directly in terms of our basis via Eq. (C.3). Because we have required each basis numerator to reflect diagram symmetry, we must specify only one numerator of each diagram topology; we can obtain the remaining ones simply by relabeling the external legs.

The coefficients in front of each basis element are straightforward to determine using simple unitarity cuts, together with previously determined representations of the three-loop four-point amplitude. We start from the $\mathcal{N} = 4$ SYM numerators as originally determined in Ref. [126], since they happen to be in a particularly compact form. Rewriting these numerators using our choice of momentum labels gives

$$
\begin{aligned}
N_{old}^{(a)} &= N_{old}^{(b)} = N_{old}^{(c)} = N_{old}^{(d)} = s^2 \,, \\
N_{old}^{(e)} &= N_{old}^{(f)} = N_{old}^{(g)} = s(\ell_5 + k_4)^2 \,, \\
N_{old}^{(h)} &= -st + 2s(k_2 + k_3) \cdot \ell_5 + 2t(\ell_6 + \ell_7) \cdot (k_1 + k_2) \,, \\
N_{old}^{(i)} &= s(k_4 + \ell_5)^2 - t(k_4 + \ell_6)^2 - \frac{1}{3}(s - t)(k_4 + \ell_5 + \ell_6)^2 \,.
\end{aligned}
\tag{C.55}
$$

To match to our basis, we start by considering the maximal cuts, where all propagators of each diagram are placed on-shell. The complete set of maximal cut solutions is unique to each diagram, so we can match coefficients by considering only a single diagram at a time. We start with diagram (a) in Table C.1. Here the numerator is a linear combination of three basis elements

$$
N^{(a)} = a_1^{(a)} N_1^{(a)} + a_2^{(a)} N_2^{(a)} + a_3^{(a)} N_3^{(a)} \,,
\tag{C.56}
$$

corresponding to $N_j^{(a)}$ in Table C.1. The $a_j^{(a)}$ are numerical parameters to be determined. This is to be compared to the old form of the numerator in Eq. (C.55). Here the maximal cuts have no effect, because both the new and old numerators are independent of loop momenta. Matching the two numerators, the coefficients in front of the numerator basis are $a_1^{(a)} = 1$,

$a_2^{(a)} = 0$ and $a_3^{(a)} = 0$.

Now consider diagram (b) in Figure C.2. Here the basis element is of a different form compared to the old version of the numerator in Eq. (C.55). The new form of the numerator is

$$N^{(b)} = a_1^{(b)} N_1^{(b)} = a_1^{(b)} s \left[(\ell_6 - k_3)^2 + (\ell_6 - k_4)^2 \right] . \tag{C.57}$$

In order to make the comparison to the old version, we impose the maximal cut conditions involving only ℓ_6:

$$\ell_6^2 = 0 , \qquad (\ell_6 - k_2 - k_3)^2 = 0 . \tag{C.58}$$

Applying these conditions:

$$\left[(\ell_6 - k_3)^2 + (\ell_6 - k_4)^2 \right] \to -s . \tag{C.59}$$

Comparing to $N_{old}^{(b)}$ in Eq. (C.55) gives us the coefficient $a_1^{(b)} = -1$.

As a more complicated example, consider diagram (i). In this case, the numerators depend only on ℓ_5 and ℓ_6. The relevant cut conditions read off from Figure C.2(i) are

$$\ell_5^2 = \ell_6^2 = (\ell_5 - k_1)^2 = (\ell_6 - k_3)^2 = (\ell_5 + \ell_6 - k_3 - k_1)^2 = (\ell_5 + \ell_6 + k_4)^2 = 0 . \tag{C.60}$$

With these cut conditions, the old numerator in Eq. (C.55) becomes

$$N_{old}^{(i)} \Big|_{cut} = 2s \left(k_4 \cdot \ell_5 \right) - 2t \left(k_4 \cdot \ell_6 \right) . \tag{C.61}$$

The full numerator for diagram (i) is a linear combination of the three basis elements for diagram (i) in Table C.1 and C.2:

$$N^{(i)} = a_1^{(i)} N_1^{(i)} + a_2^{(i)} N_2^{(i)} + a_3^{(i)} N_3^{(i)} . \tag{C.62}$$

The maximal cut conditions immediately set the last two of these numerators to zero, because

they contain inverse propagators. Applying the cut conditions Eq. (C.60) to the nonvanishing term results in

$$N^{(i)}\big|_{cut} = a_1^{(i)}\left[-2(\ell_6 \cdot k_4)t + 2(\ell_5 \cdot k_4)s\right].\tag{C.63}$$

Comparing Eq. (C.61) to Eq. (C.63) fixes $a_1^{(i)} = 1$. The two other coefficients for diagram (i), $a_2^{(i)}$ and $a_3^{(i)}$, cannot be fixed from the maximal cuts.

In order to determine all coefficients and to prove that the answer is complete and correct, we need to evaluate next-to-maximal and next-to-next-to-maximal cuts. We need only evaluate the cuts through this level because of the especially good power counting of $\mathcal{N} = 4$ SYM. We do not describe this procedure explicitly here. Details of how this is done may be found in Ref. [118]. Using these cuts, we have the solution of the numerators in terms of the basis elements as

$$
\begin{aligned}
N^{(a)} &= N_1^{(a)}, \\
N^{(b)} &= -N_1^{(b)}, \\
N^{(c)} &= -N_1^{(c)} + 2d_1 N_2^{(c)}, \\
N^{(d)} &= N_1^{(d)}, \\
N^{(e)} &= N_1^{(e)}, \\
N^{(f)} &= -N_1^{(f)} + 2d_2 N_2^{(f)}, \\
N^{(g)} &= -N_1^{(g)} + N_3^{(g)} + N_4^{(g)} + (d_1 + d_3 - 1)N_5^{(g)} + (d_1 - d_2)N_6^{(g)}, \\
N^{(h)} &= N_1^{(h)} + 2d_3 N_2^{(h)}, \\
N^{(i)} &= N_1^{(i)} + N_2^{(i)} + (d_3 - d_2)N_3^{(i)},
\end{aligned}
\tag{C.64}
$$

where the three d_i are free parameters not fixed by any physical constraint.

C.2.3 Free Parameters and Color Jacobi Identites

The ambiguity represented by the three free parameters, d_i in Eq. (C.64), derives from color factors not being independent, but instead related via color Jacobi identities. This allows us to move contact terms between different diagrams without altering the amplitude. Different choices of d_1, d_2, d_3 correspond to three degrees of freedom from color Jacobi identities. These allow us to move contact contributions of diagram (k), where two propagators are collapsed, between different parent diagrams. The contact term in diagram (j) of Table C.3 does not generate a fourth degree of freedom because the three resulting parent diagrams all have the same topology, corresponding to relabelings of the external legs of diagram (i). The potential freedom then cancels within a single diagram. We have explicitly checked that the d_i parameters in Eq. (C.64) drop out of the full amplitude after using appropriate color Jacobi identities. One choice of free parameters is to take them to all vanish

$$d_1 = 0 \,, \qquad\qquad d_2 = 0 \,, \qquad\qquad d_3 = 0 \,. \qquad\qquad \text{(C.65)}$$

In this case every remaining nonvanishing numerical coefficient in front of a basis elements is ± 1. (Recall that $N_2^{(i)}$ absorbed the $1/3$ combinatorial factor mismatch between diagram (i) and diagram (j).) Of course this is not some "best" choice of the d_i, given that the amplitude is unchanged for any other choice of d_i.

Power counting of the loop momenta forbids numerators from canceling more than two propagators, so the topologies with the fewest allowed number of propagators contain eight propagators. There is only one such topology that is not forbidden by our pole constraints: diagram (k). Since this topology has four-point contact terms, its color coefficient cannot simply be read off. Instead, we must consider expanding the diagram (k)'s two four-point contact vertices in each of the three possible ways (i.e. s, t, and u channels) to obtain nine 10-propagator topologies. Fixing the selected channel on one of the vertices and cycling through the three channels on the other vertex, we see that the color coefficients from each of the three resulting 10-propagator diagrams form a color Jacobi relation. Considering

the other two channels on the fixed vertex and doing the same procedure yields two more 10-propagator diagram triplets whose color factors satisfy color Jacobi identities.

Diagram (k) receives color contributions from all nine of these color factors. However, some of these factors are simply noncyclic permutations of each other, and thus correspond to the same 10-propagator topology. In all, diagram (k) receives color contributions to five of the nine 10-propagator topologies, corresponding to diagrams (c), (f), (g), (h), and (i).

The overall coefficients of these contributions to the amplitude are not fixed, however. Indeed, the Jacobi identities corresponding to the three Jacobi triplets each contribute one degree of freedom to our full solution, the d_i discussed above. The reason is that one can take the sum of three color factors in a Jacobi triplet (which is by definition zero) and multiply it by propagators of the diagram (k), along with an arbitrary coefficient. We can then distribute this zero among the three members of the Jacobi triplet. For each member of the triplet, take the two propagators that were generated by expanding the four-point vertices in diagram (k). Divide them by themselves to get unity, and then multiply this times the member's corresponding color factor. In this way, the arbitrary coefficient of our Jacobi times the two inverse propagators becomes a basis element in the numerator of each of the three (now color-dressed) 10-propagator diagrams in the triplet.

Let's see an explicit example of this. Diagram (k) takes the form shown in Table C.3. First, let's expand the four-point vertex connected to leg k_2 into its s-channel, i.e. moving the k_2 leg to the upper-right. We then consider all three expansions of the four-point vertex connected to k_4; the sum of their color factors is a Jacobi identity. The first term is isomorphic to diagram (i); indeed it's in a cyclic permutation of the master labels of that topology, and thus has the master color factor $c_{(1234)}$. The second term is a permutation of diagram (f); specifically, $(1234) \rightarrow (2431)$. However, the sign of the color vertex factor adjoining leg k_3 must be flipped for this identification, so its color factor is $-c_{f(2431)}$, where $c_{f(2431)}$ denotes the color factor of the master labels for f under the permutation $(1234) \rightarrow (2431)$. The final term is a copy of diagram (g), with the permutation $(1234) \rightarrow (4312)$. The vertex factors for both legs k_1 and k_4, as well as the four internal vertices, must all be flipped to make this
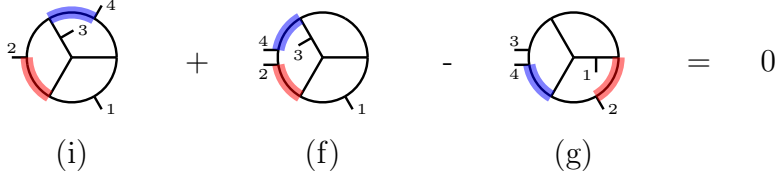
Figure C.3: A diagrammatic representation of the color Jacobi relation described in the text. The red leg is the shared expanded propagator, while the blue propagator is the propagator on which the Jacobi identity is applied. Collapsing these leads to diagram (k).

identification; since there are an even number of sign flips, the color factor is still just $c_{g(4312)}$. Note that these last two diagrams contribute to pieces that appear in the permutation sum of the master diagram, rather than to the labels that appear in Table C.1. We'll deal with this complication below.

We now wish to add this Jacobi relation (which is just zero) to the full integrand, and distribute its three pieces among the appropriate master topologies. We'll give it an overall coefficient named a_f, as this is the only Jacobi relation that contributes to diagram (f). We drew our diagrams to match the signs of the usual Jacobi relation $c_s - c_t - c_u = 0$. As noted above, our t-channel (the diagram (f) contribution) has a sign flip when discussed in terms of the master labeling. Thus we instead add

$$a_f \left(c_{i(1234)} + c_{f(2431)} - c_{g(4312)} \right), \tag{C.66}$$

labeling each color factor by its master topology and permutation of external legs, modulo cyclic permutations. This is graphically depicted in Figure C.3.

We need to distribute this among the three master topologies, and this requires giving each piece the appropriate propagator structure. All three diagrams share the eight propagators inherited from diagram (k). They also all share the first propagator we expanded. We'll call the product of these nine propagators D, and multiply it by our Jacobi relation. Next, we need the remaining propagator, which is unique to each diagram. We divide this

propagator by itself and multiply it against its corresponding color factor:

$$a_f \left(c_{i,(1234)} D_{i,(1234)} \frac{\ell_{i,(1234)}}{\ell_{i,(1234)}} + c_{f,(2431)} D_{f,(2431)} \frac{\ell_{f,(2431)}}{\ell_{f,(2431)}} - c_{g,(4312)} D_{g(4312)} \frac{\ell_{g,(4312)}}{\ell_{g,(4312)}} \right), \quad \text{(C.67)}$$

where we have distributed D throughout and labeled it according to the labels of the appropriate topology.

Remember that we are ultimately interested in the contribution this has to our basis elements, which are defined under the sum over noncyclic permutations of the external legs. Of course if we apply any permutation of the external legs to our entire Jacobi relation, it will still be a Jacobi relation, so this means we can add it to the integrand *under* the permutation sum. But this means that the specific permutations that show up in our Jacobi are irrelevant; since all permutations are summed over, they'll all appear in the sum anyway. Therefore, our Jacobi clearly contributes $a_f \ell_{i(1234)}$ to the master numerator for diagram (i); it also contributes $a_f \ell_{f(1234)}$ to the master numerator for diagram (f), and $-a_f \ell_{g,(4312)}$ to the numerator of diagram (g).

Now notice that if we had initially fixed the vertex connected to k_2 in its t- or u-channel instead, we would have gotten two other sets of Jacobi triplets. The first triplet consists of two copies of diagram (g) and one of (c). The first copy of (g) is already in exactly the master labels, contributing to $c_{g(1234)}$. The second is $-c_{g(2134)}$, with seven color vertex flips to get the sign, and the third is a copy of diagram (c) with color factor $-c_{c,(1234)}$. The second triplet gives a master copy of diagram (h), with color factor $c_{h(1234)}$; additionally there is a copy of diagram (i) with a cyclic permutation of the master labels, so we get $c_{i(1234)}$, and last a copy of diagram (g), with $-c_{g(3412)}$. We name their arbitrary coefficients a_c and a_h respectively, after the diagrams that appear only in those triplets:

$$a_c \left(c_{g,(1234)} D_{g,(1234)} \frac{\ell_{g,(1234)}}{\ell_{g,(1234)}} + c_{g,(2143)} D_{g,(2143)} \frac{\ell_{g,(2143)}}{\ell_{g,(2143)}} + c_{c,(1234)} D_{c,(1234)} \frac{\ell_{c,(1234)}}{\ell_{c,(1234)}} \right) \quad \text{(C.68)}$$

$$a_h \left(c_{h,(1234)} D_{h,(1234)} \frac{\ell_{h,(1234)}}{\ell_{h,(1234)}} - c_{i,(1234)} D_{i,(1234)} \frac{\ell_{i,(1234)}}{\ell_{i,(1234)}} + c_{g,(3412)} D_{g(3412)} \frac{\ell_{g,(3412)}}{\ell_{g,(3412)}} \right). \quad \text{(C.69)}$$

There is one more issue to deal with. We have chosen our basis elements to respect the automorphisms of their topologies, and we should expect no less from the contributions provided by Jacobi triplets. For example, diagram (i) possesses a reflection symmetry that leads to $c_{i,(1234)} = -c_{i(3214)}$. This means that in the permutation sum, the coefficients of $c_{i,(1234)}$ and $c_{i,(3214)}$ will be combined. We want this behavior to be manifest in the basis elements themselves, so instead of our first Jacobi contributing

$$a_f c_{i,(1234)} D_{i,(1234)} \frac{\ell_{i,(1234)}}{\ell_{i,(1234)}} \tag{C.70}$$

to the full numerator for diagram i, we'll have it contribute

$$\frac{1}{2} a_f c_{i,(1234)} \left(D_{i,(1234)} \frac{\ell_{i,(1234)}}{\ell_{i,(1234)}} - D_{i,(3214)} \frac{\ell_{i,(3214)}}{\ell_{i,(3214)}} \right). \tag{C.71}$$

Up to these symmetry factors, we can finally read off that a_f corresponds to d_2, a_c to d_1, and a_h to d_3, explaining the origin of these extra degrees of freedom. Note that the imposition of unit leading singularities in the pure integrand basis of Chapter 3 eliminates this freedom, as diagram (k) takes on a status equivalent to that of diagrams (a) through (i), and thus cannot have its contribution pushed around in this manner. Such rearrangement would also mess up the purity of the integrands corresponding to diagrams (a) through (i).

In any event, once the coefficients in front of each basis numerator are determined, we are left with the question of whether the basis numerators properly capture all terms that are present in the amplitude. To answer this we turn to the method of maximal cuts [118]. This is a variation on the standard generalized unitarity method, but organized by starting with maximal cuts and systematically checking cuts with fewer and fewer propagators set on shell. This method has been described in considerable detail in Ref. [118], so we only mention a few points.

The overall power counting of the three-loop $\mathcal{N} = 4$ SYM amplitude is such that it can be written with at most two powers of loop momenta in the numerator [107, 126], as discussed above. This means that in principle we can fully determine the amplitude using only

next-to-maximal cuts. However, here we use a higher-power counting representation with up to four powers of loop momenta in the numerator corresponding to as many as two canceled propagators. This implies that to completely determine the amplitude using our representation we need to check cuts down to the next-to-next-to-maximal level. We have explicitly checked all next-to-next-to-maximal cuts, proving that the amplitudes obtained by inserting the numerators in Eq. (C.64) into Eqs. (C.21) and (C.3) gives the complete amplitude, and that it is entirely equivalent to earlier representations of the amplitude [107, 126, 148]. Because each numerator basis element is constructed such that each integrand has only logarithmic singularities and no poles at infinity, this proves that the full nonplanar three-loop four-point $\mathcal{N} = 4$ SYM amplitude has these properties, as conjectured in Ref. [108].

Bibliography

[1] Sean Litsey and James Stankowicz. Kinematic Numerators and a Double-Copy Formula for $\mathcal{N} = 4$ Super-Yang-Mills Residues. *Phys. Rev.*, D90(2):025013, 2014.

[2] Zvi Bern, Enrico Herrmann, Sean Litsey, James Stankowicz, and Jaroslav Trnka. Logarithmic Singularities and Maximally Supersymmetric Amplitudes. *JHEP*, 06:202, 2015.

[3] Zvi Bern, Enrico Herrmann, Sean Litsey, James Stankowicz, and Jaroslav Trnka. Evidence for a Nonplanar Amplituhedron. *arXiv:1512.08591 [hep-th]*, 2015.

[4] Ruth Britto, Freddy Cachazo, and Bo Feng. New recursion relations for tree amplitudes of gluons. *Nucl.Phys.*, B715:499–522, 2005.

[5] Ruth Britto, Freddy Cachazo, Bo Feng, and Edward Witten. Direct proof of tree-level recursion relation in Yang-Mills theory. *Phys.Rev.Lett.*, 94:181602, 2005.

[6] Z. Bern, J.J.M. Carrasco, and Henrik Johansson. New Relations for Gauge-Theory Amplitudes. *Phys.Rev.*, D78:085011, 2008.

[7] Ronald Kleiss and Hans Kuijf. Multi-Gluon Cross-sections and Five Jet Production at Hadron Colliders. *Nucl. Phys.*, B312:616, 1989.

[8] Zvi Bern, Scott Davies, Tristan Dennen, Yu-tin Huang, and Josh Nohle. Color-Kinematics Duality for Pure Yang-Mills and Gravity at One and Two Loops. *Phys. Rev.*, D92(4):045041, 2015.

[9] Zvi Bern, John Joseph M. Carrasco, and Henrik Johansson. Perturbative quantum gravity as a double copy of gauge theory. *Physical Review Letters*, 105(6), August 2010.

[10] Z. Bern, J. J. M. Carrasco, L. J. Dixon, H. Johansson, and R. Roiban. Simplifying multiloop integrands and ultraviolet divergences of gauge theory and gravity amplitudes. *Physical Review D*, 85(10), May 2012.

[11] John Joseph M. Carrasco, Marco Chiodaroli, Murat Günaydin, and Radu Roiban. One-loop four-point amplitudes in pure and matter-coupled $\mathcal{N} \leq 4$ supergravity. *Journal of High Energy Physics*, 2013(3), March 2013.

[12] Rutger H. Boels, Reinke Sven Isermann, Ricardo Monteiro, and Donal O'Connell. Colour-kinematics duality for one-loop rational amplitudes. *Journal of High Energy Physics*, 2013(4), April 2013.

[13] John Joseph M. Carrasco and Henrik Johansson. Five-Point Amplitudes in $\mathcal{N} = 4$ Super-Yang-Mills Theory and $\mathcal{N} = 8$ Supergravity. *Phys. Rev.*, D85:025006, 2012.

[14] N. Emil J. Bjerrum-Bohr, Tristan Dennen, Ricardo Monteiro, and Donal O'Connell. Integrand oxidation and one-loop colour-dual numerators in $\mathcal{N} = 4$ gauge theory. *Journal of High Energy Physics*, 2013(7), July 2013.

[15] Rutger H. Boels, Bernd A. Kniehl, Oleg V. Tarasov, and Gang Yang. Color-kinematic duality for form factors. *Journal of High Energy Physics*, 2013(2), February 2013.

[16] Hideyuki Kawai, David C. Lewellen, and S.-HH Tye. A relation between tree amplitudes of closed and open strings. *Nuclear Physics B*, 269(1):1–23, 1986.

[17] Zvi Bern, Tristan Dennen, Yu-tin Huang, and Michael Kiermaier. Gravity as the square of gauge theory. *Physical Review D*, 82(6), September 2010.

[18] Edward Witten. Perturbative gauge theory as a string theory in twistor space. *Commun.Math.Phys.*, 252:189–258, 2004.

[19] Nathan Berkovits. Alternative String Theory in Twistor Space for $\mathcal{N} = 4$ Super-Yang-Mills Theory. *Physical Review Letters*, 93(1), June 2004.

[20] Radu Roiban, Marcus Spradlin, and Anastasia Volovich. A Googly amplitude from the B model in twistor space. *JHEP*, 0404:012, 2004.

[21] Radu Roiban, Marcus Spradlin, and Anastasia Volovich. Tree-level S-matrix of Yang-Mills theory. *Physical Review D*, 70(2), July 2004.

[22] Marcus Spradlin and Anastasia Volovich. From twistor string theory to recursion relations. *Physical Review D*, 80(8), October 2009.

[23] Dung Nguyen, Marcus Spradlin, Anastasia Volovich, and Congkao Wen. The tree formula for MHV graviton amplitudes. *Journal of High Energy Physics*, 2010(7), July 2010.

[24] Andrew Hodges. New expressions for gravitational scattering amplitudes. *JHEP*, 07:075, 2013.

[25] Andrew Hodges. A simple formula for gravitational mhv amplitudes. *arXiv:1204.1930*, 2012.

[26] Freddy Cachazo and Yvonne Geyer. A "Twistor String" Inspired Formula For Tree-Level Scattering Amplitudes in $\mathcal{N} = 8$ SUGRA. *arXiv:1206.6511*, 2012.

[27] Freddy Cachazo and David Skinner. Gravity from rational curves in twistor space. *Physical Review Letters*, 110(16), April 2013.

[28] Freddy Cachazo, Lionel Mason, and David Skinner. Gravity in Twistor Space and its Grassmannian Formulation. *SIGMA*, 10:051, 2014.

[29] Song He. A Link Representation for Gravity Amplitudes. *JHEP*, 10:139, 2013.

[30] Freddy Cachazo, Song He, and Ellis Ye Yuan. Scattering equations and Kawai-Lewellen-Tye orthogonality. *Phys. Rev.*, D90(6):065001, 2014.

[31] Freddy Cachazo, Song He, and Ellis Ye Yuan. Scattering in Three Dimensions from Rational Maps. *JHEP*, 10:141, 2013.

[32] Freddy Cachazo, Song He, and Ellis Ye Yuan. Scattering of Massless Particles: Scalars, Gluons and Gravitons. *JHEP*, 07:033, 2014.

[33] Freddy Cachazo. Fundamental BCJ Relation in $\mathcal{N} = 4$ SYM from the Connected Formulation. *arXiv:1206.5970*, 2012.

[34] Diana Vaman and York-Peng Yao. Constraints and generalized gauge transformations on tree-level gluon and graviton amplitudes. *Journal of High Energy Physics*, 2010(11), November 2010.

[35] Rutger H. Boels and Reinke Sven Isermann. On powercounting in perturbative quantum gravity theories through color-kinematic duality. *Journal of High Energy Physics*, 2013(6), June 2013.

[36] Vittorio Del Duca, Lance Dixon, and Fabio Maltoni. New color decompositions for gauge amplitudes at tree and loop level. *Nuclear Physics B*, 571(1-2):51–70, April 2000.

[37] Mathias Tolotti and Stefan Weinzierl. Construction of an effective Yang-Mills Lagrangian with manifest BCJ duality. *JHEP*, 07:111, 2013.

[38] Adi Ben-Israel and Thomas N. E. Greville. *Generalized inverses: theory and applications*. Number 15 in CMS books in mathematics. Springer, New York, 2nd edition, 2003.

[39] Carlos R. Mafra, Oliver Schlotterer, and Stephan Stieberger. Explicit BCJ numerators from pure spinors. *Journal of High Energy Physics*, 2011(7), July 2011.

[40] N. Emil J. Bjerrum-Bohr, Poul H. Damgaard, Thomas Søndergaard, and Pierre Vanhove. The momentum kernel of gauge and gravity theories. *Journal of High Energy Physics*, 2011(1):1–18, 2011.

[41] N. E. J. Bjerrum-Bohr, Poul H. Damgaard, Bo Feng, and Thomas Søndergaard. Gravity and Yang-Mills amplitude relations. *Physical Review D*, 82(10), November 2010.

[42] N. E. J. Bjerrum-Bohr, Poul H. Damgaard, Bo Feng, and Thomas Søndergaard. Proof of gravity and Yang-Mills amplitude relations. *Journal of High Energy Physics*, 2010(9), September 2010.

[43] N.E.J. Bjerrum-Bohr, Poul H. Damgaard, Bo Feng, and Thomas Søndergaard. New identities among gauge theory amplitudes. *Physics Letters B*, 691(5):268–273, August 2010.

[44] N. Bjerrum-Bohr, Poul Damgaard, and Pierre Vanhove. Minimal basis for gauge theory amplitudes. *Physical Review Letters*, 103(16), October 2009.

[45] N. E. J. Bjerrum-Bohr, Poul H. Damgaard, Ricardo Monteiro, and Donal O'Connell. Algebras for amplitudes. *Journal of High Energy Physics*, 2012(6), June 2012.

[46] Stephan Stieberger. Open & closed vs. pure open string disk amplitudes. *arXiv:0907.2211*, 2009.

[47] Nima Arkani-Hamed, Freddy Cachazo, Clifford Cheung, and Jared Kaplan. A Duality for the S-Matrix. *JHEP*, 1003:020, 2010.

[48] Nima Arkani-Hamed, Jacob Bourjaily, Freddy Cachazo, and Jaroslav Trnka. Unification of Residues and Grassmannian Dualities. *JHEP*, 1101:049, 2011.

[49] Nima Arkani-Hamed, Jacob L. Bourjaily, Freddy Cachazo, Alexander B. Goncharov, Alexander Postnikov, and Jaroslav Trnka. Scattering Amplitudes and the Positive Grassmannian. *arXiv:1212.5605 [hep-th]*, 2012.

[50] Nima Arkani-Hamed, Jacob Bourjaily, Freddy Cachazo, and Jaroslav Trnka. Local Spacetime Physics from the Grassmannian. *JHEP*, 1101:108, 2011.

[51] Freddy Cachazo, Song He, and Ellis Ye Yuan. Scattering of Massless Particles in Arbitrary Dimensions. *Phys. Rev. Lett.*, 113(17):171601, 2014.

[52] Michael Kiermaier. Gravity as the square of gauge theory. *Prog. Theor. Phys. Suppl.*, 188:177–186, 2011.

[53] Nima Arkani-Hamed and Jaroslav Trnka. The Amplituhedron. *JHEP*, 10:030, 2014.

[54] Nima Arkani-Hamed and Jaroslav Trnka. Into the Amplituhedron. *JHEP*, 12:182, 2014.

[55] Yu-tin Huang, Henrik Johansson, and Sangmin Lee. On Three-Algebra and Bi-Fundamental Matter Amplitudes and Integrability of Supergravity. *JHEP*, 11:050, 2013.

[56] Allic Sivaramakrishnan. Color-Kinematic Duality in ABJM Theory Without Amplitude Relations. *arXiv:1402.1821 [hep-th]*, February 2014.

[57] Chih-Hao Fu, Yi-Jian Du, and Bo Feng. An Algebraic Approach to BCJ Numerators. *Journal of High Energy Physics*, 2013(3), March 2013.

[58] David A. Kosower and Kasper J. Larsen. Maximal unitarity at two loops. *Physical Review D*, 85(4), February 2012.

[59] Simon Caron-Huot and Kasper J. Larsen. Uniqueness of two-loop master contours. *Journal of High Energy Physics*, 2012(10), October 2012.

[60] Zvi Bern, Scott Davies, and Josh Nohle. Double-Copy Constructions and Unitarity Cuts. *arXiv:1510.03448 [hep-th]*, 2015.

[61] Tim Adamo, Eduardo Casali, and David Skinner. Ambitwistor strings and the scattering equations at one loop. *JHEP*, 04:104, 2014.

[62] Lionel Mason and David Skinner. Ambitwistor strings and the scattering equations. *JHEP*, 07:048, 2014.

[63] Yvonne Geyer, Lionel Mason, Ricardo Monteiro, and Piotr Tourkine. Loop Integrands for Scattering Amplitudes from the Riemann Sphere. *Phys. Rev. Lett.*, 115(12):121603, 2015.

[64] Yvonne Geyer, Lionel Mason, Ricardo Monteiro, and Piotr Tourkine. One-loop ampli-tudes on the Riemann sphere. *JHEP*, 03:114, 2016.

[65] Christian Baadsgaard, N. E. J. Bjerrum-Bohr, Jacob L. Bourjaily, Poul H. Damgaard, and Bo Feng. Integration Rules for Loop Scattering Equations. *JHEP*, 11:080, 2015.

[66] J.M. Drummond, J. Henn, V.A. Smirnov, and E. Sokatchev. Magic identities for conformal four-point integrals. *JHEP*, 0701:064, 2007.

[67] Luis F. Alday and Juan Martin Maldacena. Gluon scattering amplitudes at strong coupling. *JHEP*, 0706:064, 2007.

[68] J.M. Drummond, J. Henn, G.P. Korchemsky, and E. Sokatchev. Dual superconformal symmetry of scattering amplitudes in $\mathcal{N} = 4$ super-Yang-Mills theory. *Nucl.Phys.*, B828:317–374, 2010.

[69] James M. Drummond, Johannes M. Henn, and Jan Plefka. Yangian symmetry of scattering amplitudes in $\mathcal{N} = 4$ super Yang-Mills theory. *JHEP*, 0905:046, 2009.

[70] Niklas Beisert and Matthias Staudacher. The $\mathcal{N} = 4$ SYM integrable super spin chain. *Nucl.Phys.*, B670:439–463, 2003.

[71] Niklas Beisert, Burkhard Eden, and Matthias Staudacher. Transcendentality and Crossing. *J. Stat. Mech.*, 0701:P01021, 2007.

[72] J.M. Drummond, G.P. Korchemsky, and E. Sokatchev. Conformal properties of four-gluon planar amplitudes and Wilson loops. *Nucl.Phys.*, B795:385–408, 2008.

[73] Andreas Brandhuber, Paul Heslop, and Gabriele Travaglini. MHV amplitudes in $\mathcal{N} = 4$ super Yang-Mills and Wilson loops. *Nucl. Phys.*, B794:231–243, 2008.

[74] J.M. Drummond, J. Henn, G.P. Korchemsky, and E. Sokatchev. Conformal Ward identities for Wilson loops and a test of the duality with gluon amplitudes. *Nucl.Phys.*, B826:337–364, 2010.

[75] L.J. Mason and David Skinner. The Complete Planar S-matrix of $\mathcal{N} = 4$ SYM as a Wilson Loop in Twistor Space. *JHEP*, 1012:018, 2010.

[76] Simon Caron-Huot. Notes on the scattering amplitude / Wilson loop duality. *JHEP*, 1107:058, 2011.

[77] Luis F. Alday, Burkhard Eden, Gregory P. Korchemsky, Juan Maldacena, and Emery Sokatchev. From correlation functions to Wilson loops. *JHEP*, 1109:123, 2011.

[78] Benjamin Basso, Amit Sever, and Pedro Vieira. Spacetime and Flux Tube S-Matrices at Finite Coupling for $\mathcal{N} = 4$ Supersymmetric Yang-Mills Theory. *Phys.Rev.Lett.*, 111(9):091602, 2013.

[79] Benjamin Basso, Joao Caetano, Lucia Cordova, Amit Sever, and Pedro Vieira. OPE for all Helicity Amplitudes. *JHEP*, 08:018, 2015.

[80] Benjamin Basso, Amit Sever, and Pedro Vieira. Hexagonal Wilson Loops in Planar $\mathcal{N} = 4$ SYM Theory at Finite Coupling. *arXiv:1508.03045 [hep-th]*, 2015.

[81] Lance J. Dixon, James M. Drummond, Matt von Hippel, and Jeffrey Pennington. Hexagon functions and the three-loop remainder function. *JHEP*, 12:049, 2013.

[82] Lance J. Dixon and Matt von Hippel. Bootstrapping an NMHV amplitude through three loops. *JHEP*, 10:065, 2014.

[83] Lance J. Dixon, Matt von Hippel, and Andrew J. McLeod. The four-loop six-gluon NMHV ratio function. *JHEP*, 01:053, 2016.

[84] Alexander B. Goncharov, Marcus Spradlin, C. Vergu, and Anastasia Volovich. Classical Polylogarithms for Amplitudes and Wilson Loops. *Phys.Rev.Lett.*, 105:151605, 2010.

[85] John Golden, Alexander B. Goncharov, Marcus Spradlin, Cristian Vergu, and Anastasia Volovich. Motivic Amplitudes and Cluster Coordinates. *JHEP*, 1401:091, 2014.

[86] James M. Drummond, Georgios Papathanasiou, and Marcus Spradlin. A Symbol of Uniqueness: The Cluster Bootstrap for the 3-Loop MHV Heptagon. *JHEP*, 03:072, 2015.

[87] Daniel Parker, Adam Scherlis, Marcus Spradlin, and Anastasia Volovich. Hedgehog bases for A_n cluster polylogarithms and an application to six-point amplitudes. *JHEP*, 11:136, 2015.

[88] Nima Arkani-Hamed, Freddy Cachazo, and Clifford Cheung. The Grassmannian Origin of Dual Superconformal Invariance. *JHEP*, 1003:036, 2010.

[89] L.J. Mason and David Skinner. Dual Superconformal Invariance, Momentum Twistors and Grassmannians. *JHEP*, 0911:045, 2009.

[90] Nima Arkani-Hamed, Jacob L. Bourjaily, Freddy Cachazo, Simon Caron-Huot, and Jaroslav Trnka. The All-Loop Integrand for Scattering Amplitudes in Planar $\mathcal{N} = 4$ SYM. *JHEP*, 1101:041, 2011.

[91] Yu-Tin Huang and CongKao Wen. ABJM amplitudes and the positive orthogonal Grassmannian. *JHEP*, 1402:104, 2014.

[92] Yu-tin Huang, Congkao Wen, and Dan Xie. The Positive Orthogonal Grassmannian and Loop Amplitudes of ABJM. *J. Phys.*, A47(47):474008, 2014.

[93] Joonho Kim and Sangmin Lee. Positroid Stratification of Orthogonal Grassmannian and ABJM Amplitudes. *JHEP*, 1409:085, 2014.

[94] Henriette Elvang, Yu-tin Huang, Cynthia Keeler, Thomas Lam, Timothy M. Olson, Samuel B. Roland, and David E. Speyer. Grassmannians for scattering amplitudes in 4d $\mathcal{N} = 4$ SYM and 3d ABJM. *JHEP*, 12:181, 2014.

[95] Sebastian Franco, Daniele Galloni, Alberto Mariotti, and Jaroslav Trnka. Anatomy of the Amplituhedron. *JHEP*, 03:128, 2015.

[96] Yuntao Bai and Song He. The Amplituhedron from Momentum Twistor Diagrams. *JHEP*, 02:065, 2015.

[97] Nima Arkani-Hamed, Andrew Hodges, and Jaroslav Trnka. Positive Amplitudes In The Amplituhedron. *JHEP*, 08:030, 2015.

[98] Lam, Thomas. Amplituhedron Cells and Stanley Symmetric Functions. *Communications in Mathematical Physics*, 343(3):1025–1037, 2016.

[99] Yuntao Bai, Song He, and Thomas Lam. The Amplituhedron and the One-loop Grassmannian Measure. *JHEP*, 01:112, 2016.

[100] Livia Ferro, Tomasz Lukowski, Andrea Orta, and Matteo Parisi. Towards the Amplituhedron Volume. *JHEP*, 03:014, 2016.

[101] G. Lusztig. Total positivity in partial flag manifolds. *Represent. Theory*, 2:70–78, 1998.

[102] A. Postnikov. Total positivity, Grassmannians, and networks. *arXiv:math/0609764 [math.CO]*, September 2006.

[103] Alexander Postnikov, David Speyer, and Lauren Williams. Matching polytopes, toric geometry, and the totally non-negative Grassmannian. *Journal of Algebraic Combinatorics*, 30(2):173–191, 2008.

[104] Lauren K. Williams. Enumeration of totally positive Grassmann cells. *Advances in Mathematics*, 190(2):319 – 342, 2005.

[105] A. B. Goncharov and R. Kenyon. Dimers and cluster integrable systems. *arXiv:1107.5588 [math.AG]*, July 2011.

[106] Knutson, Allen and Lam, Thomas and Speyer, David E. Positroid Varieties: Juggling and Geometry. *Compositio Mathematica*, 149:1710–1752, 10 2013.

[107] Zvi Bern, John Joseph M. Carrasco, and Henrik Johansson. Perturbative Quantum Gravity as a Double Copy of Gauge Theory. *Phys.Rev.Lett.*, 105:061602, 2010.

[108] Nima Arkani-Hamed, Jacob L. Bourjaily, Freddy Cachazo, and Jaroslav Trnka. Singularity Structure of Maximally Supersymmetric Scattering Amplitudes. *Phys. Rev. Lett.*, 113(26):261603, 2014.

[109] Stephen J. Parke and T. R. Taylor. An Amplitude for n-Gluon Scattering. *Phys. Rev. Lett.*, 56:2459, 1986.

[110] Michelangelo L. Mangano, Stephen J. Parke, and Zhan Xu. Duality and Multi - Gluon Scattering. *Nucl. Phys.*, B298:653, 1988.

[111] Nima Arkani-Hamed, Jacob L. Bourjaily, Freddy Cachazo, Alexander Postnikov, and Jaroslav Trnka. On-Shell Structures of MHV Amplitudes Beyond the Planar Limit. *JHEP*, 06:179, 2015.

[112] Lance J. Dixon, Andrew J. McLeod, Jaroslav Trnka, and Matt von Hippel. In preparation.

[113] Zvi Bern, John Joseph Carrasco, Tristan Dennen, Yu-tin Huang, and Harald Ita. Generalized Unitarity and Six-Dimensional Helicity. *Phys.Rev.*, D83:085022, 2011.

[114] Z. Bern, L.J. Dixon, D.A. Kosower, R. Roiban, M. Spradlin, et al. The Two-Loop Six-Gluon MHV Amplitude in Maximally Supersymmetric Yang-Mills Theory. *Phys.Rev.*, D78:045007, 2008.

[115] V. P. Nair. A Current Algebra for Some Gauge Theory Amplitudes. *Phys. Lett.*, B214:215, 1988.

[116] Zvi Bern, Lance J. Dixon, David C. Dunbar, and David A. Kosower. One loop n point gauge theory amplitudes, unitarity and collinear limits. *Nucl.Phys.*, B425:217–260, 1994.

[117] Zvi Bern, Lance J. Dixon, David C. Dunbar, and David A. Kosower. Fusing gauge theory tree amplitudes into loop amplitudes. *Nucl.Phys.*, B435:59–101, 1995.

[118] Z. Bern, J.J.M. Carrasco, Henrik Johansson, and D.A. Kosower. Maximally supersymmetric planar Yang-Mills amplitudes at five loops. *Phys.Rev.*, D76:125020, 2007.

[119] Andrew Hodges. Eliminating spurious poles from gauge-theoretic amplitudes. *JHEP*, 1305:135, 2013.

[120] Freddy Cachazo. Sharpening the Leading Singularity. *arXiv:0803.1988 [hep-th]*, 2008.

[121] J. M. Drummond, J. Henn, G. P. Korchemsky, and E. Sokatchev. The hexagon Wilson loop and the BDS ansatz for the six-gluon amplitude. *Phys. Lett.*, B662:456–460, 2008.

[122] Nima Arkani-Hamed, Jacob L. Bourjaily, Freddy Cachazo, and Jaroslav Trnka. Local Integrals for Planar Scattering Amplitudes. *JHEP*, 06:125, 2012.

[123] Jacob L. Bourjaily, Simon Caron-Huot, and Jaroslav Trnka. Dual-Conformal Regularization of Infrared Loop Divergences and the Chiral Box Expansion. *JHEP*, 01:001, 2015.

[124] Jacob L. Bourjaily and Jaroslav Trnka. Local Integrand Representations of All Two-Loop Amplitudes in Planar SYM. *JHEP*, 08:119, 2015.

[125] Z. Bern, J.S. Rozowsky, and B. Yan. Two loop four gluon amplitudes in $\mathcal{N} = 4$ super-Yang-Mills. *Phys.Lett.*, B401:273–282, 1997.

[126] Z. Bern, J.J. Carrasco, Lance J. Dixon, Henrik Johansson, D.A. Kosower, and Radu Roiban. Three-Loop Superfiniteness of $\mathcal{N} = 8$ Supergravity. *Phys.Rev.Lett.*, 98:161303, 2007.

[127] Z. Bern, Lance J. Dixon, D.C. Dunbar, M. Perelstein, and J.S. Rozowsky. On the relationship between Yang-Mills theory and gravity and its implication for ultraviolet divergences. *Nucl.Phys.*, B530:401–456, 1998.

[128] Z. Bern, J.J.M. Carrasco, L.J. Dixon, H. Johansson, and R. Roiban. Simplifying Multi-loop Integrands and Ultraviolet Divergences of Gauge Theory and Gravity Amplitudes. *Phys.Rev.*, D85:105014, 2012.

[129] Michelangelo L. Mangano and Stephen J. Parke. Multiparton amplitudes in gauge theories. *Phys. Rept.*, 200:301–367, 1991.

[130] Sebastian Franco, Daniele Galloni, Brenda Penante, and Congkao Wen. Non-Planar On-Shell Diagrams. *JHEP*, 06:199, 2015.

[131] Rouven Frassek and David Meidinger. Yangian-type symmetries of non-planar leading singularities. *arXiv:1603.00088 [hep-th]*, 2016.

[132] Zvi Bern, Lance J. Dixon, David C. Dunbar, and David A. Kosower. One loop self-dual and $\mathcal{N} = 4$ super-Yang-Mills. *Phys. Lett.*, B394:105–115, 1997.

[133] Z. Bern, Lance J. Dixon, M. Perelstein, and J. S. Rozowsky. Multileg one loop gravity amplitudes from gauge theory. *Nucl. Phys.*, B546:423–479, 1999.

[134] Gustav Mogull and Donal O'Connell. Overcoming Obstacles to Colour-Kinematics Duality at Two Loops. *JHEP*, 12:135, 2015.

[135] A.V. Kotikov, L.N. Lipatov, A.I. Onishchenko, and V.N. Velizhanin. Three loop universal anomalous dimension of the Wilson operators in $\mathcal{N} = 4$ SUSY Yang-Mills model. *Phys.Lett.*, B595:521–529, 2004.

[136] Johannes M. Henn. Multiloop integrals in dimensional regularization made simple. *Phys.Rev.Lett.*, 110(25):251601, 2013.

[137] Johannes M. Henn, Alexander V. Smirnov, and Vladimir A. Smirnov. Analytic results for planar three-loop four-point integrals from a Knizhnik-Zamolodchikov equation. *JHEP*, 1307:128, 2013.

[138] Simon Caron-Huot and Johannes M. Henn. Iterative structure of finite loop integrals. *JHEP*, 06:114, 2014.

[139] Johannes M. Henn. Lectures on differential equations for Feynman integrals. *J. Phys.*, A48:153001, 2015.

[140] T. Gehrmann, J. M. Henn, and N. A. Lo Presti. Analytic form of the two-loop planar five-gluon all-plus-helicity amplitude in QCD. *Phys. Rev. Lett.*, 116(6):062001, 2016.

[141] G. Passarino and M.J.G. Veltman. One Loop Corrections for e^+e^- Annihilation into $\mu^+\mu^-$ in the Weinberg Model. *Nucl.Phys.*, B160:151, 1979.

[142] Zvi Bern, Lance J. Dixon, and David A. Kosower. Dimensionally regulated pentagon integrals. *Nucl.Phys.*, B412:751–816, 1994.

[143] Z. Bern, J.J.M. Carrasco, Lance J. Dixon, H. Johansson, and R. Roiban. The Complete Four-Loop Four-Point Amplitude in $\mathcal{N} = 4$ Super-Yang-Mills Theory. *Phys.Rev.*, D82:125040, 2010.

[144] N.E.J. Bjerrum-Bohr and Pierre Vanhove. Absence of Triangles in Maximal Supergravity Amplitudes. *JHEP*, 0810:006, 2008.

[145] Nima Arkani-Hamed, Freddy Cachazo, and Jared Kaplan. What Is the Simplest Quantum Field Theory? *JHEP*, 1009:016, 2010.

[146] Henriette Elvang and Yu-tin Huang. Scattering Amplitudes. *arXiv:1308.1697 [hep-th]*, 2013.

[147] Z. Bern, J.J.M. Carrasco, H. Johansson, and R. Roiban. The Five-Loop Four-Point Amplitude of $\mathcal{N} = 4$ super-Yang-Mills Theory. *Phys.Rev.Lett.*, 109:241602, 2012.

[148] Z. Bern, J.J.M. Carrasco, Lance J. Dixon, Henrik Johansson, and R. Roiban. Manifest Ultraviolet Behavior for the Three-Loop Four-Point Amplitude of $\mathcal{N} = 8$ Supergravity. *Phys.Rev.*, D78:105019, 2008.